
Electronic Thesis and Dissertation Repository

10-18-2017 2:00 PM

Induction of alternative pathway respiration by nitrate in *Chlamydomonas*

Shanmugasundaram Pakkiriswami
The University of Western Ontario

Supervisor
Dr. Denis Philip Maxwell
The University of Western Ontario

Graduate Program in Biology
A thesis submitted in partial fulfillment of the requirements for the degree in Doctor of Philosophy
© Shanmugasundaram Pakkiriswami 2017

Follow this and additional works at: <https://ir.lib.uwo.ca/etd>



Part of the [Biology Commons](#)

Recommended Citation

Pakkiriswami, Shanmugasundaram, "Induction of alternative pathway respiration by nitrate in *Chlamydomonas*" (2017). *Electronic Thesis and Dissertation Repository*. 4966.
<https://ir.lib.uwo.ca/etd/4966>

This Dissertation/Thesis is brought to you for free and open access by Scholarship@Western. It has been accepted for inclusion in Electronic Thesis and Dissertation Repository by an authorized administrator of Scholarship@Western. For more information, please contact wlsadmin@uwo.ca.

Abstract

Besides the ubiquitous cytochrome pathway of mitochondrial respiration, the green alga *Chlamydomonas* possesses an alternative pathway of respiration, which is comprised of a single protein, alternative oxidase (AOX). AOX is induced when *Chlamydomonas* cells are shifted from a growth medium containing ammonium as the nitrogen source to one with nitrate. The primary aim of this thesis was to understand the metabolic connections between nitrate assimilation and the induction of the alternative pathway. That these two metabolic processes are closely linked is supported by the fact that the gene encoding AOX is clustered with the genes required for nitrate assimilation (NAR genes).

To investigate if the clustering of AOX with NAR genes occurs in other green algae, publicly available genome databases were searched. It was found that while the clustering of NAR genes is widespread in many lineages of green algae, the presence of AOX within a NAR cluster is a characteristic of only a single group of green algae, the chlorophytes. Interestingly, it was found that lineages that lack NAR gene clustering seem to have a preference for importing amino acids instead of nitrate as their dominant source of nitrogen.

The role of AOX in nitrate assimilation was investigated by constitutively blocking AOX expression. AOX knockdown cells displayed a slightly decreased rate of growth and distinctly different photosynthetic electron transport characteristics. Whole-cell metabolite analysis showed that the lack of AOX in the mitochondrion in knockdown cells suppressed the stimulatory effect of nitrate on oxidative pentose phosphate pathway (oxPPP) activity in the chloroplast. Interestingly, this regulation also occurred in the opposite direction. In wild-type cells, the biochemical inhibition of oxPPP by glycerol in the chloroplast decreased the accumulation of AOX in the mitochondrion.

I suggest that the induction of AOX by nitrate is to relieve respiratory electron transport from adenylate control. During nitrate assimilation increased demand by

the chloroplast for ATP would decrease the transfer of ADP and Pi to the mitochondria restricting the rate of the cytochrome pathway. Up regulation of the alternative pathway would allow for continued upstream respiratory carbon flow under limiting adenylate conditions.

Keywords

Alternative oxidase, nitrate, *Chlamydomonas*, respiration, oxidative pentose phosphate pathway

Co-Authorship Statement

Chapter 2: S. Pakkiriswami, DP Maxwell. The distribution of NAR gene clusters in green algae and its ecological significance. (Article in Preparation)

DP Maxwell – Principal Investigator, provided suggestions for experimental design and comments on the manuscript preparation.

Chapter 3: S. Pakkiriswami, AG Ivanov, NPA Hüner, DP Maxwell. Photosynthetic alterations triggered by the absence of AOX protein accumulation in the mitochondria of *Chlamydomonas* cells. (Article in Preparation)

NPA Huner – Advisory committee member and provided critical comments on the manuscript preparation.

AG Ivanov – P700 redox measurements and provided critical comments on the manuscript preparation.

DP Maxwell – Principal Investigator, provided suggestions for experimental design and comments on the manuscript preparation.

Chapter 4: S. Pakkiriswami, AG Ivanov, DP Maxwell. Induction of alternative pathway respiration is metabolically linked to the activation of oxidative pentose phosphate pathway under nitrate in *Chlamydomonas*. (Article in Preparation)

AG Ivanov – P700 redox measurements and provided critical comments on the manuscript preparation.

DP Maxwell – Principal Investigator, provided suggestions for experimental design and comments on the manuscript preparation.

Acknowledgments

It is my pleasure to thank my PhD supervisor and mentor DR. Denis Maxwell for the encouragement and guidance given by him throughout my graduate program. Without his continued and timely support completion of this dissertation would not have been possible.

I extend my sincere thanks to my PhD research advisory committee members DR. Norman Hüner and DR. Mark Bernards for their valuable suggestions and support that contributed significantly towards the development of this thesis. In addition, special thanks to DR. Norman Huner for reading my thesis and for the critical corrections and comments.

I thank DR Alexander Ivanov for thoroughly guiding me in doing the fluorescence measurements and P700 redox measurements and his valuable suggestions that helped to improve my experimental approaches. I like to extend special thanks to my lab mate Marc Possmayer for his help and memorable scientific chats happened with him. I extend my sincere gratitude to all the past and present members of Huner, Bernards, Trick and Vava Grbic lab with whom I had interacted during my stay in DR Maxwell Lab. Finally, I like to thank Ray Zabulionis, Jeni Duro and Anica for their support and friendship.

I gratefully acknowledge the funding sources QE (II) GSST, NSERC, OSAP and WGRS for the recognition and financial support provided during my graduate studies.

Table of Contents

Abstract	i
Keywords.....	ii
Co-Authorship Statement	iii
Acknowledgments	iv
Table of Contents	v
List of Tables	ix
List of Figures	x
List of Appendices	xiii
List of Abbreviations	xiv
Chapter 1.....	1
1 General Introduction.....	1
1.1 Chlamydomonas reinhardtii, the green alga	1
1.2 Chlamydomonas reinhardtii as a model organism	1
1.3 Energy Metabolism in Photoautotrophs	2
1.3.1 Photosynthesis.....	4
1.3.2 Respiration	4
1.3.3 Cytochrome Electron Transport Pathway.....	5
1.3.4 Alternative Pathway Respiration	6
1.4 The Physiological Function of Alternative Oxidase	7
1.5 AOX and its Regulation in Chlamydomonas reinhardtii	9
1.6 Nitrate Assimilation	11
1.7 Organization of nitrate assimilation related (NAR) genes	13
1.8 Thesis objectives	13
1.9 References	16

Chapter 2.....	22
2 Nitrate assimilation related (NAR) gene cluster distribution and organization in green algal species	22
2.1 Introduction	22
2.2 Material and Methods	28
2.2.1 Algal NAR Cluster I and II identification	28
2.2.2 Phylogenetic analysis.....	28
2.2.3 RNA isolation, semi-quantitative polymerase chain reaction and gel blot analysis	29
2.2.4 Isolation and cloning of 1.4 kbp intergenic fragment of AOX1 and NRT2.3 gene.....	30
2.2.5 Transformation of Chlamydomonas cells	31
2.2.6 ARS reporter gene assay	31
2.3 Results.....	33
2.3.1 Distribution of NAR Cluster I in Algae	33
2.3.2 Other metabolic genes are recruited into NAR cluster I.	37
2.3.3 Lack of a complete NAR Cluster I is linked to alternative nitrogen acquisition strategies.....	38
2.3.4 Ferredoxin-dependent Nitrite reductase of Mamiellophyceae contains three additional protein domains.....	40
2.3.5 Ferredoxin-dependent Nitrite reductase (NII) has a probable cyanobacterial origin	42
2.3.6 NAR Cluster II distribution and its regulation by nitrate	44
2.4 Discussion	48
2.5 References	55
Chapter 3.....	59
3 Generation and Molecular Characterization of Chlamydomonas strain with reduced AOX1 gene expression	59
3.1 Introduction.....	59

3.2	Material and Methods	62
3.2.1	Strain and growth conditions	62
3.2.2	Generation of knock down cell lines of AOX1	63
3.2.3	Isolation of membrane fraction for Immunoblotting	63
3.2.4	SDS-polyacrylamide gel electrophoresis and Immunoblotting	64
3.2.5	Determination of Growth Rate.....	65
3.2.6	Measurement of Photosynthetic O ₂ Evolution	65
3.2.7	Measurement of Respiration	66
3.2.8	Chlorophyll Determination	66
3.2.9	Low temperature (77K) Fluorescence Measurements	66
3.2.10	Measurement of P700 Photooxidation	67
3.2.11	Measurement of ROS	68
3.2.12	RNA extraction and Quantitative Polymerase Chain Reaction (qPCR)	68
3.3	Results.....	70
3.3.1	Isolation of AOX1 knockdown cell lines.....	70
3.3.2	Growth, Photosynthetic Oxygen Evolution and Respiration Characteristics of WT and K26	73
3.3.3	Absence of AOX increased ROS abundance.....	77
3.3.4	Nitrate and AOX1 silencing activates Photosynthetic Cyclic Electron Flow	78
3.4	Discussion	88
3.5	References	94
Chapter 4	99
4	Role of oxidative pentose phosphate pathway in the nitrate dependent induction of AOX	99
4.1	Introduction	99
4.2	Material and Methods	102

4.2.1	Analysis of cell metabolome by GC-MS method	102
4.2.2	RNA extraction and Quantitative Polymerase Chain Reaction....	102
4.2.3	Glycerol treatment and protein blot analysis of AOX and COX ...	104
4.3	Results.....	105
4.3.1	AOX1 silencing alters the effect of nitrate on the cell metabolome	105
4.3.2	Oxidative Pentose Phosphate Pathway (oxPPP) activity is differentially modified by nitrate and alternative oxidase	113
4.3.3	Modification of oxPPP activity by glycerol downregulates AOX accumulation in the presence of nitrate.....	115
4.4	Discussion	117
4.5	References	120
Chapter 5	122
5	General Discussion and Future Perspectives	122
5.1	Understanding the significance of AOX induction in response to nitrate in Chlamydomonas	122
5.2	Summary of Major Contributions	130
5.3	Future Directions	131
5.4	References	133
Appendices	135
Curriculum Vitae	141

List of Tables

Table 2-1 Predicted number of amino acid transporters and ammonium transporter proteins in various green and red algal genomes.....	40
Table 3-1 Rate of dark reduction ($t_{1/2}$) of P700+ in the dark for WT and K26 cells grown in ammonium and nitrate.	87

List of Figures

Figure 1-1 Picture of <i>C. reinhardtii</i> cell showing the cellular location of Photosynthesis, Calvin cycle, Glycolysis, Tricarboxylic acid (TCA) cycle and Oxidative phosphorylation.	3
Figure 1-2 Mitochondrial Electron Transport Chain	7
Figure 1-3 Diagram of a <i>C. reinhardtii</i> cell showing the major steps of nitrate assimilation.....	12
Figure 2-1 Nitrate assimilation related (NAR) Cluster I (A) and Cluster II (B).	27
Figure 2-2 Representative semi-quantitative RT-PCR analysis of NAR genes transcript abundance in <i>Chlamydomonas</i>	34
Figure 2-3 NAR Cluster I distribution in species of the four classes of algae.	36
Figure 2-4 Phylogenetic tree of the distribution of NAR2 among various lineages. ..	37
Figure 2-5 Diagram illustrating the position of NAR2, MDH, NIA1 and NII1 in <i>Coccomyxa</i> (top) in relation to the NAR Cluster I organization of <i>Chlamydomonas</i> (bottom).	39
Figure 2-6 Representative protein domains of ferredoxin-dependent nitrite reductase from (A) <i>Chlamydomonas reinhardtii</i> (B) <i>Micromonas pusilla</i>	41
Figure 2-7 Distribution of the nitrite transporter (NRT2) protein (A) and ferredoxin-dependent nitrite reductase (NII1) protein (B) among various taxa.	43
Figure 2-8 The NAR Cluster II genes in three species of Chlorophyceae: <i>Chlamydomonas</i> compared with <i>Volvox</i> and <i>Gonium</i>	44
Figure 2-9 RNA blot analysis of NRT2.3 and AOX1 transcript abundance in <i>Chlamydomonas</i> cells shifted to the medium containing as nitrate the sole nitrogen source.....	45

Figure 2-10 Measuring transcription of the NRT2.3:AOX1 intergenic region.....	47
Figure 3-1 Growth characteristics and Immunoblot analysis of AOX and COX in WT and K26 cells.....	72
Figure 3-2 Growth of WT (solid line) and K26 (dashed line) strains grown in high salt-ammonium (HS-A) and high salt-nitrate (HS-N) nutrient medium.	74
Figure 3-3 Respiration profile of WT and K26 strains.	75
Figure 3-4 Measurement of photosynthetic oxygen evolution in WT and K26. Oxygen evolution measured as a function of irradiance for WT and K26 cells.	76
Figure 3-5 Changes in intracellular reactive oxygen species (ROS) abundance in WT and K26 cells.	78
Figure 3-6 Representative Immunoblots showing the abundance of various photosynthesis-related proteins in WT and K26 strains grown in ammonium (A) or nitrate (N) containing media.....	80
Figure 3-7 Quantitative PCR (qPCR) analysis of the abundance of FDX2 transcripts in WT and K26 cells grown in ammonium (A) and nitrate (N) containing medium... ..	82
Figure 3-8 Quantitative PCR (qPCR) analysis of the transcript level of NDA2 and PGRL in WT and K26 strains grown in ammonium (A) and nitrate (N) containing medium.....	83
Figure 3-9 Energy distribution pattern between PSII and PSI in WT and K26.....	85
Figure 3-10 Representative traces of the spectrophotometric measurement of the redox state of P700 in WT cells grown in ammonium and nitrate.	87
Figure 3-11 Model showing the non-photochemical reduction of PQ pool by the enzymic action of NDA2 complex. Increased electron donation through NDA2 complex could either be used to increase the cyclic electron flow around PSI or reduce the ferredoxins.	93

Figure 4-1 Venn diagram analysis and Heat map construction for metabolites altered in their status in WT and K26 in response to nitrate.	107
Figure 4-2 PCA scores plot showing the separation of the metabolome of WT and K26 cells grown in ammonium and nitrate.	108
Figure 4-3 PCA Loading plot showing metabolites that contribute to the variation for PC1 and PC2.....	110
Figure 4-4 Abundance of specific sugar phosphates in WT and K26 grown in ammonium and nitrate.	112
Figure 4-5 Changes in the abundance of metabolites glucose-6-phosphate and ribulose-6-phosphate.....	114
Figure 4-6 Quantitative PCR analysis of transcript abundance of GLD1 (glucose-6-phosphate dehydrogenase) and PGL/PGD (phosphogluconolactonase) in WT and K26 strains.....	115
Figure 5-1 Model showing the metabolic interactions between the chloroplast and mitochondria in Chlamydomonas cells grown in ammonium.	127
Figure 5-2 Model showing the relevant interactions between photosynthesis, Calvin cycle, oxPPP and mitochondrial electron transport in response to nitrate in WT cells.	128
Figure 5-3 Model showing the relevant interactions between photosynthesis, Calvin cycle and mitochondrial electron transport in response to nitrate in K26 cells.....	129

List of Appendices

Appendix S1: Gaussian parameters for the sub-band decomposition of low temperature (77K) chlorophyll fluorescence emission spectra of WT and K26 cells.	135
Appendix S2: List of gene specific primers used in PCR.....	136
Appendix S3: Changes in the accumulation of 26 different types of metabolites in WT and K26 that are used for heat map analysis.....	137
Appendix S4: PLS (DA) algorithm scores plot showing the separation of the metabolome of WT and K26 cells grown in ammonium and nitrate.....	140

List of Abbreviations

AA	antimycin A
ADP	adenosine diphosphate
AOX	alternative oxidase
amiRNA	artificial microRNA
AP	alternative pathway
ARS	arylsulfatase
ATP	adenosine 5' -triphosphate
BLAST	basic local alignment search tool
Chl	chlorophyll
COX3	third subunit of cytochrome oxidase
CP	cytochrome pathway
Cyt b6	cytochrome b6 of cytochrome b6f complex
Cyt f	cytochrome f of cytochrome b6f complex
D1	reaction center protein of PSII
DEPC	diethyl pyrocarbonate
FDX	ferredoxin
LHC	light harvesting complex
NADP ⁺	nicotinamide adenine dinucleotide phosphate (oxidized form)

NADPH	nicotinamide adenine dinucleotide phosphate (reduced form)
NAR	nitrate assimilation related
NIA1	nitrate reductase
NII1	nitrite reductase
NRT	nitrate transporter
NAR1	nitrite transporter
NAR2	nitrate transporter accessory protein
OEC	oxygen evolving complex
oxPPP	oxidative pentose phosphate pathway
PSI	photosystem I
PSII	photosystem II
P700	reaction center Chl a of PSI (reduced form)
P700 ⁺	reaction center Chl of PSI (oxidized form)
PAGE	polyacrylamide gel electrophoresis
PQ	plastoquinone (oxidized form)
PQH ₂	plastoquinone (reduced form)
P _{max}	maximum photosynthetic efficiency
PsaA/B	reaction center protein of Psi
RBCL	rubisco 1,5-bisphosphate carboxylase/oxygenase large subunit
ROS	reactive oxygen species

RNAi	RNA interference
RT-PCR	polymerase chain reaction
SDS	sodium dodecyl sulphate
SQ-RTPCR	semi-quantitative reverse transcriptase polymerase chain reaction
X-SO ₄	5-bromo-4-chloroindolyl sulfate

Chapter 1

1 General Introduction

1.1 *Chlamydomonas reinhardtii*, the green alga

Chlamydomonas is a genus of biflagellate unicellular green algae commonly found in soil and fresh water environments and has a nearly cosmopolitan distribution (Harris 2009). While it is most common in temperate regions, species of *Chlamydomonas* have been isolated from high altitude snowfields (e.g. *Chlamydomonas nivalis*) (Williams et al., 2003) and Antarctica (*Chlamydomonas* sp. UWO241) (Possmayer et al., 2016). How these so-called extremophile species differ genetically and physiologically from their temperate counterparts is beginning to be elucidated (Dolhi et al., 2013).

Phylogenetically, *Chlamydomonas* belongs to the Chlorophyceae (green algae) that diverged from the lineage leading to Streptophytes (land plants) approximately one billion years ago (Leliaert et al., 2012). The species *C. reinhardtii* was first described by Pierre Danegard (Danegard 1888) with most laboratory strains being derived from soil isolates collected by Gilbert Smith in 1945 near Amherst, Massachusetts, USA (Harris 2009).

1.2 *Chlamydomonas reinhardtii* as a model organism

Like other organisms including *Drosophila melanogaster*, *Caenorhabditis elegans* and *Arabidopsis thaliana*, *C. reinhardtii* possesses a set of traits that makes it particularly amenable for experimentation and thus it has become a widely adopted model system. First, it can be easily grown and maintained in the laboratory and has a relatively fast growth rate (doubling time of around 10 hours). Second, besides growing photoautotrophically like plants, *C. reinhardtii* is able to grow completely heterotrophically in the dark if it is supplied with acetate (Harris 2009). This specific trait has allowed researchers to characterize a wide

range of photosynthetic mutants (Spreitzer and Mets 1981, Grossmann et al., 2010) that are unable to grow in the presence of carbon dioxide alone.

Chlamydomonas has been widely exploited by geneticists because it is amenable to both forward and reverse genetic techniques for the elucidation of the molecular basis of various traits. Both insertional and chemical mutagenesis have been widely adopted (McCarthy et al., 2004, Dent et al., 2005, Gonzalez-Ballester et al., 2005), aided by the fact that vegetative cells of *C. reinhardtii* are haploid and reproduce simply by fission. Diploid cells, produced by the fertilization of haploid zygotes, can also be maintained (Harris 2009). In addition to forward genetic approaches, the completion of the *C. reinhardtii* genome sequencing project (Merchant et al., 2007) along with a wealth of expressed sequence tag (EST) libraries has made it possible to use the techniques of RNA interference (RNAi), for example, to specifically block the expression of a known gene and study the functional consequences of knocking it out (Reviewed in Cerutti et al., 2011).

1.3 Energy Metabolism in Photoautotrophs

As a photoautotrophic eukaryote, a *C. reinhardtii* cell possesses both a chloroplast and mitochondria. It can be argued that in many ways a single *C. reinhardtii* cell is metabolically similar to a single leaf cell of a plant. Structurally however, a notable difference is that a *C. reinhardtii* cell has a single chloroplast and 2-4 mitochondria whereas a single mesophyll cell of a leaf typically contains hundreds of each of these organelles.

As the two energy-transducing organelles of the cell the mitochondria and the chloroplast display metabolic interconnectivity (Krömer 1995; Nunes-Nesi et al. 2011). Both cellular respiration and photosynthesis, for example, exchange adenylate (e.g. ATP) and pyridine nucleotides (NADH, NADPH). The chloroplast is the site of photosynthesis where light energy is used to drive the reduction of carbon dioxide into sugar. While some of this sugar is stored in the chloroplast as starch much of it is exported to the cytosol, where it is used as the starting

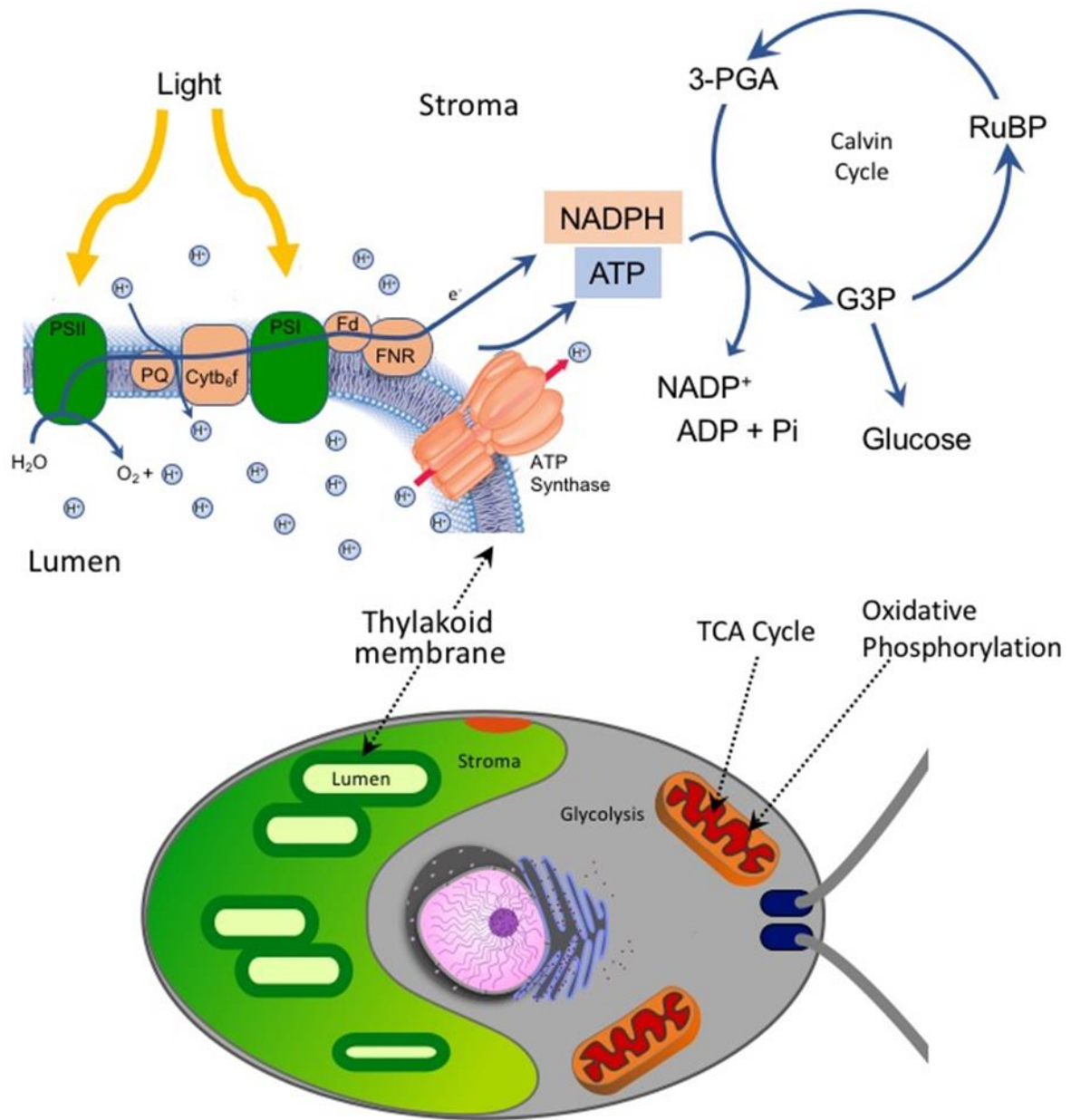


Figure 1.1 Picture of *C. reinhardtii* cell showing the cellular location of photosynthesis, Calvin cycle, glycolysis, tricarboxylic acid (TCA) cycle and oxidative phosphorylation. Photosystem II (PSII) and Photosystem I (PSI) are the two photosystems of photosynthesis; CYTB6F mediates the electron transfer between the two photosystems by oxidizing the PQ (plastoquinone) pool. The electrons are finally accepted by NADP $^+$ catalyzed by the enzyme ferredoxin NADP $^+$ reductase. NADPH formed and ATP synthesized by the ATP synthase complex are utilized in the Calvin cycle for the generation of photo assimilates.

molecule for two distinct processes. First, these carbon molecules represent a key source of the carbon skeletons used to synthesize a wide range of molecules (e.g. amino acids, fatty acids). Second this reduced carbon is oxidized by the components of cellular respiration with the energy conserved in the generation of ATP, the common energy currently required to support a wide array of anabolic processes (biosynthetic reactions).

1.3.1 Photosynthesis

The chloroplast contains an internal organized membrane called the thylakoid within which is embedded the components of photosynthetic electron transport (e.g. the light reactions). Photosystem I (PSI) and photosystem II (PSII) are the two supramolecular complexes that bind chlorophyll and other pigments that harvest light energy and use that energy to drive electron transport that oxidizes H_2O molecules and uses the released electrons to reduce NADP^+ to NADPH (Figure 1.1). Concurrently with electron transport, proton pumping generates an electrochemical gradient of protons across the thylakoid membrane that is used for the chemiosmotic generation of ATP using the enzyme complex ATP synthase (Hopkins and Hüner 2008).

The NADPH and ATP generated by the light reactions are consumed by the reactions of the Calvin Cycle, which are localized in the stroma of the chloroplast. The primary product of the Calvin cycle is the three-carbon sugar glyceraldehyde-3-phosphate (G3P). Within the chloroplast, G3P can be used for the synthesis of various molecules including glucose and other six carbon compounds, as well as the synthesis of starch. In addition, G3P can be readily exported into the cytosol where it can enter glycolysis or be used as a precursor for a range of biosynthetic reactions.

1.3.2 Respiration

Cellular respiration encompasses a range of metabolic reactions that collectively are used to oxidize a diverse group of molecules (carbohydrates, fatty acids and proteins) and use the released energy to produce adenosine triphosphate (ATP).

Cellular respiration is divided into three distinct stages: glycolysis, the tricarboxylic acid cycle (TCA) and oxidative phosphorylation (Figure 1.1). During glycolysis, which occurs in the cytosol, glucose is oxidized to pyruvate, producing both ATP and NADH. The pyruvate is subsequently transported into the matrix of the mitochondrion where it is further oxidized and converted to acetyl CoA, which is subsequently completely oxidized to CO₂ by the enzymes of the TCA cycle, generating ATP, NADH and FADH₂ in the process. Additional ATP is generated by the oxidation of NADH and FADH₂ by a respiratory electron transport chain that is located on the inner mitochondrial membrane. Oxidation of these substrates generates a proton gradient that represents potential energy that is conserved in the chemiosmotic generation of ATP (oxidative phosphorylation). In a number of species this is denoted as the cytochrome pathway as they also possess a second, alternative pathway of mitochondrial respiration.

1.3.3 Cytochrome Electron Transport Pathway

All eukaryotes possess a respiratory electron transport chain that is referred to as the cytochrome pathway (CP). This electron transport chain consists of four major protein complexes —Complex I (NADH dehydrogenase), Complex II (succinate dehydrogenase), Complex III (cytochrome bc₁) and Complex IV (cytochrome c oxidase) that are associated with the inner mitochondrial membrane and which facilitate the transfer of electrons from NADH or FADH₂ to molecular oxygen, reducing it to water (Figure 1.2). Electron flow along the CP is coupled to chemiosmotic ATP generation through the generation of a proton gradient, which is facilitated by proton pumping at three sites (Complex I, Complex III, and Complex IV) (Figure 1.2). This movement of positively charged protons from the matrix into the intermembrane space establishes an electrochemical gradient across the membrane. The gradient is dissipated by ATP synthase (Complex V) where the free energy released by the movement of protons back into the matrix is used to drive the formation of ATP (adenine triphosphate) from ADP (adenine diphosphate) and inorganic phosphate (Pi).

1.3.4 Alternative Pathway Respiration

In addition to the ubiquitous cytochrome pathway, plants and algae contain a second respiratory chain called the alternative pathway (AP) (For review see Vanlerberghe and McIntosh 1997). The AP branches from the cytochrome chain at ubiquinone and consists of a single protein, the alternative oxidase (AOX), which serves to transfer electrons from reduced ubiquinone directly to O₂ (Figure 1.2). AOX is a ~32-kDA interfacial membrane protein that contains a non-heme di-iron carboxylate active site and interacts with a single leaflet of the inner mitochondrial membrane (For review see Moore et al. 2013).

As shown in Figure 1.2, electron flow along the AP bypasses two of the three sites where electron transport is coupled to proton pumping into the intermembrane space. Because of this, AP respiration does not contribute to the trans-membrane pH gradient used to synthesize ATP by chemiosmosis. Besides being present in all plants and algae examined to date, the AP has more recently been shown to be present in protozoa, some fungi and in some lower animal phyla (McDonald and Vanlerberghe 2004).

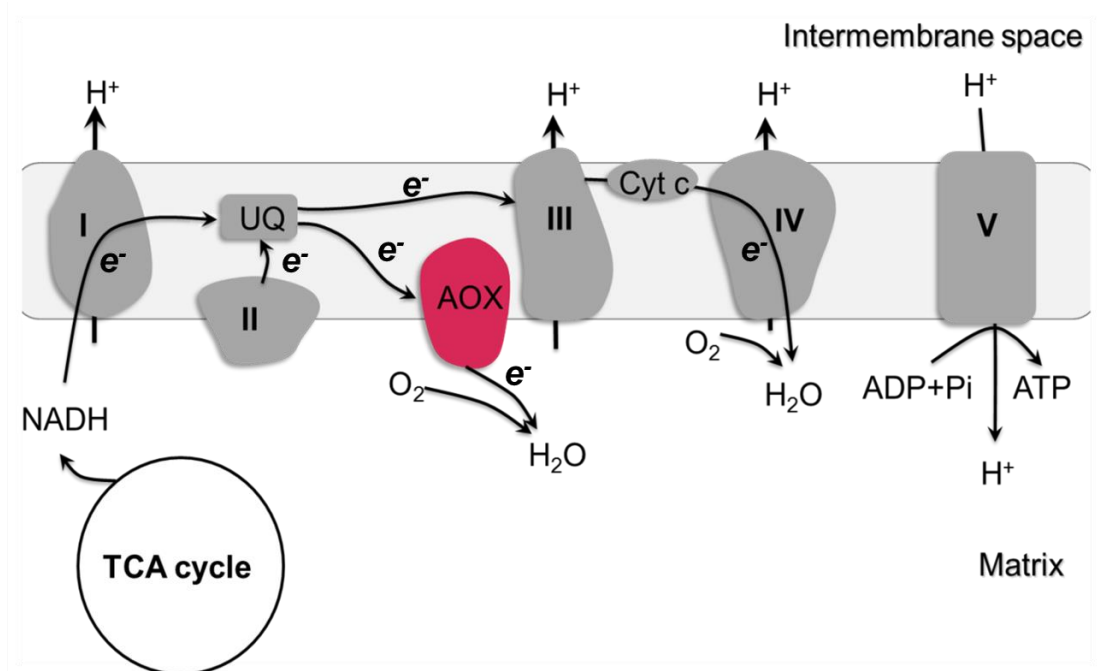


Figure 1.2 Mitochondrial Electron Transport Chain

Complex I – NADH dehydrogenase complex; Complex II- Succinate dehydrogenase; UQ- ubiquinone; AOX- Alternative oxidase; Complex III- Cytochrome bc_1 ; Cyt c- Cytochrome C; Complex IV- Cytochrome oxidase complex (COX); Complex V- ATP synthase complex.

1.4 The Physiological Function of Alternative Oxidase

Alternative oxidase has been shown to play an important role in pollination in certain families of angiosperms (for a review see Seymour 2001). For example, in species of the Araceae, including *Sauromattum guttatum* (skunk cabbage) and *S. venosum* (voodoo lily) high AP activity in the mitochondria of floral tissue cause thermogenesis resulting in high temperature within the flower that can exceed 45°C . These high temperatures have been shown to facilitate the volatilization of compounds critical for the attraction of insect pollinators (Elthon et al., 1989, Moore and Siedow 1991).

The role of AOX in non-thermogenic plants remains an active area of research. It has been suggested that the shunting of electrons through the AP allows for continued operation of glycolysis and the tricarboxylic acid cycle under conditions where the cytochrome pathway is impaired or otherwise restricted (Lambers 1982, Vanlerberghe 2013). By providing a second pathway of electron flow, AP respiration may also serve to prevent the over-reduction of electron transport components, particularly the ubiquinone pool, which would in turn reduce the formation of damaging reactive oxygen species (ROS). Using transgenic tobacco cells, Maxwell et al., (1999) showed that cells lacking AOX had increased mitochondrial-derived ROS formation and an up regulation of key genes such as catalase involved in antioxidant defense, when compared with wild-type cells.

AOX has been shown to be induced by a diverse array of stress conditions. This includes: pathogen attack (Cvetkovska and Vanlerberghe 2012), low oxygen (Clifton et al., 2005), nutrient limitation (Noguchi and Terashima 2006), salinity (Wang et al., 2010), metal toxicity (Tan et al., 2010), low temperature (Wang et al., 2011), high light and drought (Giraud et al., 2008, Yoshida et al., 2011, Zhang et al., 2012), and high CO₂ (Gandin et al., 2010). A common consequence of many of these stressors that increase AOX expression is that they also increase intracellular ROS. An increase in H₂O₂ levels, for example, have been shown to be a key secondary messenger in many responses of plants to stress and it has been proposed as a key intermediate in AOX signaling (Maxwell et al., 2002, Vanlerberghe 2013).

Several research studies in plants have investigated the role of AOX by employing molecular tools to alter AOX expression. Interestingly it was reported that the growth and development of plants was unaffected by altering the AOX expression levels under normal growth conditions. However, under drought (Giraud et al., 2008, Dahal et al., 2015), high light (Yoshida et al., 2011) and high CO₂ (Vishwakarma et al., 2015), AP respiration is shown to be essential in optimizing photosynthetic performance through its ability to manage the energy

imbalances in the metabolism. The role for AOX under such situations was explained as follows; stress conditions promote reductant generation through photosynthesis and mechanisms to dissipate excess reducing power while continuing to support ATP synthesis. Such mechanisms in the chloroplast can be continued without much interruption only if other cellular processes like respiratory NADH oxidation became less coupled to ATP synthesis. To achieve this, AP respiratory route in the mitochondrial respiration is increased to oxidize the excess carbon with lowered ATP synthesis and thereby manage the whole cell energy imbalance.

1.5 AOX and its Regulation in *Chlamydomonas reinhardtii*

In all species investigated to date AOX is encoded by a small family of nuclear genes. In plants, the individual members have been shown to be differentially regulated in a tissue or developmental stage-dependent manner (Finnegan et al., 1997). Earlier work in *Arabidopsis*, in which four AOX genes have been identified, has shown that these genes display different spatial patterns of expression (Saisho et al., 1997). Among the four AOX encoding genes, AOX1a and AOX1c are expressed in all organs of the plant. While AOX1b is expressed in flowers and buds, AOX2 was found to be upregulated in stem, rosette and roots (Saisho et al., 1997). Interestingly, in non-plant species, it seems that AOX is encoded by only a single gene. This is the case for *Trypanosoma brucei* (Chaudhri et al., 1998), *Hansenula anomala* (Sakajo et al., 1999), and *Aspergillus niger* (Kirimura et al., 1999). However, in the yeast, *Candida albicans* there are two AOX encoding genes found in its nuclear genome (Huh et al., 1999).

In *C. reinhardtii*, two nuclear genes have been identified that encode for AOX (Dinant et al., 2001), AOX1 and AOX2; both showing the greatest similarity to the single AOX gene of the fungus *Aspergillus niger* (Kirimura et al., 1999) although both AOX genes are clearly evolutionarily related to plant AOX genes. A common feature of the AOX protein in plants is that it is functional as a

homodimer (Umbach et al., 2006). The dimerization is facilitated by the presence of conserved cysteine residues that are conspicuous in all plant AOX protein sequences. Interestingly, AOX from *Chlamydomonas* and fungal species examined to date lack the regulatory features found in the plant enzyme, including the conserved cysteine residues. Because of this, it is assumed that in these species AOX is a functional monomer.

Comparison of the predicted protein sequences coded by AOX1 and AOX2 show that at the amino acid level they share 57.6 % identity (Dinant et al., 2001), and undoubtedly the two copies were the product of a gene duplication event. While the two genes share significant sequence similarity, their regulation seems quite distinct. Only AOX1 seems to be inducible; it is up regulated by a wide range of stress factors (cold stress, H₂O₂ treatment, antimycin A), and was strongly expressed in the dum15 strain, a mutant that lacks complex III electron transport activity (Dinant et al., 2001). Regardless of treatment, the expression of AOX2 remains almost imperceptible using RNA blot analysis (Molen et al., 2006, Dinant et al., 2001). However, more recent work has shown that AOX2 expression is upregulated when *C. reinhardtii* is exposed to copper and oxygen deprivation (Ostroukhova et al., 2016).

The transcriptional regulation of AOX1 in *C. reinhardtii* has been investigated through the use of a reporter gene; promoter regions of AOX1 were fused to the coding region of the gene coding aryl sulfatase (Davies et al., 1992), and aryl sulfatase activity is readily assayed in cells transformed with the reporter construct. Unlike plants, the reporter gene as well as AOX abundance and AP respiration were induced when *C. reinhardtii* cells were shifted from a medium containing ammonium to one containing nitrate (Molen et al., 2006, Baurain et al., 2003). Additional work by Molen et al., (2006) showed that transcriptional up regulation of AOX1 by antimycin A, H₂O₂ and cold stress requires one or more enhancers which are not found in the proximal promoter region of the gene that is responsible for nitrate-dependent induction. Overall, the work of Molen et al., (2006) suggests the existence of two distinct pathways regulating AOX1 in *C.*

reinhardtii – one in response to oxidative stress and second due to metabolic changes brought about by a shift in nitrogen source from ammonia to nitrate.

1.6 Nitrate Assimilation

Of all the inorganic molecules that *C. reinhardtii* needs to take up from the environment the requirement for nitrogen exceeds all other nutrients (Richmond and Grobbelaar 2007). The different forms of nitrogen in the environment include nitrate, ammonium and urea and amino acids. Among these, nitrate is the most common nitrogen form available in the aerobic soil for the growth of plants and algae (Giordano and Raven 2004).

While ammonium import into the cell is followed rapidly by its direct assimilation into amino acid biosynthesis, which occurs in the chloroplast, nitrate must first be reduced to ammonium through stepwise reduction to nitrite in the cytosol (using nitrate reductase) and to ammonia in the chloroplast (using nitrite reductase) (Hopkins and Hüner 2008) (Figure 1.3). The fundamental difference between ammonium and nitrate assimilation is the additional energy (ATP and reducing power) required for nitrate reduction. In the chloroplast stroma, nitrite reductase directly interacts with reduced ferredoxin, generated by electron transport, as the source of electrons to convert nitrite to ammonium (Figure 1.3). That nitrite reductase syphons off electrons from the acceptor side of PSI explains the stimulatory effect a shift into nitrate containing media has on the rate of photosynthesis. This has been shown in *C. reinhardtii* as well as a range of plant species (Bloom et al., 1989, Young and Beadall 2003).

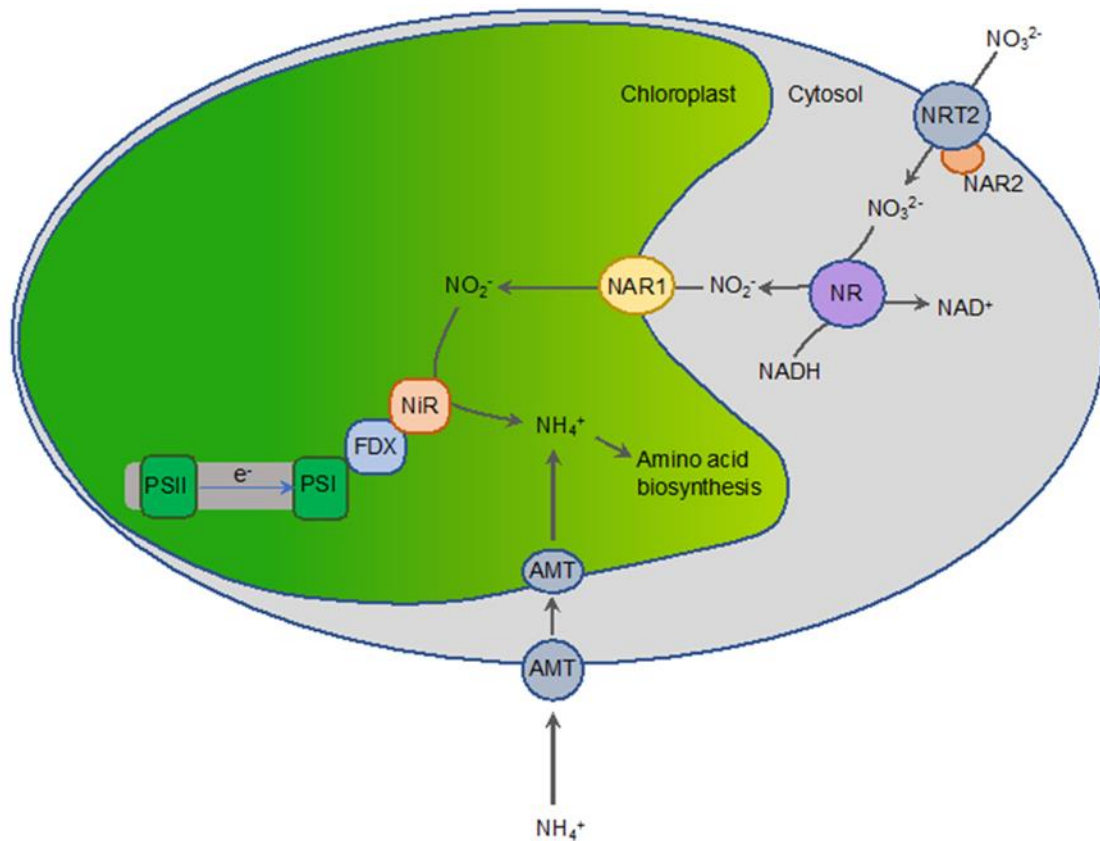


Figure 1.3 Diagram of *C. reinhardtii* cell showing the major steps of nitrate assimilation. Nitrate is imported by the NRT2-NAR2 transport complex localized in the plasma membrane of the cell. NRT2 is the transporter and NAR2, the accessory protein. In the cytosol, nitrate is reduced to nitrite by Nitrate reductase (NR) by consuming a NADH molecule and transported to the chloroplast by nitrite specific transporter protein, NAR1. In the chloroplast, nitrite is reduced to ammonium by accepting electrons from ferredoxin (FDX), a component of photosynthetic electron transport chain. The conversion of nitrite to ammonium is catalyzed by the enzyme nitrite reductase (NIR). In case of ammonium, it is transported via ammonium transporters (AMT) present in the cell and the chloroplast membrane.

1.7 Organization of nitrate assimilation related (NAR) genes

A complex network of genes and their encoded proteins (transporters and enzymes) define the nitrate assimilation pathway (Galvan and Fernandez 2001). To date, a total of five genes have been identified as being nitrate assimilation related (NAR). Primarily through mutant analysis, these genes have been shown to play essential roles in either nitrate transport or its reduction to ammonium (Galvan and Fernandez 2007). In *C. reinhardtii*, NAR genes are found localized in two distinct gene clusters within the nuclear genome and they exhibit coordinated regulation (Quesada et al., 1998); the genes are strongly induced by nitrate while being repressed by ammonium (Quesada and Fernandez 1994).

It was the early work by Quesada et al., (1998) that serendipitously identified AOX1 as being a member of the smaller of the two NAR clusters. Originally denoted as NAR5, AOX1 was positioned very close, but in opposite orientation to NRT2.3, which encodes a nitrite/nitrate transporter (Quesada et al., 1998). The regulation of many NAR genes including nitrate reductase, nitrite reductase, and nitrate/nitrite transporters is under transcriptional control by the regulator protein NIT2, which seems to exert overarching control of the entire nitrate assimilation pathway (Schnell and Lefebvre 1993, Fernandez et al., 1989, Quesada and Fernandez 1994, Quesada et al., 1998).

1.8 Thesis objectives

It has been hypothesized by Quesada et al. (2000) that increased AOX expression and AP respiration within the mitochondrion in response to nitrate may be triggered by changes in photosynthetic metabolism owing to the increased demand for cellular reductant (NADPH) and ATP by nitrate assimilation as compared to ammonium assimilation. While this hypothesis has not been directly tested it is based on a wealth of data from both plant and algal systems that have been published showing that respiratory metabolism

associated with the mitochondria and photosynthetic metabolism in the chloroplast do not occur in isolation, but rather that metabolic events in these two organelles are intimately connected by a range of metabolites (For review Foyer et al., 1998). These metabolites include NADH (NADPH), ATP and carbon compounds such as oxaloacetate and malate, which provide metabolic flexibility to energy metabolism.

In *C. reinhardtii*, Dang et al., (2014) showed that a photosynthetic mutant of *C. reinhardtii* deficient in ATP generation is supported by the ATP synthesized through CP respiration in the mitochondria. This was shown by the data that the mutant's growth was lowered only when CP respiration is blocked by the inhibitor antimycin A. Other research showed the compensatory role played by photosynthetic electron transport in a *C. reinhardtii* mutant defective in CP respiration (Cardol et al., 2003). It was shown that the lowered ATP synthesis in the mitochondria was compensated by increased ATP generation in the chloroplast by the stimulation of cyclic photosynthetic electron transport.

The overarching goal of my doctoral thesis was to provide a metabolic rationale for why AOX and alternative pathway respiration are induced in *C. reinhardtii* (hereafter, *Chlamydomonas*) when cells are grown in the presence of nitrate. The data provided by Baurain et al., (2003) and Molen et al., (2006) clearly show that AOX is strongly induced by nitrate and other work by Quesada et al (1998) show that AOX1 is a component of a NAR gene cluster, suggesting a possibility of co-regulation of these genes. Yet to date, the physiological and metabolic link between increased alternative pathway respiration and nitrate assimilation has not been directly addressed.

The specific objectives of my thesis are to address the following questions:

(1) Does AOX1 cluster with NAR genes in other green algal species?

While AOX1 is shown to belong to a NAR cluster in *Chlamydomonas*, it is unknown if this clustering is found in other species of green algae. A

bioinformatics approach will be employed to address this question taking advantage of the algal genome sequencing projects that have been carried out over the past few years. Using annotated genome information, the position of AOX genes relative to known NAR genes will be used to determine the extent of clustering.

(2) Characterize the consequences of knocking down AOX expression on overall cell growth and physiology.

It is hypothesized that knocking down AOX expression will have little effect on cell growth and physiology when cells are grown in ammonium as the sole nitrogen source. Under these conditions the expression of AOX has been shown to be very low (Molen et al. 2006). However, it is hypothesized that compared to wild-type (WT) cells, AOX knockdown cells will display significant decreases in growth, respiration and photosynthesis when cultured in the presence of nitrate. Such findings would indicate a critical role played by AOX in the ability of *Chlamydomonas* to assimilate nitrate.

(3) Compared to wild-type cells, how are AOX knockdown cells metabolically distinct?

Previous studies in *Arabidopsis* showed that plants lacking AOX displayed altered carbon/nitrogen balance and decreased photosynthetic efficiency (Giraud et al., 2008; Yoshida et al., 2011) compared to wild-type plants when exposed to environmental stresses. It is hypothesized that knocking down AOX in *Chlamydomonas* will result in a remodeling of overall cell metabolism. Compared to wild-type cells, it is hypothesized that knockdown cells will display clear metabolome differences when grown in either ammonium or nitrate. Changes in the metabolites associated with photosynthesis, carbon metabolism and nitrogen metabolism will be assessed using whole cell metabolomics analysis using gas-chromatography mass spectrometry (GC-MS).

1.9 References

- Baurain D, Dinant M, Coosemans N, Matagne RF (2003) Regulation of the Alternative Oxidase Aox1 Gene in *Chlamydomonas reinhardtii*. Role of the Nitrogen Source on the Expression of a Reporter Gene under the Control of the Aox1 Promoter. *Plant Physiol* 131: 1418–1430
- Bloom AJ, Caldwell RM, Finazzo J, Warner RL, Weissbart J (1989) Oxygen and Carbon Dioxide Fluxes from Barley Shoots Depend on Nitrate Assimilation. *Plant Physiol* 91: 352–356
- Cerutti H, Ma X, Msanne J, Repas T (2011) RNA-Mediated Silencing in Algae: Biological Roles and Tools for Analysis of Gene Function. *Eukaryotic Cell* 10: 1164–1172
- Chaudhuri M, Ajayi W, Hill GC (1998) Biochemical and molecular properties of the *Trypanosoma brucei* alternative oxidase. *Molecular and Biochemical Parasitology* 95: 53–68
- Clifton R, Lister R, Parker KL, Sappl PG, Elhafez D, Millar AH, Day DA, Whelan J (2005) Stress-induced co-expression of alternative respiratory chain components in *Arabidopsis thaliana*. *Plant Mol Biol* 58: 193
- Cvetkovska M, Vanlerberghe GC (2012) Coordination of a mitochondrial superoxide burst during the hypersensitive response to bacterial pathogen in *Nicotiana tabacum*. *Plant, Cell & Environment* 35: 1121–1136
- Dahal K, Martyn GD, Vanlerberghe GC (2015) Improved photosynthetic performance during severe drought in *Nicotiana tabacum* overexpressing a nonenergy conserving respiratory electron sink. *New Phytol* 208: 382–395
- Danegard PA (1888) Recherches sur les algues inferieures. *Ann.Sci.Nat.*, 7th series., Bot. 4: 105-275
- Davies JP, Weeks DP, Grossman AR (1992) Expression of the arylsulfatase gene from the beta 2-tubulin promoter in *Chlamydomonas reinhardtii*. *Nucleic Acids Res* 20: 2959–2965
- Dent RM, Haglund CM, Chin BL, Kobayashi MC, Niyogi KK (2005) Functional Genomics of Eukaryotic Photosynthesis Using Insertional Mutagenesis of *Chlamydomonas reinhardtii*. *Plant Physiol* 137: 545–556
- Dinant M, Baurain D, Coosemans N, Joris B, Matagne RF (2001) Characterization of two genes encoding the mitochondrial alternative oxidase in *Chlamydomonas reinhardtii*. *Curr Genet* 39: 101–108
- Dolhi JM, Maxwell DP, Morgan-Kiss RM (2013) Review: the Antarctic *Chlamydomonas raudensis*: an emerging model for cold adaptation of

photosynthesis. *Extremophiles* 17: 711–722

Elthon TE, Nickels RL, McIntosh L (1989) Mitochondrial events during development of thermogenesis in *Sauromatum guttatum* (Schott). *Planta* 180: 82–89

Fernandez E, Galvan A (2007) Inorganic nitrogen assimilation in *Chlamydomonas*. *J Exp Bot* 58: 2279–2287

Fernández E, Schnell R, Ranum LP, Hussey SC, Silflow CD, Lefebvre PA (1989) Isolation and characterization of the nitrate reductase structural gene of *Chlamydomonas reinhardtii*. *PNAS* 86: 6449–6453

Finnegan PM, Whelan J, Millar AH, Zhang Q, Smith MK, Wiskich JT, Day DA (1997) Differential Expression of the Multigene Family Encoding the Soybean Mitochondrial Alternative Oxidase. *Plant Physiol* 114: 455–466

Foyer C, Noctor G, Hodges M (2011) Respiration and Nitrogen metabolism. *J Exp Bot* 62(4): 1467–1482

Galván A, Fernández E (2001) Eukaryotic nitrate and nitrite transporters. *CMLS, Cell Mol Life Sci* 58: 225–233

Gandin A, Duffes C, Day DA, Cousins AB (2012) The absence of alternative oxidase AOX1A results in altered response of photosynthetic carbon assimilation to increasing CO₂ in *Arabidopsis thaliana*. *Plant Cell Physiol* 53: 1627–1637

Giraud E, Ho LHM, Clifton R, Carroll A, Estavillo G, Tan Y-F, Howell KA, Ivanova A, Pogson BJ, Millar AH, et al (2008) The Absence of ALTERNATIVE OXIDASE1a in *Arabidopsis* Results in Acute Sensitivity to Combined Light and Drought Stress. *Plant Physiol* 147: 595–610

González-Ballester D, Montaigu A de, Higuera JJ, Galván A, Fernández E (2005) Functional Genomics of the Regulation of the Nitrate Assimilation Pathway in *Chlamydomonas*. *Plant Physiol* 137: 522–533

Grossman AR, Karpowicz SJ, Heinnickel M, Dewez D, Hamel B, Dent R, Niyogi KK, Johnson X, Alric J, Wollman F-A, et al (2010) Phylogenomic analysis of the *Chlamydomonas* genome unmask proteins potentially involved in photosynthetic function and regulation. *Photosynth Res* 106: 3–17

Harris E (2009). *The Chlamydomonas sourcebook*, 2nd Edition, Elsevier

Hopkins and Huner (2008). *Introduction to Plant Physiology*. 4th edition, John Wiley and sons Inc. New York.

Huh W-K, Kang S-O (1999) Molecular Cloning and Functional Expression of Alternative Oxidase from *Candida albicans*. *J Bacteriol* 181: 4098–4102

- Kirimura K, Yoda M, Usami S (1999) Cloning and expression of the cDNA encoding an alternative oxidase gene from *Aspergillus niger* WU-2223L. *Curr Genet* 34: 472–477
- Kromer S (1995) Respiration during photosynthesis. *Ann Rev Plant Physiol Plant Mol Bio* 46:45-47
- Lambers H (1982) Cyanide-resistant respiration: A non-phosphorylating electron transport pathway acting as an energy overflow. *Physiologia Plantarum* 55: 478–485
- Leliaert F, Smith DR, Moreau H, Herron MD, Verbruggen H, Delwiche CF, Clerck OD (2012) Phylogeny and Molecular Evolution of the Green Algae. *Critical Reviews in Plant Sciences* 31: 1–46
- Maxwell DP, Nickels R, McIntosh L (2002) Evidence of mitochondrial involvement in the transduction of signals required for the induction of genes associated with pathogen attack and senescence. *The Plant Journal* 29: 269–279
- Maxwell DP, Wang Y, McIntosh L (1999) The alternative oxidase lowers mitochondrial reactive oxygen production in plant cells. *PNAS* 96: 8271–8276
- McCarthy SS, Kobayashi MC, Niyogi KK (2004) White Mutants of *Chlamydomonas reinhardtii* Are Defective in Phytoene Synthase. *Genetics* 168: 1249–1257
- McDonald AE, Vanlerberghe GC (2004) Branched Mitochondrial Electron Transport in the Animalia: Presence of Alternative Oxidase in Several Animal Phyla. *IUBMB Life* 56: 333–341
- Merchant SS, Prochnik SE, Vallon O, Harris EH, Karpowicz SJ, Witman GB, Terry A, Salamov A, Fritz-Laylin LK, Maréchal-Drouard L, et al (2007) The *Chlamydomonas* Genome Reveals the Evolution of Key Animal and Plant Functions. *Science* 318: 245–250
- Molen TA, Rosso D, Piercy S, Maxwell DP (2006a) Characterization of the alternative oxidase of *Chlamydomonas reinhardtii* in response to oxidative stress and a shift in nitrogen source. *Physiologia Plantarum* 127: 74–86
- Moore AL, Siedow JN (1991) The regulation and nature of the cyanide-resistant alternative oxidase of plant mitochondria. *Biochimica et Biophysica Acta (BBA) - Bioenergetics* 1059: 121–140
- Moore AL, Shiba T, Young L, Harada S, Kita K, Ito K (2013) *Annu Rev Plant Bio* 64:637-663.

- Noguchi K, Terashima I (2006) Responses of spinach leaf mitochondria to low N availability. *Plant, Cell & Environment* 29: 710–719
- Nunes-Nesi A, Sulpice R, Gibon Y, Fernie A (2008) The enigmatic contribution of mitochondrial function in photosynthesis. *J Exp Bot* 59(7):1675-1684
- Ostroukhova M, Zalutskaya Z, Ermilova E (2017) New insights into AOX2 transcriptional regulation in *Chlamydomonas reinhardtii*. *European Journal of Protistology* 58: 1–8
- Pakkiriswami S, Beall BFN, Maxwell DP (2009) On the role of photosynthesis in the nitrate-dependent induction of the alternative oxidase in *Chlamydomonas reinhardtii*. *Botany* 87: 363–374
- Quesada A, Fernández E (1994) Expression of nitrate assimilation related genes in *Chlamydomonas reinhardtii*. *Plant Mol Biol* 24: 185–194
- Quesada A, Galvan A, Fernandez E (1994) Identification of nitrate transporter genes in *Chlamydomonas reinhardtii*. *The Plant Journal* 5: 407–419
- Quesada A, Gómez-García I, Fernández E (2000) Involvement of chloroplast and mitochondria redox valves in nitrate assimilation. *Trends in Plant Science* 5: 463–464
- Quesada A, Hidalgo J, Fernández E (1998) Three Nrt2 genes are differentially regulated in *Chlamydomonas reinhardtii*. *Mol Gen Genet* 258: 373–377
- Richmond A and Grobbelaar JU (2007). *Handbook of Microalgal Culture*, First Edition, Blackwell Publishing Ltd.
- Saisho D, Nambara E, Naito S, Tsutsumi N, Hirai A, Nakazono M (1997) Characterization of the gene family for alternative oxidase from *Arabidopsis thaliana*. *Plant Mol Biol* 35: 585–596
- Schnell RA, Lefebvre PA (1993) Isolation of the *Chlamydomonas* regulatory gene NIT2 by transposon tagging. *Genetics* 134: 737–747
- Seymour S (2001) Biophysics and Physiology of temperature regulation in thermogenic flowers. *Bio Sci Rep* 21(2):223-236.
- Shigeru Sakajo, Nabuko Minagawa, Tadazumi Komiyama, Akio Yoshimoto (1991) Molecular cloning of cDNA for antimycin A-inducible mRNA and its role in cyanide-resistant respiration in *Hansenula anomala*. *Biochimica et Biophysica Acta (BBA) - Gene Structure and Expression* 1090: 102–108
- Spreitzer RJ, Mets L (1981) Photosynthesis-deficient Mutants of *Chlamydomonas reinhardtii* with Associated Light-sensitive Phenotypes. *Plant Physiol* 67: 565–569

Tan Y-F, O'Toole N, Taylor NL, Millar AH (2010) Divalent Metal Ions in Plant Mitochondria and Their Role in Interactions with Proteins and Oxidative Stress-Induced Damage to Respiratory Function. *Plant Physiol* 152: 747–761

Umbach AL, Fiorani F, Siedow JN (2005) Characterization of Transformed Arabidopsis with Altered Alternative Oxidase Levels and Analysis of Effects on Reactive Oxygen Species in Tissue. *Plant Physiol* 139: 1806–1820

Umbach AL, Ng VS, Siedow JN (2006) Regulation of plant alternative oxidase activity: A tale of two cysteines. *Biochimica et Biophysica Acta (BBA) - Bioenergetics* 1757: 135–142

Vanlerberghe GC (2013) Alternative Oxidase: A Mitochondrial Respiratory Pathway to Maintain Metabolic and Signaling Homeostasis during Abiotic and Biotic Stress in Plants. *International Journal of Molecular Sciences* 14: 6805–6847

Vanlerberghe GC, McIntosh L (1994) Mitochondrial Electron Transport Regulation of Nuclear Gene Expression (Studies with the Alternative Oxidase Gene of Tobacco). *Plant Physiol* 105: 867–874

Vanlerberghe GC, McIntosh L (1997) ALTERNATIVE OXIDASE: From Gene to Function. *Annual Review of Plant Physiology and Plant Molecular Biology* 48: 703–734

Vishwakarma A, Tetali SD, Selinski J, Scheibe R, Padmasree K (2015) Importance of the alternative oxidase (AOX) pathway in regulating cellular redox and ROS homeostasis to optimize photosynthesis during restriction of the cytochrome oxidase pathway in *Arabidopsis thaliana*. *Ann Bot* 116: 555–569

Wang H, Liang X, Huang J, Zhang D, Lu H, Liu Z, Bi Y (2010) Involvement of Ethylene and Hydrogen Peroxide in Induction of Alternative Respiratory Pathway in Salt-Treated *Arabidopsis* Calluses. *Plant Cell Physiol* 51: 1754–1765

Wang J, Rajakulendran N, Amirsadeghi S, Vanlerberghe GC (2011) Impact of mitochondrial alternative oxidase expression on the response of *Nicotiana tabacum* to cold temperature. *Physiologia Plantarum* 142: 339–351

Williams WE, Gorton HL, Vogelmann TC (2003) Surface gas-exchange processes of snow algae. *PNAS* 100: 562–566

Yoshida K, Watanabe CK, Terashima I, Noguchi K (2011) Physiological impact of mitochondrial alternative oxidase on photosynthesis and growth in *Arabidopsis thaliana*. *Plant, Cell & Environment* 34: 1890–1899

Young EB, Beardall J (2003) Rapid ammonium- and nitrate-induced

perturbations to chl a fluorescence in nitrogen-stressed *Dunaliella tertiolecta* (Chlorophyta). *J Phycol* 39: 332–342

Zhang L-T, Zhang Z-S, Gao H-Y, Meng X-L, Yang C, Liu J-G, Meng Q-W (2012) The mitochondrial alternative oxidase pathway protects the photosynthetic apparatus against photodamage in *Rumex K-1* leaves. *BMC Plant Biology* 12: 40

Chapter 2

2 Nitrate assimilation related (NAR) gene cluster distribution and organization in green algal species

2.1 Introduction

The location of genes in a genome is no longer considered to be random. In prokaryotes, the genes that participate in many metabolic pathways are physically linked and organized in a specific manner termed an operon (Jacob and Monod 1961, Rocha 2008). The widely studied lac operon contains regulator as well as structural genes that are coordinately regulated; genes of the operon are repressed by glucose and induced by lactose under carbon starvation (Jacob and Monod 1961). A single promoter activates the transcription of the operon genes, which are expressed as a polycistronic mRNA allowing for the tight coupling of transcription and translation. Many operons in bacteria have been shown to be involved in nutrient (carbon and nitrogen source) utilization (Luque-Almagro et al., 2011) and secondary metabolite synthesis (Garcia et al., 2009).

Compared to bacteria, gene clusters are not a common feature of eukaryotes, but they have been found in organisms as diverse as fungi and mammals. Some of the most well studied examples of gene clusters in eukaryotes include the homeobox (HOX) gene cluster for embryonic patterning and the beta-globin gene loci for hemoglobin synthesis in animals, and in plants the leucine-rich repeat genes associated with disease resistance (For review see Hurst et al., 2004).

A common feature of some gene clusters is that member genes are evolutionarily related, having arisen by gene duplication followed by structural and functional divergence (Chu et al., 2011). Unlike genes that share a common ancestor, functionally related non-homologous genes are usually dispersed randomly throughout the genome with coordination of expression

being exercised by a transcription factor. However, with the increasing availability of large amount of genome data, functional clusters containing non-homologous genes in eukaryotic genomes have been identified and are beginning to be well characterized (Hoffmeister and Keller 2007, Chu et al., 2011). Evidence to date indicates that genes in these clusters most often participate in a single metabolic pathway and do not share sequence similarity (they are non-homologous genes). These gene clusters in eukaryotes are considered equivalent to bacterial operons except that each gene in the cluster is regulated by its own promoter and produces a monocistronic transcript.

Evidence suggests that the clustering of genes in eukaryotes seems to have evolved related to specific challenges: to support organism growth and survival under changing environmental conditions (Reviewed in Chu et al., 2010), exploitation of new environment (Wong and Wolfe 2004), or for the management of interactions with other organisms (Horton et al., 2004). Common examples that support this claim include the DAL gene cluster of yeast, which is involved in allantoin utilization (Wong and Wolfe 2004) and the GAL gene cluster of yeasts and fungi, which is critical for galactose assimilation (Slot and Rokas, 2010).

The DAL gene cluster, which contains six genes, is found in *Saccharomyces cerevisiae* and its close relatives including *S. castellii*. Collectively, the six genes are involved in the import and catabolism of the nitrogen source allantoin, a product of purine degradation. Interestingly, there is no DAL cluster in any of the more distantly related hemi-ascomycete yeast species, yet homologs of each of the six DAL genes are found scattered throughout their genomes. Research has shown that the clustering of DAL genes occurred on a single branch of the yeast phylogenetic tree and coincided with a biochemical reorganization of the purine degradation pathway (Wong and Wolfe 2004). Species lacking the DAL cluster rely on the classical purine degradation pathway including the products of two genes, urate permease

(UAP) and urate oxidase (UOX) that are involved in the transport and oxidation of urea.

The development of the DAL cluster seems to have been adaptive, driven by selection for the ability to grow in low oxygen environments (Wonga and Wolfe 2004). Species with the DAL cluster lack urate oxidase, which requires molecular oxygen as a substrate. Development of the DAL cluster, and other adaptations, including the loss of other oxygen-requiring enzymes, led *S. cerevisiae* and related species the ability to grow vigorously under anaerobic conditions by fermentation (Wonga and Wolfe, 2004).

Other adaptive gene clusters include major histocompatibility (MHC) complex loci of animals (Horton et al., 2004) required for innate and adaptive immunity and secondary metabolite gene clusters in filamentous fungi (Hoffmeister and Keller 2007). Various secondary metabolite clusters identified in fungi have antibiotic properties to suppress the growth of competing organisms in the environment and some clusters of fungi synthesize toxins for the colonization of plant and animal hosts (eg., Aflatoxin gene cluster in *Aspergillus flavus*) (Turgeon and Bushley 2010). Very recently, several secondary metabolite gene clusters were identified in plants involved in the synthesis of chemical defense compounds (Nützmann and Osbourn 2014).

So why are genes for certain metabolic pathways clustered whereas genes for other pathways remain unclustered? According to the co-regulation model, first proposed by Jacob and colleagues (Jacob et al., 1960), it would be easier to regulate all genes of a pathway if they were proximate to each other. An often-cited condition under which coregulation would be particularly important occurs when metabolic intermediates are potentially deleterious (Hurst et al., 2004). Under such conditions it would be critical to regulate the expression of all enzymes in a pathway so that toxic intermediates do not accumulate.

The major benefit associated with proximal arrangement of genes in the cluster may be related to coordinate regulation (Sproul et al., (2005), Chu et al., (2011), Takos and Rook 2012). Locating genes adjacent to each other allows the genome to have an additional tier of regulatory control. For example, a long distance cis element can be placed near the gene cluster or a chromatin level modification can be added specific to the cluster (Sproul et al., 2005, Nuttmann and Osbourn 2014, Nuttmann and Osbourn 2015). A report on operon-like secondary metabolite gene clusters in plants illustrated the significance of forming gene clusters especially in sub-telomeric region of chromosomes (Field et al., 2011) where there is less heterochromatin formation. These regions tend to be particularly active in chromosomal rearrangement, which would facilitate gene clustering.

In contrast to the co-regulation model, an alternative hypothesis referred to as the selfish cluster model (referred to as the selfish operon model in bacteria) posits that clustering was originally only beneficial to the member genes themselves and not the host organism (Lawrence and Roth, 1996). The advantage to the member genes of being organized into a cluster is that they can be readily propagated and spread by horizontal as well as vertical transmission. Unlike vertical transmission, there are clearly delineated constraints that limit the size of DNA that can be moved by horizontal gene transfer processes (Walton 2000). The selfish cluster model thus suggests that the gene cluster is a promiscuous package of DNA that is essential for related genes (members of a single pathway) to be propagated by horizontal transfer mechanisms. If the formation and maintenance of a particular gene set is expected to be beneficial, then this may lead natural selection to favor decreased recombination to reduce the distance between the pathway genes (Nei 1967). For example, if the metabolic genes involved in a pathway are located at random in the genome, chances of becoming functionally weak due to mutation pressure or getting deleted by genetic drift in the absence of selection is possible (Lawrence and Roth 1996). Additionally, Slot and Rokas (2010) reported that the GAL gene cluster of fungi contains features of both

coregulation and selfish cluster (operon) model. Under this hybrid model, the GAL gene cluster, once formed in the fungi by positive selection for coordinate regulation, was more likely to be propagated to other lineages by horizontal gene transfer.

In the green alga *Chlamydomonas*, nitrate assimilation related (NAR) genes are found in two clusters of the nuclear genome (Quesada et al., 1998). One of these clusters designated NAR Cluster I (Figure 2.1A) spans 37.5 kbp of genomic DNA and encodes the following seven genes: NADH dependent nitrate reductase (NIA1); ferredoxin-dependent nitrite reductase (NII1); high affinity nitrate transporters (NRT2.1) and (NRT2.2); formate/nitrite transporter (NAR1.1); nitrate high affinity transporter accessory protein (NAR2) and a chloroplastic malate dehydrogenase (MDH5).

NAR Cluster II is about 10 kbp in size and codes for a high affinity nitrate transporter (NRT2.3) and the mitochondrial alternative oxidase (AOX1) (Figure 2.1B) (Quesada et al., 1998). These two genes are found to be positioned in opposite orientation to each other while being separated by a 1.4 kbp intergenic region.

A common characteristic of all NAR genes in both clusters is that they are strongly induced by nitrate and repressed by ammonium (Quesada et al., 1998). The protein NIT2 is considered as a central regulatory component essential for nitrate signaling in *Chlamydomonas*. It activates the transcription of all NAR genes and requires the presence of nitrate for its function (Camargo et al., 2007). The predicted NIT2 protein sequence contains domains typically found in the transcriptional activators and coactivators of major signaling pathways (Camargo et al., 2007).

While the genes involved in nitrate assimilation are clustered in *Chlamydomonas*, interestingly this seems not to be the case in plants. For example, in *Arabidopsis* genes required for nitrate transport and assimilation are distributed randomly throughout the genome (Orsel et al., 2002). This

then leads to the obvious question: how widespread is the NAR gene cluster? Is it found only in *Chlamydomonas* or do other algal species possess the cluster as well? Furthermore, if some species have the cluster and others don't, can this be explained by differences in the nitrogen sources common in the habitat occupied by specific species? The goal of this chapter is to address these questions by taking advantage of the wealth of genome sequence information that has become available over the past few years.

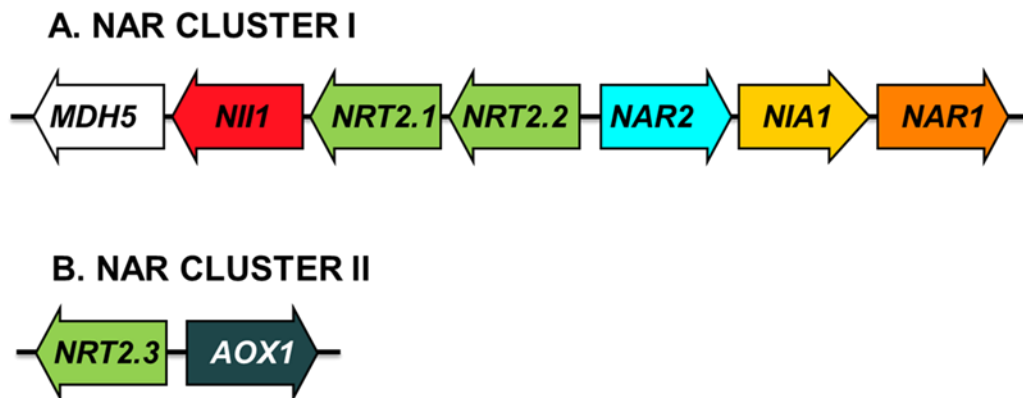


Figure 2.1 Nitrate assimilation related (NAR) Cluster I (A) and Cluster II (B).

A. NAR Cluster I: NIA1- Nitrate reductase, NII1- ferredoxin dependent Nitrite reductase, NRT2.1&2.2 – high affinity nitrate/nitrite transporter, NAR2- nitrate transporter accessory protein, NAR1- Nitrite transporter, MDH5 – Chloroplastic Malate dehydrogenase. B. NAR Cluster II: NRT2.3 high affinity nitrate transporter, AOX1- mitochondrial alternative oxidase. The organization of Cluster I and II shown here is originally reported by Quesada et al., (1998).

2.2 Material and Methods

2.2.1 Algal NAR Cluster I and II identification

The distribution of NAR Cluster I and II in different green algal genomes was determined by searching the NCBI (www.ncbi.nlm.nih.gov/genome) and Phytozome (www.phytozome.org) genome databases. Using the *Chlamydomonas* NAR protein sequences as query, synteny searches were performed by utilizing the NCBI protein blast program to retrieve the homologous NAR gene clusters in the ten-available green algal genomes (Figure 2. 3). Specifically, to identify the NAR Cluster in different algal species, *Chlamydomonas* nitrate reductase gene was used as a query to obtain the list of other algal species that contains nitrate reductase. Then each blast hit of corresponding algal species obtained as HTML link was chosen and followed. The link has provided the chromosomal map (graphical) of the nitrate reductase gene in the corresponding algal species. Then in the map, manual search was done to locate the other NAR genes present in the upstream or downstream region of the nitrate reductase gene. Likewise, the presence of AOX1 and NRT2.3 physical association in the genomes of other algal species was also searched and identified.

2.2.2 Phylogenetic analysis

To construct a phylogenetic tree of NAR genes (NIA1, NII1, NRT2, NAR1.1), protein sequences of the respective genes from different organisms were retrieved from NCBI. The algorithm MEGA 6.0 platform (Tamura et al., 2013) was used to generate the phylogenetic trees of NAR protein sequences. The downloaded protein sequences from NCBI databases were aligned with the MUSCLE program in MEGA 6.0 and the aligned sequences were later used to construct the phylogenetic tree using the maximum-likelihood method. The stability of internal nodes was assessed by bootstrap analysis with 100 replicates. The protein blast hits retrieved with the expected threshold value higher than e^{-70} were selected and used for sequence alignment. The

bacterial close relatives of NAR genes were obtained by blasting the *Chlamydomonas* NAR genes (as query) selectively against all bacterial genomes in the NCBI genome database.

2.2.3 RNA isolation, semi-quantitative polymerase chain reaction and gel blot analysis

For RNA isolation, 40 mL of cells harvested by centrifugation in 50 ml disposable centrifuge tubes was immediately frozen in liquid nitrogen and stored at -80°C. RNA was extracted using a modified hot phenol method described by Molen et al., 2006.

One mL of a hot (80°C) phenol/extraction buffer (P/EB) solution was added to the 40 mL of frozen pellet collected by centrifugation. The P/EB extraction reagent consisted of one-part buffered phenol (pH 6.8) and one-part extraction buffer (1 M LiCl, 10 methylenediaminetetraacetic acid (EDTA), 1% SDS, 0.1 M Tris pH 8.0). Before vortexing the cells with the extraction reagent, (v/v) betamercaptoethanol and 4% (w/v) polyvinylpyrrolidone was added to the mixture. Then 0.5 mL of 24:1 (v/v) chloroform: isoamyl alcohol was added and vortexed for one minute. Immediately after, mixture was transferred to a microfuge and centrifuged at 16 000 *g* for 10 min at room temperature to collect the supernatant. The aqueous phase collected was used to selectively precipitate RNA by the addition of 1 vol. of 4 M LiCl. Then the whole mixture was stored at -20°C for at least 2 h, RNA was pelleted at 16 000 *g* for 10 min at room temperature. For final purification, the RNA pellet was dissolved in 400 µl of diethyl pyrocarbonate (DEPC)-treated water and precipitated using standard ethanol precipitation. The precipitated RNA was centrifuged to remove the supernatant and air dried to quantify using spectrometry.

For semi-quantitative PCR, 1 µg RNA was treated with DNase (dexoxyribonuclease, Promega) to remove contaminating genomic DNA. To prepare cDNA from 1 µg of RNA, 1 µl Oligo (dT) (500 µg/ml) and 1 µL 10 mM

dNTP mix was added. Then the mixture was heated at 65°C for 5 min and snap cooled on ice followed by short spin. To the cooled mixture, 4 µL 5X first strand buffer, 2 µL 0.1 M DTT and 1 µL RNase-OUT (Recombinant ribonuclease inhibitor (40 units/ µL) was added and incubated at 42°C for 2 min. One µL of Superscript II Reverse transcriptase was added and the incubation was continued at 42°C for 50 mins. Finally, the mixture is incubated at 70°C for 15 mins. PCR reaction of 35 cycles was performed with the following reaction conditions: 5 µL 10x PCR buffer (200 mM Tris-HCl (pH 8.4) 500 mM KCl), 1 µL 50 mM MgCl₂, 1 µL 10 mM dNTP mix, 1 µL gene specific forward primer (10 µM), 1 µL gene specific reverse primer (10 µM), 0.4 µL Taq DNA polymerase (5 U/ µL) (Invitrogen), 2 µL cDNA.

For gel blot analysis, samples of total RNA (25 µg) were separated on agarose gels and transferred to Hybond-N membrane (GE Healthcare). Northern hybridization was performed at 65°C in Church buffer using the gene specific probes (Molen et al., 2006). Using the High Prime Kit (Roche Applied Science) probes were labelled with dCT³²P. After hybridization, blots were washed at high stringency solution (0.1% SDS/0.1 X SSC, 65°C) and exposed to X-ray film. Using cDNA as the template, the gene specific probes for AOX1 and NRT2.3 are generated with the following forward and reverse primers: AOX1-Forward Primer- CCTAGGCACGGCAGTATGAC, AOX1-Reverse Primer- CATTACACTTTTCTCCAGACA, NRT2.3 –Forward Primer- GAATGTCTA CAGGCGTCGACTACTTG, NRT2.3-Reverse Primer- CTGGTAGATGAGC GGCATGATGAAGT.

2.2.4 Isolation and cloning of 1.4 kbp intergenic fragment of AOX1 and NRT2.3 gene

Using the bacterial artificial chromosome (BAC) clone 10N7 as template DNA (Molen et al., 2006), a 1402 bp fragment extending between the start codons of AOX1 and NRT2.3 was amplified using Pfu Turbo DNA polymerase (Stratagene, CA). The primers (forward primer-GGTACCTCTTGCGCGTCTCGCTACAAG, reverse primer-GGTACCGTAACGTTGAGTTCTTGGGTAAGTG) designed with

the KPN1 restriction enzyme site was used to amplify the intergenic DNA fragment. Initially, the fragment was cloned into pGEM-T (Promega) and sequenced for verification. Then the fragment was sub cloned into the plasmid pJD54 (Davies et al., 1992) which contains the coding region of the aryl sulfatase (ARS2) reporter gene. A unique KPN1 restriction site present upstream of the reporter gene was used to insert the 1.4 kbp fragment in the pJD vector. The resulting plasmids contained the intergenic DNA fragment in either orientation upstream of the ARS2 gene.

2.2.5 Transformation of Chlamydomonas cells

The *Chlamydomonas reinhardtii* strain, CC 4351 (cw15, arg⁻, mt⁺) is a cell wall less and an auxotroph of the amino acid arginine. This strain is co transformed with pARG7.8 (contains arginosuccinate lyase gene, ARG7) and the plasmid containing the ARS reporter gene driven by the 1.4 kbp upstream sequences of AOX1 or the plasmid containing the ARS reporter gene driven by 1.4 kbp upstream sequences of NRT2.3 using the glass bead method described by Kindle (1990). The transformation was performed in a 15mL polypropylene tube containing 0.6 ml of cells, 0.2 ml of 20% (w/v) polyethylene glycol 8000, 0.6 g of acid-washed 0.5 mm glass beads, 6 µg pAOX1.4 or pNRT1.4 and 3 µg pARG7.8. The mixture was vortexed twice for 15 s followed by 15 s stop. Then the entire cell suspension was immediately spread onto TAP-nitrate plates containing the arylsulfatase substrate 5-bromo-4-chloro-indolylsulfate (X-SO₄). After 15 days, colonies that appeared blue were selected as positive transformants.

2.2.6 ARS reporter gene assay

For the ARS assay, 1 mL of cells were collected and immediately stored at -20°C. Thawed samples were centrifuged at 16000 rpm for 5 mins and the supernatant was used to measure the ARS activity according to Ohresser et al., (1997). The reaction mixture of 500 µL contained 400 µL supernatant, 0.4 M glycine-NaOH, pH 9.0, 10 mM imidazole and 0.8 mM α-naphthylsulfate was

incubated at 37°C for 1 h. After incubation, the reaction was stopped by adding 500 µL of 4% SDS in 0.2 M sodium acetate buffer (pH 4.8) and 100 µl of 10 mg/mL tetrazotized-o-dianisidine (fast Blue, Sigma). ARS activity was measured immediately at 540 nm and calculated by dividing the A₅₄₀ value by the culture turbidity at 750 nm (Kucho et al., 2003).

2.3 Results

2.3.1 Distribution of NAR Cluster I in Algae

As shown in Figure 2.2, in *Chlamydomonas* the seven genes that are found in NAR Cluster I exhibit coordinate regulation: they are all repressed by ammonium displaying undetectable levels of transcript abundance and are rapidly induced within thirty minutes after a shift to a medium containing nitrate. The exception to this trend is MDH5, which codes for the enzyme malate dehydrogenase. It shows constitutive expression regardless of the nitrogen source (Figure 2.2).

For this project, a complete NAR Cluster I was defined as one containing the following five genes involved in nitrate transport or assimilation: nitrate reductase (NIA1), ferredoxin-dependent nitrite reductase (NII1), the nitrate transporter accessory protein (NAR2), nitrite transporter (NAR1.1), and at least one copy of the nitrate transporter (NRT2). To determine the presence or absence of these five genes and whether or not they are clustered, all algal genome databases (including those deposited at NCBI, JGI and Phytozome) were searched using the *Chlamydomonas* NAR gene sequences as search queries. As shown in Figure 2.3, a complete cluster was found in nine species of green algae distributed among three phylogenetic classes (Chlorophyceae, Trebouxiophyceae, and Mamiellophyceae). Complete NAR gene clustering was however not found when non-green algal genomes were searched, including *Porphyridium purpureum* (red algae), *Galderia sulphuraria* (red algae), *Guillardia theta* (red algae), *Thalassiosira pseudonana* (diatoms), *Phaeodactylum tricornutum* (diatoms). It is important to note that although clustering of NAR genes was determined not to occur in these species, the individual genes were clearly identified and shown to be scattered throughout the genome (data not shown). Interestingly, in one of the red algal species, *Cyanidioschyzon merolae*, a partial cluster consisting of three genes (NIA1, NII1, and NRT2) was identified (Figure 2.3).

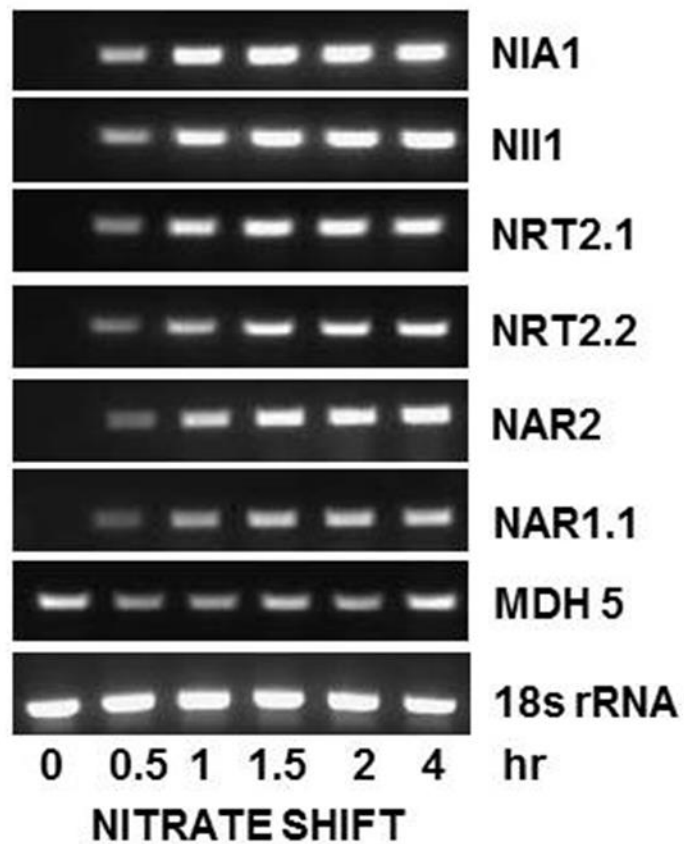


Figure 2.2 Representative semi-quantitative RT-PCR analysis of NAR genes transcript abundance in *Chlamydomonas*. Cells grown in a medium with ammonium as the sole nitrogen source were shifted at time 0 hr to a medium containing nitrate as the sole source of nitrogen.

As shown in Figure 2.3 the Chlorophyte species *Gonium* and *Volvox* have an identical complement of genes within the NAR Cluster I as *Chlamydomonas*, including the presence of an additional copy of the nitrate transporter gene NRT2 and MDH5. One conspicuous difference among the genes is that MDH5 and NAR1 have swapped positions at the cluster ends in *Gonium* and *Volvox* as compared to *Chlamydomonas*. By comparison, the six species belonging to the class Mamiellophyceae display much more variability in terms of the specific member genes found within the cluster as well as the ordering and orientation of those genes.

Among the eleven green algal species shown in Figure 2.3, *Chlorella variabilis* NC164A and *Coccomyxa subellipsoidea* C169 are the two species that lack a complete NAR Cluster I. The *Chlorella* cluster retains all genes except the NAR1.1 (nitrite transporter), while in *Coccomyxa*; the cluster has only the genes that code for nitrate reductase and nitrite reductase (NIA1 and NII1).

While clusters of NAR genes are also found in both bacteria and fungi, a gene common to all green algal NAR clusters that is absent from the genomes of other algae as well as their fungal and bacterial counterparts is NAR2 (Figure 2.4). This gene has been shown to code for a membrane accessory protein that associates with the NRT2 transporter and seems to be essential for its function (Fernandez and Galvan 2007). Interestingly, a NAR2-like protein is also present in plants. Detailed work in *Arabidopsis* indicates that the NAR2 protein serves a crucial role in ferrying nitrate transporters to the plasma membrane and that it also aids in the uptake of nitrate under varied concentration in the environment (Feng et al., 2011).

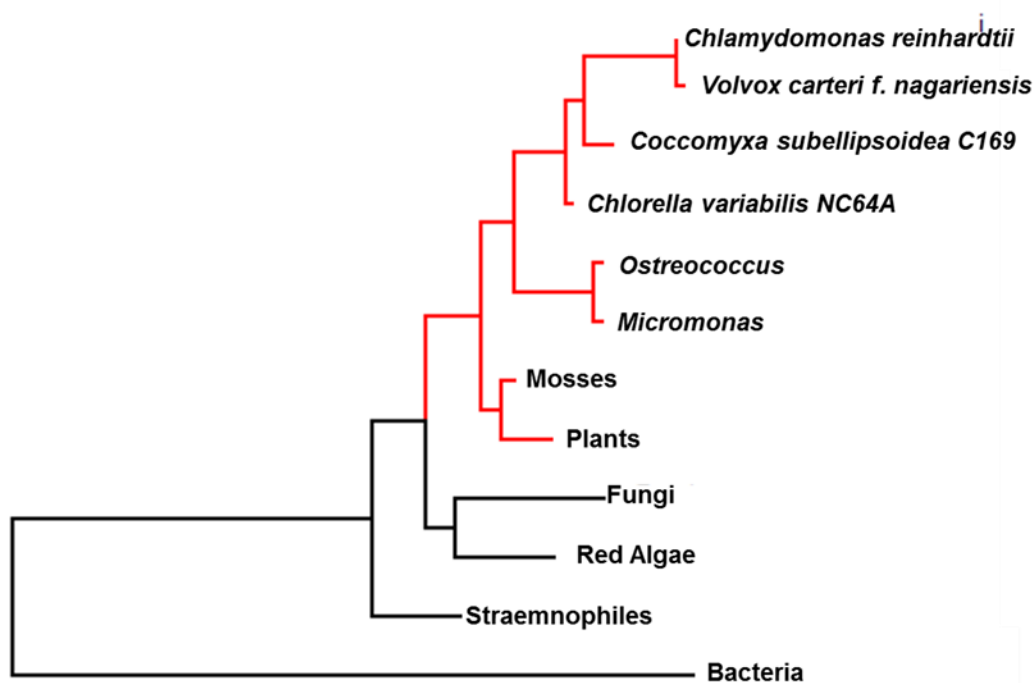


Figure 2.4 Phylogenetic tree of the distribution of NAR2 among various lineages. The tree was constructed using the ribosomal RNA gene sequence of the small subunit. The tree was constructed using maximum-likelihood method in MEGA 6.0 software program. Branches shaded red represents the species containing NAR2.

2.3.2 Other metabolic genes are recruited into NAR cluster I.

Like bacterial and fungal metabolic gene clusters (Luque-Almagro et al., 2011; Slot et al., 2010), the NAR Cluster I of green algae contain one or more additional genes that are not directly involved in nitrate transport or assimilation but do have a related function. For example, the gene encoding chloroplastic malate dehydrogenase (MDH5) present in NAR Cluster I of Chlamydomonas, Gonium and Volvox plays an important role in the ferrying of reducing power between cellular compartments (cytosol, chloroplast, mitochondria). Thus, its inclusion in the cluster likely reflects the high energetic demands of nitrate assimilation and the need for the rapid movement of reducing power into the chloroplast.

The NAR clusters of the class Mamiellophyceae have genes involved in molybdenum metabolism. For example, the NAR Cluster I of *Ostreococcus* contains the gene MOT1 that codes for a molybdate transporter. As well, many members of this class contain the genes CNX2 and CNX5, which are involved in molybdenum cofactor biosynthesis. The presence of a molybdenum cofactor is essential for the catalytic activity of nitrate reductase (Li et al., 2009).

2.3.3 Lack of a complete NAR Cluster I is linked to alternative nitrogen acquisition strategies

Recall that both *Coccomyxa* and *Chlorella* possess an incomplete NAR Cluster I (Figure 2.3). A closer examination of the genes surrounding the *Coccomyxa* cluster revealed that the NAR Cluster I genes NAR2 and MDH found in the Chlorophyceae, were located approximately 125 and 80 kbp upstream, respectively (Figure 2.5). Both the *Coccomyxa* and *Chlorella* clusters lack NAR1.1. In both species this gene was not present on the same chromosome as the NAR cluster.

That both *Coccomyxa* and *Chlorella* lack a complete NAR Cluster I suggests that formation of a complete NAR cluster or its maintenance may not be advantageous in these species. This may be a consequence of compensatory changes that result in the dominance of other nitrogen acquisition systems. Specifically, the absence or loss of the complete NAR Cluster I may reflect a shift in nitrogen uptake strategies away from nitrate and towards the import of ammonium or organic nitrogen sources (e.g. amino acids). To test this hypothesis, the genomes of both *Coccomyxa* and *Chlorella* were searched for genes involved in ammonium and amino acid transport. Both species were found to contain a similar number of ammonium transporters to species, like *Chlamydomonas*, that possess a complete NAR Cluster I. However, a surprising finding was that both *Coccomyxa* and *Chlorella* had between three and four times the number of amino acid transport-related proteins (both amino acid permeases and transporters) than

Chlamydomonas. As shown in Table I, there are 42 proteins annotated as amino acid transporters in Chlorella and 36 in Coccomyxa whereas the other algal species examined in this study contain only between 12 and 14 amino acid transporters (Table 2.1).

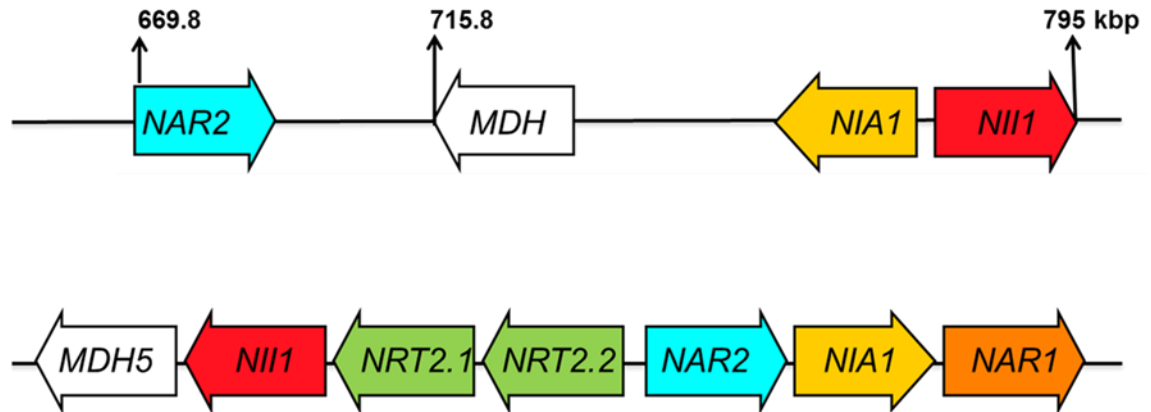


Figure 2.5 Diagram illustrating the position of NAR2, MDH, NIA1 and NII1 *Coccomyxa* (top) in relation to the NAR Cluster I organization of *Chlamydomonas* (bottom). The NAR cluster of *Chlamydomonas* is not scaled. The numbers in kbp indicate the chromosomal position of the gene.

Table 2.1 Predicted number of amino acid transporters and ammonium transporter proteins in various green and red algal genomes. Data compiled using annotated genome information found in NCBI and other published reports.

Organism	Amino acid Transporters	Ammonium Transporters
Chlamydomonas	12	10
Volvox	12	10
Chlorella	42	6
Coccomyxa	37	4
Ostreococcus	5-7	3-4
Micromonas	8-11	4-6
Bathycoccus	9	6
Cyanidioschyzon	4	2

2.3.4 Ferredoxin-dependent Nitrite reductase of Mamiellophyceae contains three additional protein domains

In addition to looking at NAR cluster organization, this investigation afforded an opportunity to examine in closer detail the diversity of domain structure of specific proteins. While most of the NAR cluster genes displayed very similar predicted protein structure, distinct differences were found in the domain structure for NII1, the gene that codes for the enzyme nitrite reductase. This enzyme catalyzes the reduction of nitrite to ammonium using electron donation from ferredoxin. As shown in Figure 2.6, all nitrite reductase proteins possess two conserved nitrite/sulfite ferredoxin domains and two nitrite/sulfite reductase 4 iron-4 sulphur (4Fe-4S) domains. However, in the

class Mamiellophyceae, the predicted nitrate reductase contains three additional domains, a rubredoxin domain, an oxidoreductase FAD-binding domain and an oxidoreductase NAD-binding domain all located at the C-terminal end (Figure 2.6). The three conserved domains share similarity with cytochrome b5 reductase and the ferredoxin: NADP (H) oxidoreductase (FNR) family of enzymes (Ghoshroy and Robertson 2014). These additional domains may provide a unique flexibility by allowing for the non-photosynthetic reduction of nitrite in the chloroplast (Hanke et al., 2005). The NAD and FAD binding domains may allow the transfer of electrons from NADPH/NADH and FADH to support nitrite reduction especially under low light and dark environment (Hanke et al., 2005; Kamp et al., 2011).

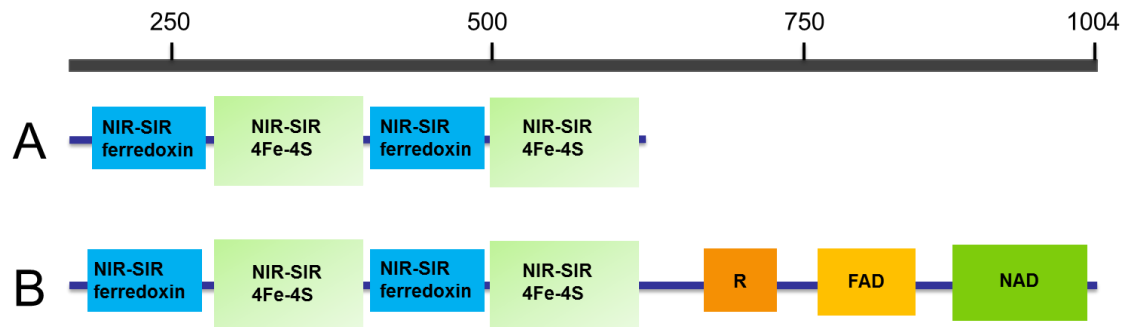


Figure 2.6 Representative protein domains of ferredoxin-dependent nitrite reductase from (A) *Chlamydomonas reinhardtii* (B) *Micromonas pusilla*. Numbers in the scale indicate amino acid position. Abbreviations: NIR_SIR ferredoxin- Nitrite/sulfite reductase ferredoxin binding domain, NIR_SIR superfamily- Nitrite/Sulfite reductase 4Fe-4S domain; R- Rubredoxin, FAD- Oxidoreductase FAD binding domain, NAD- Oxidoreductase NAD binding domain

2.3.5 Ferredoxin-dependent Nitrite reductase (NII) has a probable cyanobacterial origin

As discussed briefly in the introduction, nitrate transport and assimilation are carried out by a range of organisms including non-photosynthetic bacteria as well as fungi, which are heterotrophic. Of the five genes that we have defined as constituting a complete NAR Cluster I, most are homologous to genes found in non-photosynthetic species (both bacteria and fungi). As an example, molecular phylogenetic analysis using the maximum likelihood algorithm, illustrates that the plasma membrane-localized nitrate transporter, encoded by the gene NRT2, is evolutionarily related to genes found in non-photosynthetic bacteria (Figure 2.7A). From this, one can conclude that NRT2 is ancient, having arisen in prokaryotic cells prior to the development of the eukaryotic cell by endosymbiosis.

Unlike NRT2 and most other NAR genes, molecular phylogenetic analysis of the nitrite reductase (NII1) gene provides evidence of a different evolutionary history (Figure 2.7B). Within the phylogenetic domain of bacteria, genes with high sequence similarity for *Chlamydomonas* NII1 are not found in heterotrophic bacteria but are only found in cyanobacteria. According to the theory of endosymbiosis as initially proposed by Margulis (1970), the present-day chloroplast of plants and algae is the descendant of free living cyanobacteria. This explains the chloroplast localization of nitrite reductase. Incorporation of NII1 into the nuclear genome of *Chlamydomonas* and other photosynthetic eukaryotes is through the process of horizontal gene transfer, where DNA was relocated from proto-chloroplast (the engulfed cyanobacterium) to the nucleus very early in the development of the photosynthetic eukaryotic cell (Rockwell et al., 2014).

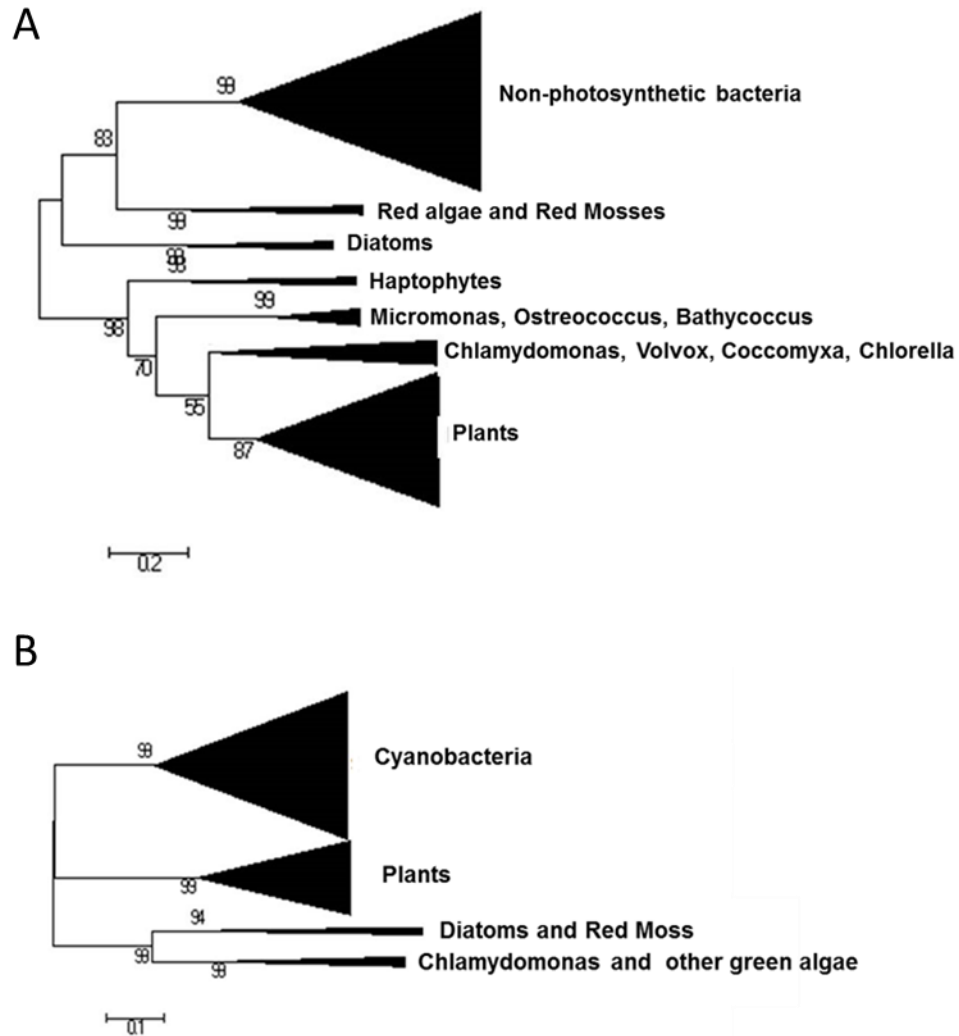


Figure 2.7 Distribution of the nitrite transporter (NRT2) protein (A) and ferredoxin-dependent nitrite reductase (NII1) protein (B) among various taxa. The size of the shaded triangles indicates the number of species within that taxon that contain a protein sequence homologous to the respective proteins in *Chlamydomonas*. The tree was made using the maximum-likelihood method in MEGA 6.0 software program of aligned protein sequences. Numbers in the node indicates the bootstrap values.

2.3.6 NAR Cluster II distribution and its regulation by nitrate

NAR Cluster II in *Chlamydomonas* consists of only two genes: the nitrate transporter gene, NRT2.3, and the mitochondrial alternative oxidase gene, AOX1. As shown in Figure 2.8, this cluster is found in *Chlamydomonas*, *Volvox* and *Gonium*, where the two genes are organized in opposite orientation to each other. A search of all other available algae genomes (a total of 22 genomes) failed to identify the presence of this cluster.

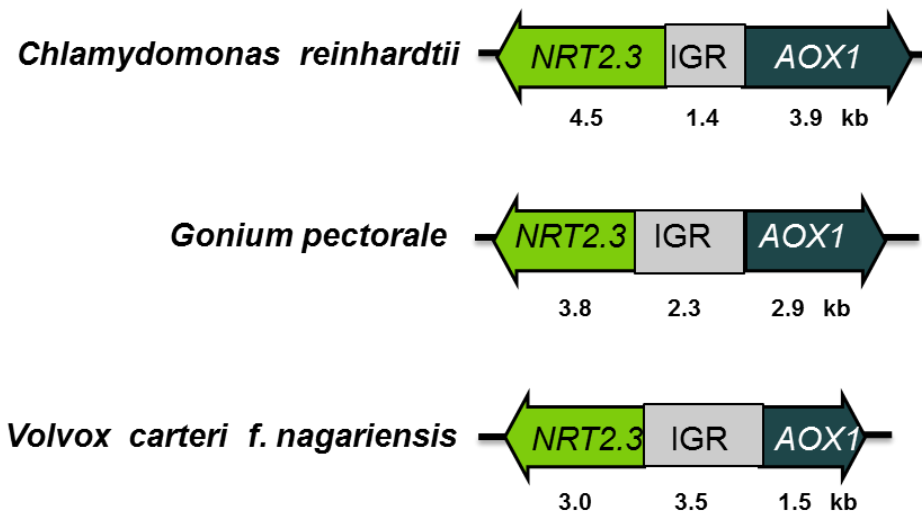


Figure 2.8 The NAR Cluster II genes in three species of Chlorophyceae: *Chlamydomonas* compared with *Volvox* and *Gonium*. IGR-intergenic region.

The structure of NAR cluster II suggests the presence of a bidirectional promoter (Wang et al., 2009). That is, the two genes are transcribed on different strands of DNA and are separated by approximately 1,400 bp of DNA. In a recent genome-wide study of *Arabidopsis*, 2,471 bidirectional gene pairs were identified (Wang et al., 2009). While in humans, about 10% of about 23,000 genes were identified as being arranged bidirectionally (Trinklein et al, 2004). Bidirectional gene pairs tend to share common cis-regulatory elements within the intergenic region and the fact that they tend to

be conserved among species of a particular lineage suggests that it serves an important function, mostly likely related to coordinate regulation.

It has previously been shown that both NRT2.3 and AOX1 are induced by nitrate (Quesada et al., 1998). To investigate the expression of these two genes in more detail, the kinetics of the change in transcript abundance for each gene was determined using RNA blot analysis for cells grown in ammonium and shifted to nitrate. As shown in Figure 2.9, AOX1 shows higher basal expression compared to NRT2.3, both are rapidly induced within 30 minutes, but the expression of NRT2.3 is far more transient than that of AOX1, returning to ammonium control levels after about 4 hours in nitrate.

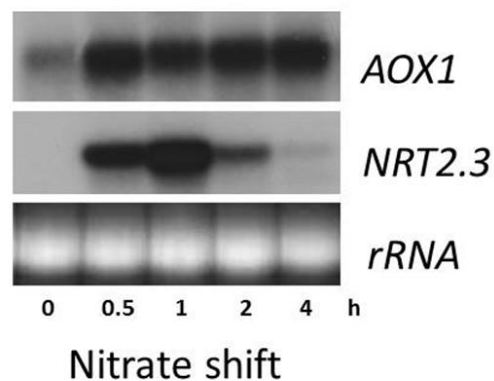


Figure 2.9 Northern blot analysis of NRT2.3 and AOX1 transcript abundance in *Chlamydomonas* cells shifted to the medium containing as nitrate the sole nitrogen source. Cells were grown in media containing HS-ammonium and total RNA was isolated as a function of time following transfer to nitrate containing HS medium. RNA was gel electrophoresed and transferred to nylon membrane to probe against AOX1 and NRT2.3 genes. A major ribosomal RNA separated in electrophoresis gel and stained by ethidium bromide was used as control for equal loading of 25 µg of RNA.

To look into the bidirectional nature of the transcriptional regulation of NAR Cluster II, the 1.4kbp intergenic region was fused to the arylsulfatase (ARS) reporter gene in both orientations (Figure 2.10A). Each construct was then transformed into wild-type *Chlamydomonas* and ARS enzyme activity was measured (Ohresser et al., 1997) in cells grown in ammonium and shifted to nitrate. As shown in Figure 2.10B, ARS expression was far stronger in the orientation that drives the expression of AOX1 than NRT2.3. While both NRT2.3 and AOX1 have both previously been shown to be regulated by the transcription factor NIT2 (Quesada et al., 1998), these data suggest that there are additional levels of regulation that differentiate the two genes. It may be that NIT2 interacts more strongly with 5' region of the AOX1 coding strand than the region upstream of the start site of NRT2.3. Alternatively, there may be additional co-transcription factors that have binding sites only to the promoter region of AOX1 that accounts for its heightened rate of transcription. More detailed analysis of the intergenic region is required to determine the biochemical basis for the large difference in transcription found between the two genes.

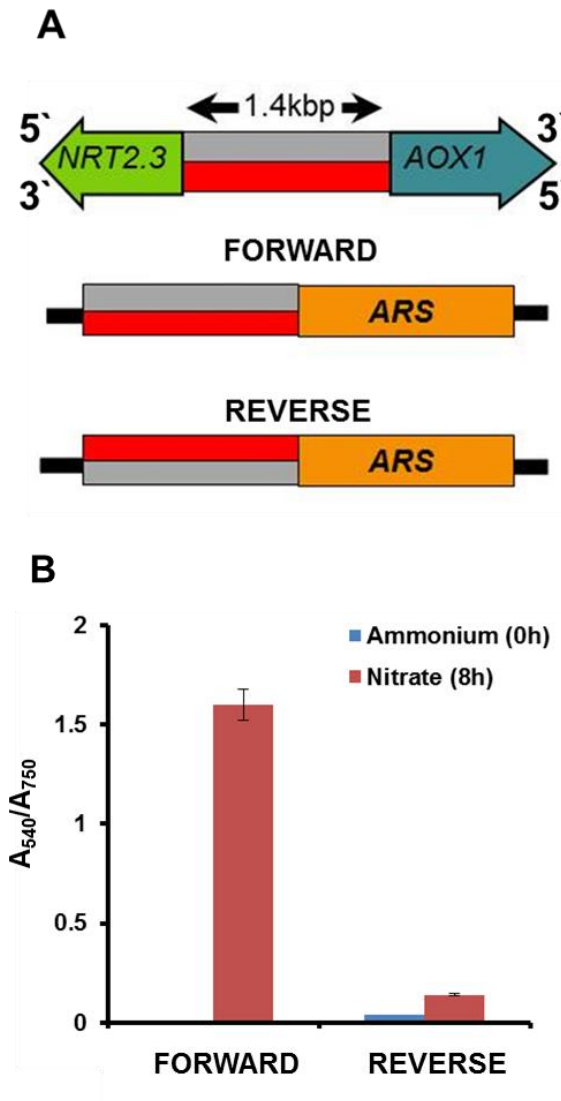


Figure 2.10 Measuring transcription of the NRT2.3:AOX1 intergenic region.

A. Two constructs were made with the arylsulfatase (ARS) coding sequence under control of the NRT2.3:AOX1 intergenic region. B. ARS expression was measured in cells transformed with either the FORWARD or REVERSE construct by assaying ARS enzyme activity. Data was standardized to the number of cells calculated by dividing the absorbance at 540nm by the culture turbidity at 750nm. Cells were initially grown under ammonium and shifted to nitrate contacting growth medium for 8 hrs before the ARS assay is performed. Data represent the mean of three independent experiments +/- SE.

2.4 Discussion

The genome of *Chlamydomonas* contains two nitrate assimilation gene (NAR) clusters: one that contains seven genes that encode proteins primarily involved in nitrate transport and assimilation (NAR Cluster I) and a second one that contains a gene for a nitrate transporter and the gene encoding the mitochondrial alternative oxidase (NAR Cluster II). NAR genes have been shown to be clustered in many lineages of fungi and bacteria. Following those findings, the purpose of the current study was to determine how widely NAR genes are found clustered within algal lineages.

Using whole genome data, the NAR Cluster I was identified in all three classes of the green algae (division Chlorophyta): clustering was found in two additional members of the Chlorophyceae, besides *Chlamydomonas*; two species within the Trebouxiophyceae and six members of the Mamiellophyceae. This analysis led to three major findings regarding NAR Cluster I. First, the basic cluster can be defined as having five genes: nitrate reductase (NIA1), ferredoxin-dependent nitrite reductase (NII1), nitrate transporter accessory protein (NAR2) and nitrite transporter (NAR1.1) and one copy of the gene that codes for nitrate transporter (NRT2). Second, the organization of these five core genes within a cluster is not conserved. Both the ordering of the genes as well as their orientation to each other is highly variable. Third, the NAR Cluster I from almost all species examined contained additional genes that were not directly involved in either nitrate transport or assimilation.

The variability in the number of nitrate assimilation genes above the core five can be explained by gene duplication. Gene duplication is considered as one of the mechanisms that contribute significantly to the formation and augmentation of the metabolic gene clusters in fungi and plants (Proctor et al., 2009, Chu et al., 2011)

Among the 11 different NAR clusters of green algal species analyzed in this study, most of the clusters contain genes that arose from duplication. For example, in the Chlorophyceae (*Chlamydomonas*, *Gonium*, and *Volvox*) and Trebouxiophyceae (*Chlorella*) the NAR clusters were found to contain an additional nitrate transporter gene (NRT2.1 and NRT2.2). Sequence conservation between the genes clearly indicates that they share an evolutionary history that was the result of a gene duplication event early in an ancestral species that propagated across lineages. Interestingly in Chlorophyceae members, a copy of NRT2 gene was relocated after duplication to form part of the NAR Cluster II along with AOX1. This is similar to what is reported in tricothecene (TRI) gene cluster of *Fusarium* (Proctor et al., 2009). From the primary TRI gene cluster, two of the genes TRI1 and TRI101 are duplicated and relocated separately to other loci of the genome and form a small cluster with other genes (Proctor et al., 2009).

Unlike these two groups of green algae, NAR clusters of Mamiellophyceae showed a lesser degree of gene duplication. NAR2 is duplicated only in *Micromonas pusilla* RCC299 and then gene CNX is duplicated only in *Ostreococcus*. The importance of this gene duplication in Mamiellophyceae NAR Cluster I is not very clear yet and it needs a detailed analysis.

The differences found in the order and orientation of NAR Cluster I members among the different lineages may be biologically relevant and thus deserves further investigation. It is intriguing to note that in all *Saccharomyces* species, but not *Naumovia castellii*, gene order within the DAL cluster is conserved (Naseeb and Delneri 2012). Compared to *Saccharomyces cerevisiae*, *Naumovia castellii* was found to grow much slower in the presence of allantoin. Interestingly, this slow growth phenotype could be mimicked in *S. cerevisiae*, by recreating the gene inversions found in *N. castellii*. Such experiments could easily be carried out in *Chlamydomonas* to determine the fitness implications of altering the gene order and orientation of the members of NAR Cluster I.

The major driving force that influences the formation and maintenance of eukaryotic gene clusters is selective pressure from the environment (Chu et al., 2011). In yeast for example, urate oxidase was selected against and eliminated from the DAL gene cluster when the yeast adapted to a low oxygen environment (Wonga and Wolfe 2004). Likewise, the GAL gene cluster seems only to be maintained when the habitat is rich in galactose. Otherwise, the cluster is dissociated and the genes in the cluster are relocated elsewhere in the genome (Slot and Rokas 2010).

The research from yeast and fungi discussed above clearly illustrates that cluster maintenance as well as gene order and orientation are targets for selection, as changes in these can alter organism fitness. Support for this from the current work comes from an examination of the NAR Cluster I in *Coccomyxa subellipsoidea* (which lacks three of the five core genes) and *Chlorella variabilis* (which lacks one of the five core genes). In both cases, the loss of the core complement of genes is correlated with an improved ability to preferentially import organic forms of nitrogen instead of nitrate. In both species, the absence of a complete NAR Cluster I is correlated with an unusually high number of amino acid transport related proteins.

Chlorella variabilis is a facultative photosynthetic symbiont of *Paramecium* and thus relies heavily on its host for nitrogen. *Paramecium* obtains nutrition by feeding on bacteria, algae and other microorganisms and generates free amino acids by protein catabolism (Johnson 2011, Karakashian 1963). Adaptation of *C. variabilis* to such an ecological niche would thus favour an increased number of amino acid transporters. A corollary to this would be that maintenance of the NAR Cluster I would not be selected for and thus its retention would not confer an advantage when organic nitrogen is the dominant form of nitrogen taken up from the environment. The cluster would break apart most likely as a result of genetic recombination during mitosis and may account for the loss of nitrite transporter gene NAR1 from the cluster.

Unlike *Chlorella variabilis* NC64A, *Coccomyxa subellipsoidea* C169 is a free living obligate photoautotroph, but the loss of a complete NAR Cluster I in this species can also be attributed to the organism occupying an uncommon ecological niche. The strain *Coccomyxa* used for genome sequencing was isolated from Antarctica in a dry environment characterized by being particularly rich in organic matter (Blanc et al., 2012). This then could explain the preponderance of amino acid transporters in the *Coccomyxa* genome.

Another interesting finding from in silico genome analysis is that the NAR Cluster I contains additional genes besides those directly required for nitrate transport and assimilation. For example, *Chlamydomonas*, *Gonium* and *Volvox*, all contain MDH, a gene that encodes malate dehydrogenase. While members of the Mamiellophyceae examined contain genes involved in molybdenum metabolism (MOT/CNX). While these genes are not directly involved in nitrate transport or assimilation, they are associated with the process. For example, malate dehydrogenase is part of the metabolic shuttle (Scheibe 2004) that is involved in the transfer of reducing power between cellular compartments to support the high energy requiring nitrate reduction reactions. Likewise, molybdenum metabolism is crucial to nitrate assimilation as molybdenum is a key component of the cofactor required for nitrate reductase activity (Li et al., 2009).

The presence of non-core genes is a characteristic of clusters in other organisms. Cooption of other genes is also reported in various bacterial NAR clusters and it is common in different kinds of fungal metabolic gene clusters (Luque-Almagro et al., 2011, Hoffmeister and Keller 2007). For example, kinase gene is present in the GAL gene cluster of yeasts and fungi (Slot and Rokas 2010). In each case, including the ones described in this research for NAR Cluster I, the non-core genes do encode components that are clearly related to the function of the core genes.

Unlike the NAR clusters found in bacteria and yeast, this study provides evidence that in green algae the formation of NAR Cluster I involved a distinct evolutionary path that included gene transfer and rearrangement events involving more than one prokaryotic genome. Based on a wealth of phylogenetic analysis, it is now well established that modern green algae arose by an endosymbiotic event whereby a cyanobacterium was engulfed by a heterotrophic eukaryote cell that already possessed a proto-mitochondrion (Falkowski et al., 2005, Keeling 2010). During early eukaryote evolution there was extensive genome reorganization that included not only the loss of redundant genes but also the transfer of genes from the engulfed cyanobacterium (destined to become the chloroplast) to the host nuclear genome. For example, most photosynthetic genes were transferred to the nucleus, with only a small number of genes being retained by the chloroplast genome (De Clerck et al., 2012).

Based upon the molecular phylogenetic analysis presented here, one can speculate a putative series of events, which would result in the unique features of the NAR cluster I organization seen in green algae. The basic cluster already existed in bacteria and thus was present in the nucleus of the earliest eukaryotic cells. It is likely that there was no transfer of NAR genes from the proto-mitochondrion to the early nucleus, instead redundant genes were deleted. However, the analysis presented here clearly shows evidence that there was a transfer of NII1, encoding nitrite reductase, from the genome of the engulfed cyanobacterium to the nucleus. Interestingly, it is likely that the NAR cluster within the nucleus already contained a gene that would encode nitrite reductase, but that gene was replaced by the one from the cyanobacterium. Why would this swap take place? It is important to realize that the two nitrite reductase genes are not equivalent. The bacterial enzyme is NADH-dependent, while the cyanobacterial is a ferredoxin-dependent form of the enzyme. This distinction is critical because only the later would be able to interact with ferredoxin, a key component of photosynthetic electron

transport allowing for nitrite reduction to occur within the chloroplast of the early photosynthetic cell.

So, what can explain the clustering of NAR genes in *Chlamydomonas*? The data presented in this chapter provides evidence of a hybrid model: there are data that support the coregulation model as well as data that supports the selfish cluster model.

Based on the phylogenetic analysis, it is clear that four of the member genes of the cluster (nitrate reductase, nitrite reductase, nitrate transporter and nitrite transporter) were present in bacteria and their close association led to widespread propagation throughout bacterial and eventually eukaryotic lineages. This supports the selfish cluster model, that having genes tightly associated with each other facilitates their rapid horizontal transfer across species. During the genome reshuffling process, nitrite reductase from the host (non-photosynthetic parent) NAR cluster was replaced by the nitrite reductase of cyanobacterium NAR cluster. Once moved into the cluster for coregulation, nitrite reductase from cyanobacteria was retained and co-inherited along with the host NAR cluster.

Support for the coregulation comes from the finding that all genes in the cluster show a remarkable degree of coordinate activation in the presence of nitrate and strong repression under ammonium. This is consistent with previous findings and is associated with the involvement of the transcription factor NIT2 that regulates the expression of NAR genes (Camargo et al., 2009). Recall from the introduction that support for the coregulation hypothesis comes from the notion that metabolic intermediates of some pathways are toxic and thus expression of all enzymes of a pathway concurrently would avoid accumulation of any toxic metabolites. This could be considered as a reason for the clustering of NAR genes in *Chlamydomonas*. A major by-product of nitrate reduction as catalyzed by nitrate reductase in the cytosol is nitric oxide, which is generated by a reaction with nitrite

(Sakihama et al., 2002). Formation of nitric oxide, which is a reactive nitrogen species and potentially harmful can be mitigated by rapidly transporting nitrite into the chloroplast to be reduced to ammonium. To allow uninterrupted transfer of nitrite molecules for enzymic reduction in the chloroplast, it would be critical to keep NAR1.1 and NII1 in a cluster for coordinate regulation. Within the chloroplast, high activity of nitrite reductase would also be important as nitrite itself is known to be a reactive nitrogen species causing nitration of proteins and lipids.

Unlike the distribution of NAR Cluster I observed among different green algal species, NAR Cluster II formation is restricted only to the three members of Chlorophyceae group and no other taxonomic group of algae seems to possess this NAR cluster. Since the NRT2.3 located next to AOX1 is a duplicated copy of the high affinity nitrate transporter gene present in the NAR cluster I, the biological significance of this association is not known yet. That AOX1 would become closely associated with a NAR gene and a component of NAR Cluster II suggests that coordinate expression of its transcription (induced by nitrate and repressed by ammonium) is important for nitrate assimilation. This is explored in chapters 3 and 4 of this thesis.

2.5 References

- Camargo A, Llamas Á, Schnell RA, Higuera JJ, González-Ballester D, Lefebvre PA, Fernández E, Galván A (2007) Nitrate Signaling by the Regulatory Gene NIT2 in *Chlamydomonas*. *The Plant Cell Online* 19: 3491–3503
- Chu HY, Wegel E, Osbourn A (2011) From hormones to secondary metabolism: the emergence of metabolic gene clusters in plants. *The Plant Journal* 66: 66–79
- Davies JP, Weeks DP, Grossman AR (1992) Expression of the arylsulfatase gene from the beta 2-tubulin promoter in *Chlamydomonas reinhardtii*. *Nucleic Acids Res* 20: 2959–2965
- De Clerck O, Bogaert K, Leliaert F (2012) Diversity and evolution of algae: primary endosymbiosis. *Advances in Botanical Research* 64: 55–86
- Falkowski PG, Katz ME, Milligan AJ, Fennel K, Cramer BS, Aubry MP, Berner RA, Novacek MJ, Zapol WM (2005) The Rise of Oxygen over the Past 205 Million Years and the Evolution of Large Placental Mammals. *Science* 309: 2202–2204
- Feng H, Fan X, Yan M, Liu X, Miller AJ, Xu G (2011) Multiple roles of nitrate transport accessory protein NAR2 in plants. *Plant Signal Behav* 6: 1286–1289
- Fernandez E, Galvan A (2007) Inorganic nitrogen assimilation in *Chlamydomonas*. *J Exp Bot* 58: 2279–2287
- Field B, Fiston-Lavier A-S, Kemen A, Geisler K, Quesneville H, Osbourn AE (2011) Formation of plant metabolic gene clusters within dynamic chromosomal regions. *PNAS* 108: 16116–16121
- Field B, Osbourn A (2012) Order in the playground. *Mobile Genetic Elements* 2: 46–50
- Ghoshroy S, Robertson DL (2015) Molecular Evolution of Nitrogen Assimilatory Enzymes in Marine Prasinophytes. *J Mol Evol* 80: 65–80
- Hanke GT, Okutani S, Satomi Y, Takao T, Suzuki A, Hase T (2005) Multiple iso-proteins of FNR in *Arabidopsis*: evidence for different contributions to chloroplast function and nitrogen assimilation. *Plant, Cell & Environment* 28: 1146–1157
- Hoffmeister D, Keller NP (2007) Natural products of filamentous fungi: enzymes, genes, and their regulation. *Nat Prod Rep* 24: 393–416
- Horton R, Wilming L, Rand V, Lovering RC, Bruford EA, Khodiyar VK, Lush MJ, Povey S, Talbot CC, Wright MW, et al (2004) Gene map of the extended human MHC. *Nat Rev Genet* 5: 889–899

- Hurst LD, Pál C, Lercher MJ (2004) The evolutionary dynamics of eukaryotic gene order. *Nat Rev Genet* 5: 299–310
- Jacob F, Monod J (1961) Genetic regulatory mechanisms in the synthesis of proteins. *Journal of Molecular Biology* 3: 318–356
- Jacob F, Perrin D, Sánchez C, Monod J (2005) L'opéron : groupe de gènes à expression coordonnée par un opérateur [C. R. Acad. Sci. Paris 250 (1960) 1727–1729]. *Comptes Rendus Biologies* 328: 514–520
- Johnson MD (2011) Acquired Phototrophy in Ciliates: A Review of Cellular Interactions and Structural Adaptations¹. *Journal of Eukaryotic Microbiology* 58: 185–195
- Kamp A, Beer D de, Nitsch JL, Lavik G, Stief P (2011) Diatoms respire nitrate to survive dark and anoxic conditions. *PNAS* 108: 5649–5654
- Karakashian SJ (1963) Growth of *Paramecium bursaria* as Influenced by the Presence of Algal Symbionts. *Physiological Zoology* 36: 52–68
- Keeling PJ (2010) The endosymbiotic origin, diversification and fate of plastids. *Philosophical Transactions of the Royal Society of London B: Biological Sciences* 365: 729–748
- Kindle KL (1990) High-frequency nuclear transformation of *Chlamydomonas reinhardtii*. *PNAS* 87: 1228–1232
- Koonin EV (2009) Evolution of genome architecture. *The International Journal of Biochemistry & Cell Biology* 41: 298–306
- Krapp A, David LC, Chardin C, Girin T, Marmagne A, Leprince A-S, Chaillou S, Ferrario-Méry S, Meyer C, Daniel-Vedele F (2014) Nitrate transport and signalling in *Arabidopsis*. *J Exp Bot* 65: 789–798
- Kucho K, Yoshioka S, Taniguchi F, Ohyama K, Fukuzawa H (2003) Cis-acting Elements and DNA-Binding Proteins Involved in CO₂-Responsive Transcriptional Activation of *Cah1* Encoding a Periplasmic Carbonic Anhydrase in *Chlamydomonas reinhardtii*. *Plant Physiol* 133: 783–793
- Lawrence JG, Roth JR (1996) Selfish Operons: Horizontal Transfer May Drive the Evolution of Gene Clusters. *Genetics* 143: 1843–1860
- Li W, Fingrut DR, Maxwell DP (2009) Characterization of a mutant of *Chlamydomonas reinhardtii* deficient in the molybdenum cofactor. *Physiol Plant* 136: 336–350

Luque- Almagro VM, Gates AJ, Moreno-Vivian C, Ferguson SJ, Richardson DJ, Rolda MD (2011) Bacterial nitrate assimilation: gene distribution and regulation. *Biochemical Society Transactions* 39: 1838-1843

Mariscal V, Moulin P, Orsel M, Miller AJ, Fernández E, Galván A (2006) Differential Regulation of the *Chlamydomonas* Nar1 Gene Family by Carbon and Nitrogen. *Protist* 157: 421–433

Molen TA, Rosso D, Piercy S, Maxwell DP (2006) Characterization of the alternative oxidase of *Chlamydomonas reinhardtii* in response to oxidative stress and a shift in nitrogen source. *Physiologia Plantarum* 127: 74–86

Naseeb S, Delneri D (2012) Impact of Chromosomal Inversions on the Yeast DAL Cluster. *PLOS ONE* 7: e42022

Nei M (1967) Modification of Linkage Intensity by Natural Selection. *Genetics* 57: 625–641

Nützmann H-W, Osbourn A (2014) Gene clustering in plant specialized metabolism. *Current Opinion in Biotechnology* 26: 91–99

Nützmann H-W, Osbourn A (2015) Regulation of metabolic gene clusters in *Arabidopsis thaliana*. *New Phytol* 205: 503–510

Ohresser M, Matagne RF, Loppes R (1997) Expression of the arylsulphatase reporter gene under the control of the nit1 promoter in *Chlamydomonas reinhardtii*. *Current Genetics (Germany)*

Orsel M, Krapp A, Daniel-Vedele F (2002) Analysis of NRT2 transporter family in *Arabidopsis*. *Structure and Expression Plant Physiol* 129(2): 886-896

Pearson WR (2013) An Introduction to Sequence Similarity (“Homology”) Searching. *Curr Protoc Bioinformatics*. doi: 10.1002/0471250953.bi0301s42

Price MN, Huang KH, Arkin AP, Alm EJ (2005) Operon formation is driven by co-regulation and not by horizontal gene transfer. *Genome Res* 15: 809–819

Proctor RH, McCormick SP, Alexander NJ, Desjardins AE (2009) Evidence that a secondary metabolic biosynthetic gene cluster has grown by gene relocation during evolution of the filamentous fungus *Fusarium*. *Molecular Microbiology* 74: 1128–1142

Quesada A, Gómez I, Fernández E (1998) Clustering of the nitrite reductase gene and a light-regulated gene with nitrate assimilation loci in *Chlamydomonas reinhardtii*. *Planta* 206: 259–265

Rocha EPC (2008) The Organization of the Bacterial Genome.
<http://dx.doi.org/10.1146/annurev.genet.42.110807091653>. doi:
10.1146/annurev.genet.42.110807.091653

Rockwell NC, Lagarias JC, Bhattacharya D (2014) Primary endosymbiosis and the evolution of light and oxygen sensing in photosynthetic eukaryotes. *Front Ecol Evol* 2:

Sakihama Y, Nakamura S, Yamasaki H (2002) Nitric Oxide Production Mediated by Nitrate Reductase in the Green Alga *Chlamydomonas reinhardtii*: an Alternative NO Production Pathway in Photosynthetic Organisms. *Plant Cell Physiol* 43: 290–297

Slot JC, Hibbett DS (2007) Horizontal Transfer of a Nitrate Assimilation Gene Cluster and Ecological Transitions in Fungi: A Phylogenetic Study. *PLOS ONE* 2: e1097

Slot JC, Rokas A (2010) Multiple GAL pathway gene clusters evolved independently and by different mechanisms in fungi. *PNAS* 107: 10136–10141

Takos AM, Rook F (2012) Why biosynthetic genes for chemical defense compounds cluster. *Trends in Plant Science* 17: 383–388

Tamura K, Stecher G, Peterson D, Filipowski A, Kumar S (2013) MEGA6: Molecular Evolutionary Genetics Analysis Version 6.0. *Mol Biol Evol* 30: 2725–2729

Trinklein ND, Aldred SF, Hartman SJ, Schroeder DI, Otillar RP, Myers RM (2004) An Abundance of Bidirectional Promoters in the Human Genome. *Genome Res* 14: 62–66

Turgeon BG, Bushley KE (2010) Secondary Metabolism. 376–395 Elsevier Inc.

Wang Q, Wan L, Li D, Zhu L, Qian M, Deng M (2009) Searching for bidirectional promoters in *Arabidopsis thaliana*. *BMC Bioinformatics* 10: S29

Wong S, Wolfe KH (2005) Birth of a metabolic gene cluster in yeast by adaptive gene relocation. *Nat Genet* 37: 777–782

Chapter 3

3 Generation and Molecular Characterization of *Chlamydomonas* strain with reduced AOX1 gene expression

3.1 Introduction

In all species in which it has been examined, the alternative pathway (AP) of mitochondrial respiration is comprised of a single protein, alternative oxidase (AOX) (Vanlerberghe and McIntosh 1997). In *Chlamydomonas*, AOX is coded by two nuclear genes, AOX1 and AOX2 and share 57.6% similarity in predicted protein sequence (Dinant et al., 2001). Out of these two homologs, only AOX1 has been found to be transcriptionally active under both optimal growth conditions and stress (Molen et al., 2006). In most plant species examined AOX functions as a dimer that can be activated by various metabolites (Elthon et al., 1989; Vanlerberghe et al., 1992; Vanlerberghe 2013). In contrast, in *Chlamydomonas*, AOX1 is predicted to function as a monomer (Molen et al., 2006, Baurain et al., 2003).

In *Chlamydomonas*, AOX1 is influenced by nitrogen (Quesada et al., 1998). It has been shown that AOX1 gene expression, AOX protein abundance and the corresponding AP capacity are upregulated when nitrate is used as the sole nitrogen source (Baurain et al., 2003, Molen et al., 2006). This specific induction of AOX by nitrate is not seen in plants or in other species that contain this protein (Reviewed in Vanlerberghe et al., 2016).

The current knowledge of the functional importance of AP respiration to respiratory metabolism in plants has been gained mainly from studies conducted in transgenic lines of tobacco and *Arabidopsis* plants with altered levels of AOX. (Umbach et al., 2005; Vishwakarma et al., 2015). It is well known that when induced, AP respiration competes with the energy conserving cytochrome pathway (CP) respiration for reductants at the ubiquinone level. As a result, this

pathway bypasses two of the three proton translocating sites that contribute to the transmembrane pH gradient and thus compromise ATP synthesis.

In transgenic tobacco cells, Maxwell et al., (1999) examined the role of AP respiration in lowering reactive oxygen species (ROS) formation and reported that cells lacking AOX have higher ROS compared with the cell of wild type. The general belief is that AOX provides a second outlet for reduced ubiquinone to be oxidized. In the absence of AOX, high levels of reduced ubiquinone have been shown in a range of systems to be a major source of ROS within the mitochondrion (Reviewed in Vanlerberghe et al., 2016). It is generally accepted, that H_2O_2 is the specific kind of ROS generated by the reduction of superoxide generated in the mitochondria. In tobacco cells, restricting CP respiration with the addition of the inhibitor antimycin A causes massive increase in ROS and AOX protein abundance (Vanlerberghe and McIntosh 1992). Further work in *Arabidopsis* showed that an antisense line of AOX1 showed greater oxidative damage when the CP respiration was chemically inhibited (Umbach et al., 2005). A similar result was also obtained in a study conducted in tobacco plants with the reduced levels of AOX (Amirsadeghi et al., 2006).

It has been more recently shown that altering AOX abundance within the mitochondria can impact photosynthesis in the chloroplast (Reviewed in Vanlerberghe et al., 2016). In plants exposed to high irradiance, a role for AP respiration in optimizing photosynthesis was shown in AOX1 knockdown plants of *Arabidopsis* and tobacco (Giraud et al., 2008, Yoshida et al., (2008, 2011), Vishwakarma et al., 2015, Vanlerberghe et al., 2016). It was found that AOX1 knockdown plants cultivated at higher irradiance levels had lower electron transport through photosystem II (PSII) and enhanced electron transport activity around photosystem I (PSI) (Yoshida et al., 2011).

In *Chlamydomonas*, experiments designed to understand the regulation of AOX1 gene expression have revealed some features that are distinct from the research conducted on plants. A study by Molen et al., (2006) identified that two distinct

pathways that induce AOX in *Chlamydomonas*: First – a pathway mediated by cold, antimycin A and H_2O_2 which explains the role of AP respiration in preventing ROS formation and second, a pathway in response to metabolic alterations triggered by a shift in nitrogen source from ammonium to nitrate in the growth medium. The physiological importance of the induction of AOX and increased AP respiratory capacity by nitrate remains elusive. A number of hypotheses have been proposed to explain this phenomenon: (i) induction of AOX during nitrate assimilation is in response to higher level of photosynthetically derived ATP than that generated during ammonium assimilation (Quesada et al., 2000); (ii) it is a response to the accumulation of nitric oxide that may be generated by the action of nitrate reductase on nitrite, which has been shown previously by Sakihama et al., (2002); (iii) activation of AOX1 expression by nitrate is simply due to the gene's close proximity to a nitrate transporter gene, NRT2.3 in the nuclear genome (Baurain et al., 2003).

One way to investigate the physiological role of AP respiration during nitrate assimilation in *Chlamydomonas* is to develop and characterize transgenic lines with silenced AOX1 gene expression. To achieve this, reverse genetics tools developed for *Chlamydomonas* based on RNA interference principle can be employed (Molnar et al., 2009, Zhao et al., 2009). In the past decade, RNA interference (RNAi) has emerged as an efficient tool to study gene function in *Chlamydomonas* (Cerutti et al., 2011). The amiRNA (artificial microRNA) technology developed by Molnar et al., (2009) and Zhao et al., (2009) has proven successful in silencing several genes of *Chlamydomonas*. Hence to elucidate the function of AOX induced during nitrate assimilation, artificial miRNA targets specific to AOX1 were designed according to Molnar et al., (2009) to develop cell lines silenced with AOX1 gene expression.

In this chapter I report 1) the development of a *Chlamydomonas* strain lacking AOX1 gene expression and 2) the effect of AOX1 silencing on growth, photosynthesis and respiration.

3.2 Material and Methods

3.2.1 Strain and growth conditions

Chlamydomonas reinhardtii strain CC-4351(cw15, arg7-8, mt+) used in this study was obtained from the *Chlamydomonas* resource center, University of Minnesota, St. Paul, MN 55108. This strain lacks cell wall and an auxotroph of amino acid arginine. To maintain the stock, cells were grown in TAP (Tris-acetate phosphate) liquid medium containing arginine under constant light ($50 \mu\text{mol m}^{-2} \text{s}^{-1}$) and temperature ($28^\circ \pm 1.0^\circ\text{C}$) (Harris 2009). The strain obtained from the resource center lacks arginosuccinate lyase (ARG7) gene involved in the synthesis of the amino acid, arginine. So before using the strain in actual experiments, it was transformed with the plasmid pARG7.8 containing the ARG7 (arginosuccinate lyase) gene for complementation to avoid using arginine every time in the growth medium. For transformation, cells maintained in small Erlenmeyer flasks were used as inoculum for larger flasks containing 500 mL TAP liquid medium and transformed using the glass bead method described by Kindle (1990). One of the transformed colonies found positive for ARG7 was selected and used in all the experiments conducted in this study. The selected line will be referred as wild type (WT) in our studies for convenience.

In all other growth and characterization experiments, cells were grown photoautotrophically in high salt (HS) medium containing either 4.0 mM NH_4Cl or 4 mM KNO_3 (Sager and Granick 1953, Harris 2009) in 200 mL glass tubes suspended in temperature controlled aquaria ($28^\circ \pm 1.0^\circ\text{C}$). Cultures were continuously aerated by air that was passed through a sterile cotton plug before being delivered to the bottom of the tube via a thin glass pipe. Cells were maintained under constant irradiance ($150 \mu\text{mol m}^{-2} \text{s}^{-1}$) which was supplied by fluorescent tubes fixed along one side of the aquaria. Irradiance was measured using a light meter (model LI-I89, LI-COR, Lincoln, NE).

Contamination of cultures was identified by routinely plating a small aliquot of culture onto a Luria Broth containing agar plate and incubating overnight at 37°C. Contaminated cultures were discarded.

3.2.2 Generation of knock down cell lines of AOX1

Different artificial miRNA targets specific for AOX1 gene were designed, synthesized as oligonucleotides and cloned into pChlamiRNA3int vector according to the protocol detailed by Molnar et al., (2009). The miRNA targets specific to the 5'UTR region, middle region and 3'UTR region of the AOX1 gene coding sequence were identified using the web designer tool, WMD2 developed by Dr. Weigel's Lab (wmd2.weigelworld.org). Two miRNA targets specific to each region of the gene were synthesized with miRNA backbone nucleotide sequence and later cloned into the plasmid vector for transformation as explained by Molnar et al., (2009). The transformation experiment was performed by vortexing the *Chlamydomonas* cells and plasmid with the glass beads (Kindle 1990). The plasmid vector pChlamiRNA3int contains a phosphotransferase (APHVIII) gene, which confers resistance against the antibiotic paramomycin. To transform the plasmid pChlamiRNA3int, CC4351 (cw15, mt+) strain already transformed with the plasmid pARG7.8 was employed. To screen colonies silenced with the AOX1 gene, individual colonies were collected and transferred into the TAP agar plate containing antimycin A (10 µM), a potent inhibitor of CP respiration. This screening procedure is based on an assumption that colonies that failed to express AOX1 and establish AP respiration, would be severely inhibited in their growth compared to WT cells.

3.2.3 Isolation of membrane fraction for Immunoblotting

Crude membranes were isolated by sonication and differential centrifugation following the protocol described in Pakkiriswami et al., (2009). Cells were pelleted and resuspended in 10 mL of isolation buffer (280 mM mannitol, 100 µM EDTA, 100 mM MOPS-KOH, pH 7.4, 0.1% (w/v) BSA). Then cells were disrupted by three short sonications of 20 s using the ultrasonic cell disrupter

(VirSonic 100, SP Industries Inc.) Then the whole suspension was centrifuged for 4 min at 3000 g. The supernatant which is expected to contain the mitochondrial membranes was decanted into new tubes and subsequently centrifuged at 27000 g for 15 min. The obtained pellet was resuspended in wash buffer (280 mM mannitol, 100 μ M EDTA, 100mM MOPS-KOH, pH 7.4) and again centrifuged at 27000g for 15 min. The final crude membrane pellet was collected and proteins present in the pellet were solubilized in 4% (w/v) SDS and routinely stored at - 20°C. The protein content was determined using the BCATM Protein Assay Kit (Pierce Biotechnology, Thermo Fisher Scientific Corporation).

3.2.4 SDS-polyacrylamide gel electrophoresis and Immunoblotting

SDS-polyacrylamide gel electrophoresis (SDS-PAGE) was carried out using standard protocols using a Bio-rad Mini-Protean II apparatus. Gels were cast using a 12% resolving and 4% stacking gel and each lane was loaded with 25 μ g total protein which was suspended in 2X sample buffer (100 mM Tris pH 6.8, 4% (w/v) SDS, 40% Glycerol, 0.01% (w/v) Bromophenol blue). Total protein content was determined using the BCA Protein Assay Kit (Pierce Biotechnology, Rockford, IL), using the provided bovine serum albumin as a protein standard. Samples in the gel were run at room temperature for approximately 3 hr at a constant voltage of 90v once it reaches the resolving gel. For stacking gel, the voltage was set at 70 for 20-30 min. Gels were routinely run in duplicate with one gel being stained with coomassie blue and the other gel being used for immunoblotting.

For immunoblotting, membrane polypeptides separated by SDS-PAGE were transferred to nitrocellulose membranes (HyBond ECL Nitrocellulose membrane, Amersham Biosciences) using a SDS gel transfer apparatus. Then membranes were blocked with a Tris-buffered saline (TBS) (20mM Tris, 135mM NaCl, pH 7.6) containing 5%(w/v) skim milk powder and 0.1% (w/v) Tween 20 and the immunoblotting was performed as explained in Molen et al., (2006). Membranes were probed with the respective primary antibodies raised against the various

proteins (AOX, COX3, D1, PsaA/B, OEC23, CYTB6F, Lhcb1, Lhcb2, FDX1, RBCL) analyzed in this study. All primary antibodies were obtained from Agrisera AB, Vannas, Sweden and diluted at the recommended rate before usage. After incubation with secondary antibody (1:20000 dilution) conjugated with horse radish peroxidase (Catalog NO: A6154, Anti-Rabbit IgG, Sigma-Aldrich), the antibody- protein complexes were detected by incubation of the blots in ECL Chemiluminescent detection kit (GE healthcare).

3.2.5 Determination of Growth Rate

To measure the growth rate of WT and K26, exponentially grown cultures were inoculated separately into Pyrex glass tubes containing HS-ammonium (HS-A) and HS-nitrate (HS-N) medium. Cultures were collected every 12 hrs and growth was measured spectrometrically as an increase in absorbance at 750 nm (Cary 50 Bio UV-Visible Spectrophotometer, Varian Inc.). The doubling time or generation time was calculated using the formula $t_{\text{gen}} = .693/\mu$ (μ -represents the specific rate constant). The value of the slope of the curve was substituted for specific rate constant to find the generation time.

3.2.6 Measurement of Photosynthetic O₂ Evolution

Photosynthetic oxygen evolution was measured using a thermostated, aqueous phase Clark-type oxygen electrode (Hansatech Ltd, King's Lynn, UK).

Measurements were carried out using a 1.5 mL aliquot of cells transferred into a closed chamber which was agitated with a magnetic stirrer at 28° C. Before each measurement, 6 μ l of sodium bicarbonate (NaHCO₃ 1M) was added to ensure saturating CO₂ concentration (4mM) inside the chamber. Light response curves were made by exposing the cells to different photon flux densities from 10-1500 $\mu\text{mol m}^{-2} \text{s}^{-1}$. The level of irradiance and exposure time was automated using the oxygraph software associated with the electrode. Photosynthetic rates were calculated as $\mu\text{mol oxygen evolution} [\text{mg (Chl)}^{-1} \text{h}^{-1}]$.

3.2.7 Measurement of Respiration

Respiratory rates were measured as oxygen uptake in the dark at 28° C using the same Clark-type oxygen electrode used for measuring photosynthetic O₂ evolution. The total capacity of electron flow through CP and AP can be determined by the sequential addition of two inhibitors: potassium cyanide (KCN), which inhibits the CP and salicylhydroxamic acid (SHAM) which inhibits the AP. CP capacity was taken to be that portion of the oxygen consumption that could be inhibited by 1 mM KCN in the presence of 2 mM SHAM (Peltier and Thibault 1985). The capacity of AP was taken to be that portion of oxygen consumption inhibited by 2 mM SHAM in the presence of 1mM KCN. Residual respiration after the addition of both inhibitors was subtracted from all measures of total respiration. Stock solution of KCN (1 M) was prepared by dissolving it in sterile water and SHAM (0.45 M) was made by dissolving in ethanol.

3.2.8 Chlorophyll Determination

Aliquots (2 mL) of culture were collected in micro centrifuge tubes and pelleted by centrifugation at 5000 g for 5 min. After the media was aspirated, each cell pellet was resuspended in 1.5 ml of 90% (v/v) acetone and vortexed vigorously for 2 min. Cellular debris was pelleted by centrifugation at 12000 g for 5 min. Total concentration of chlorophyll a and chlorophyll b were determined spectrophotometrically using the supernatant according to the method of Jeffrey and Humphrey (1975).

3.2.9 Low temperature (77K) Fluorescence Measurements

Low temperature (77K) fluorescence emission spectra of *Chlamydomonas* cells were measured using a PTI QM-7/2006 spectrofluorometer (Photon Technology International, South Brunswick, NJ, USA) equipped with a double monochromator, R928P red-sensitive photomultiplier tube (Hamamatsu Photonics, Shizuoka-ken, Japan) and a liquid nitrogen device as described previously (Morgan-Kiss et al., 2008). Cell cultures with chlorophyll concentration of 5 µg/mL were dark adapted at room temperature for 30 min and quickly frozen

in liquid nitrogen in the presence of 30% glycerol before the measurements. Corrected fluorescence emission spectra were excited at 436 nm and recorded from 650 nm to 800 nm using slit width of 2.5 nm for both excitation and emission. All fluorescence spectra were normalized to the PSII emission peak at 695 nm. Deconvolution analysis of the spectra in terms of Gaussian bands was carried out by a non-linear least squares algorithm that minimizes the chi-square function (Morgan-Kiss et al., 2008) using a Microcal™ Origin™ Version 7.0 software package (Microcal Software Inc., Northampton, MA, USA). The fitting parameters for the five Gaussian components, that is, position, area and full width at the half maximum were free-running parameters.

3.2.10 Measurement of P700 Photooxidation

Far-red light induced photooxidation of P700 in *Chlamydomonas* strains was estimated as a change in absorbance around 820 nm ($\Delta A_{820-860}$) using a PAM-101 chlorophyll fluorescence measuring system equipped with a dual wavelength emitter-detector ED-P700DW and PAM-102 units (Heinz Walz GmbH, Effeltrich, Germany) as described in detail earlier (Klughammer and Schreiber, 1994; Ivanov et al., 2012). Samples were prepared as described by Herbert et al. (1995). The relative redox state of P700 was determined in vivo under ambient CO₂ conditions at room temperature. Far-red light (FR; $\lambda_{\text{max}} = 715$ nm, 10 W m⁻², Schott filter RG 715) was provided by a FL-101 light source. After reaching a steady state level of P700⁺ in the presence of FR background, single turn over (half peak width 14 μ s) and multiple turn over (50 ms) pulses of actinic light were applied with a XMT-103 and XST-103 power/control units, respectively, via a multi branched fibre optic system connected to the emitter-detector unit and the cuvette. The spectral data were analyzed in terms of Gaussian bands by a nonlinear least-squares algorithm using a Microcal™ Origin™ Version 7.0 software package (Microcal Software Inc., Northampton, MA, USA).

3.2.11 Measurement of ROS

Intracellular generation of ROS in WT and AOX1 knock down cells were measured using 2',7'-dichlorofluorescein diacetate (H₂DCF-DA) (Maxwell et al., 1999). This nonpolar compound is converted to the membrane-impermeant polar derivative H₂-DCF, which is non-fluorescent but is immediately oxidized by intracellular H₂O₂ and other peroxides to fluorescent DCF (Zhu et al., 1994). Dichlorofluorescein fluorescence was determined using a microplate spectrofluorometer (Molecular Devices Spectra Max Gemini). Before loading the microplate into the fluorometer, excitation and emission wavelengths were set at 488 nm and 520 nm for the measurement. Cells were grown in HS-A and HS-N and treated with H₂DCF-DA. After 15 min exposure, cells were pelleted and resuspended with fresh growth medium treated with antimycin A, 10 µM. For the measurement, samples were transferred to the 96-well microplate and placed in the spectrofluorometer for the fluorescence reading. Three biological replicates for each treatment or condition were used for the analyses.

3.2.12 RNA extraction and Quantitative Polymerase Chain Reaction (qPCR)

For RNA isolation, 40 mL of cells harvested by centrifugation in 50 ml disposable centrifuge tubes was immediately frozen in liquid nitrogen and stored at -80°C. RNA was extracted using a modified hot phenol method described by Molen et al., 2006.

One mL of a hot (80°C) phenol/extraction buffer (P/EB) solution was added to the 40 mL of frozen pellet collected by centrifugation. The P/EB extraction reagent consisted of one-part buffered phenol (pH 6.8) and one-part extraction buffer (1 M LiCl, 10 methylenediaminetetraacetic acid (EDTA), 1% SDS, 0.1 M Tris pH 8.0). Before vortexing the cells with the extraction reagent, (v/v) betamercaptoethanol and 4% (w/v) polyvinylpyrrolidone was added to the mixture. Then 0.5 mL of 24:1 (v/v) chloroform: isoamyl alcohol was added and vortexed for one minute. Immediately after, mixture was

transferred to a microfuge and centrifuged at 16 000 *g* for 10 min at room temperature to collect the supernatant. The aqueous phase collected was used to selectively precipitate RNA by the addition of 1 vol. of 4 M LiCl. Then the whole mixture was stored at -20°C for at least 2 h, RNA was pelleted at 16 000 *g* for 10 min at room temperature. For final purification, the RNA pellet was dissolved in 400 µl of diethyl pyrocarbonate (DEPC)-treated water and precipitated using standard ethanol precipitation. The precipitated RNA was centrifuged to remove the supernatant and air dried to quantify using spectrometry.

Complementary DNA (cDNA), primed by oligo dT was prepared with the action of Superscript II Reverse Transcriptase (SS II RT) as described in Chapter 2, Material and Methods section 2.2.3 and used in the quantitative PCR. The amplification was performed in CFX96™ touch system (Bio-Rad laboratories) with qPCR reagents of iTaq Universal SYBR® Green Super mix qPCR kit (Bio-Rad Laboratories). All reactions contained the vendor's super mix, 200nm of each gene specific primer, and cDNA from WT or AOX1 knock down cells grown in HS-A or HS-N growth medium. The primers are designed as per the guidelines suggested by Bio-Rad Laboratories. The primers designed using PRIMER3 algorithm are listed in Appendix S2. The reaction was performed as per the manufacturer's protocol: 95°C for 5min, followed by 95°C for 15s, 65°C for 30s, 72°C for 30s up to a total of 40 cycles. The $2^{-\Delta\Delta CT}$ method was used to analyze the data (Livak and Schmittgen, 2001). The product was analyzed later by gel electrophoresis to verify that it represented the gene of interest based on its size. The final data are presented as fold change in mRNA abundance, normalized to an endogenous reference gene, ubiquitin ligase (UBL) (Montaigu et al., 2010). The accumulation of endogenous gene mRNA did not vary between the WT and AOX1 knock down cells.

3.3 Results

3.3.1 Isolation of AOX1 knockdown cell lines

A strain of *Chlamydomonas* lacking AOX1 gene expression (often referred to as a "knockdown") was generated using the RNA interference (RNAi) method described by Molnar et al., (2009). Briefly, cells were transformed with a DNA construct that generates microRNAs, which would bind to the native AOX1 transcript causing its degradation. This results in very low or undetectable levels of AOX protein being produced through translation.

The RNAi constructs containing the AOX1 artificial miRNA targets were produced by cloning gene specific DNA fragments into the plasmid vector pChlamiRNA3int. This plasmid contains a novel phosphotransferase (APHVIII) gene, which confers resistance to the antibiotic paramomycin on cells that take up the construct (Molnar et al., 2009). The transformation of cloned pChlamiRNA3int vector with amiRNA targets was carried out in the strain CC4351 (cw15, mt⁺) using the glass bead method and plated on growth medium containing the selectable marker, paramomycin. After about one week, cells successfully transformed with pChlamiRNA3int could be visualized as individual colonies.

To identify AOX1 silenced strains, individual colonies were picked and transferred to fresh TAP agar plates containing antimycin A (10 μ m), a potent inhibitor of CP respiration. This screening protocol is based on the understanding that strains unable to express AOX1 and thus unable to synthesize AOX and establish AP respiration, would be severely inhibited in their growth compared to WT cells on plates containing antimycin A.

After allowing colonies to grow up for two weeks, three clear phenotypes became apparent: colonies that could grow as well as WT cells in the presence of antimycin A, a second that showed clear inhibition of growth and a third phenotype where growth was almost completely arrested (Figure 3.1A). It was assumed that strains that showed the strongest inhibition of growth on AA lacked AP respiration due to the strong silencing of AOX1 gene expression. This

assumption was tested by growing up a number of these strains in liquid HS or TAP medium containing nitrate as the sole nitrogen source. Using cell extracts, the abundance of AOX was determined through western blotting using a polyclonal antibody raised specifically against the *Chlamydomonas* AOX protein. As shown in Figure 3.1C, the expression of AOX varied widely among the different lines, which reflected the variability in gene silencing. The difference in the strength of silencing observed among the transgenic lines could be attributed to the positional effect of the genomic region, where the plasmid vector is integrated.

For every two hundred original transformants screened there were at least ten colonies showing partial suppression of AOX protein accumulation, as determined through western blot analysis (data not shown). However, strains in which AOX was close to undetected using western blotting were very rare.

Figure 3.1A shows an example of transformed cells re-plated onto agar containing antimycin A. While many lines grew equally well as WT, a small number showed clear growth restriction (Figure 3.1A). Immunoblot analysis on cell extracts of these different strains indicated that the lines that grew most poorly in the presence of AA had very low levels of AOX expression (Figure 3.1C). It was interesting to observe that cells in which AOX1 was not strongly knocked down and thus showed strong AOX abundance were able to grow in the presence of antimycin A which is a strong inhibitor of the CP pathway (Figure 3.1A).

One of the colonies numbered 26, which showed strong inhibition of growth and reduced AOX abundance was selected (Figure 3.1C). In a separate growth experiment, growth of K26 was monitored spectrometrically as a change in the absorbance at 750 nm along with WT and a partially silenced line of

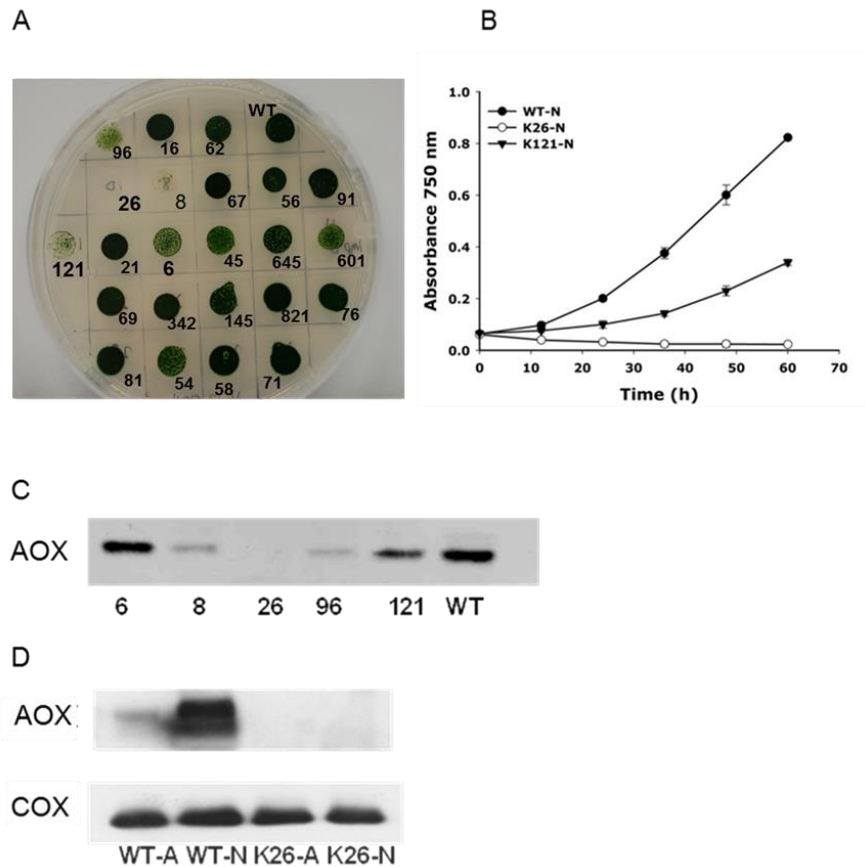


Figure 3.1 Growth characterization and immunoblot analysis of AOX and COX in WT and K26 cells. A) Spotted cell suspensions of individual transformed colonies. The colonies numbered are transformed with pChlamiRNA3int plasmid vector with the AOX1 target sequence. The agar contained nitrate (4 mM) and antimycin A (10 μ M). B) Growth of WT, K26, K121 in TAP liquid medium containing nitrate (WT-N, K26-N) in the presence of antimycin A (10 μ M). C) Immunoblot analysis of AOX protein showing the variation in AOX abundance in various transformed cell lines. D) Immunoblot analysis of AOX and COX protein in WT and K26 (K-knock down) strains grown in ammonium (A) and nitrate (N). Each lane of SDS-PAGE gel contains 25 μ g of protein.

AOX1(K121). Cells were cultured in the liquid growth medium containing nitrate in the presence of antimycin A. As shown in Figure 3.1B, compared to WT, the growth of K121 was restricted moderately; it was completely arrested in K26. This result confirms the previous work in tobacco cells showing the importance of

AP in maintaining respiration rate to support growth in the absence of CP respiration (Vanlerberghe et al., 1997). Figure 3.1D shows the accumulation of AOX in nitrate and ammonium grown cells of WT and the AOX1 knock down line, K26. Compared to WT cells, AOX1 knock down cells showed no accumulation of AOX indicating successful silencing of AOX1 gene expression in K26 strain grown in ammonium and nitrate.

3.3.2 Growth, Photosynthetic Oxygen Evolution and Respiration Characteristics of WT and K26

To determine the effects of decreased AP capacity on cell growth, photosynthesis and respiration, cells were grown under photoautotrophic condition in HS media containing either ammonium or nitrate as the nitrogen source. Unlike the more commonly used TAP medium, which contains a reduced carbon source (acetate), HS is a minimal medium that, while resulting in slower growth, it more accurately reflects growth conditions in the natural environment.

Log transformation of OD data was used to determine the exponential portion of the growth curve. During the exponential growth phase, it was found that WT cells grown in either ammonium or nitrate had almost identical generation time of around 8.0 h. Compared to WT, the doubling time of K26 cells in ammonium and nitrate-containing media was reduced by 17% (9.5 h) and 19% (9.6 h), respectively (Figure 3.2).

To further assess the impact of AOX1 silencing in *Chlamydomonas*, whole cell respiration was measured using a Clark-type oxygen electrode. The capacity of the AP to support electron flow was determined under conditions where the CP pathway was blocked using KCN. Alternatively, the capacity of the CP pathway that contributes for electron flow was determined by blocking AP pathway using SHAM. In WT cells, AP capacity accounts for at least 20% of total respiration in ammonium, while in nitrate it contributes nearly 70%. As expected, there was a complete absence of AP respiration in K26 cells grown in either ammonium or

nitrate (Figure 3.3). However, the total respiratory rate of K26 cells, measured in the absence of inhibitors remained similar to the rate observed in WT cells. This data indicates that CP respiration is the only pathway that is functional in the K26 strain. Interestingly, while AP pathway is totally inhibited in the K26 strain, this did not result in an increase of COX 3 abundance, a protein component of cytochrome c oxidase (Figure 3.1D).

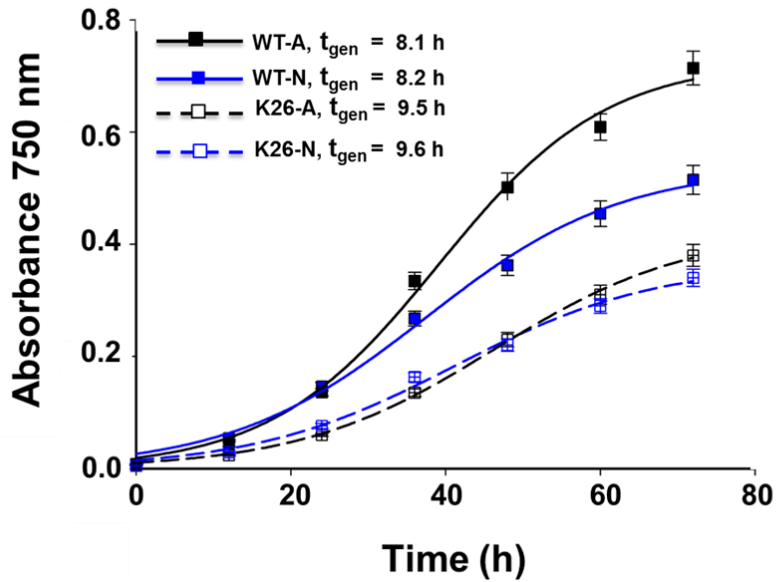


Figure 3.2 Growth of WT (solid line) and K26 (dashed line) strains grown in high salt-ammonium (HS-A) and high salt-nitrate (HS-N) nutrient medium. Growth was measured as an absorbance at 750 nm. Prior to measurements, cells are acclimated to the growth medium. Generation times (t_{gen}) represent the mean of three independent growth curves. Mean \pm SE values are calculated for each curve. Doubling time calculated during log phase cells are significantly different between WT and K26 identified by two-way ANOVA (Post-hoc Tukey test, $P < 0.05$).

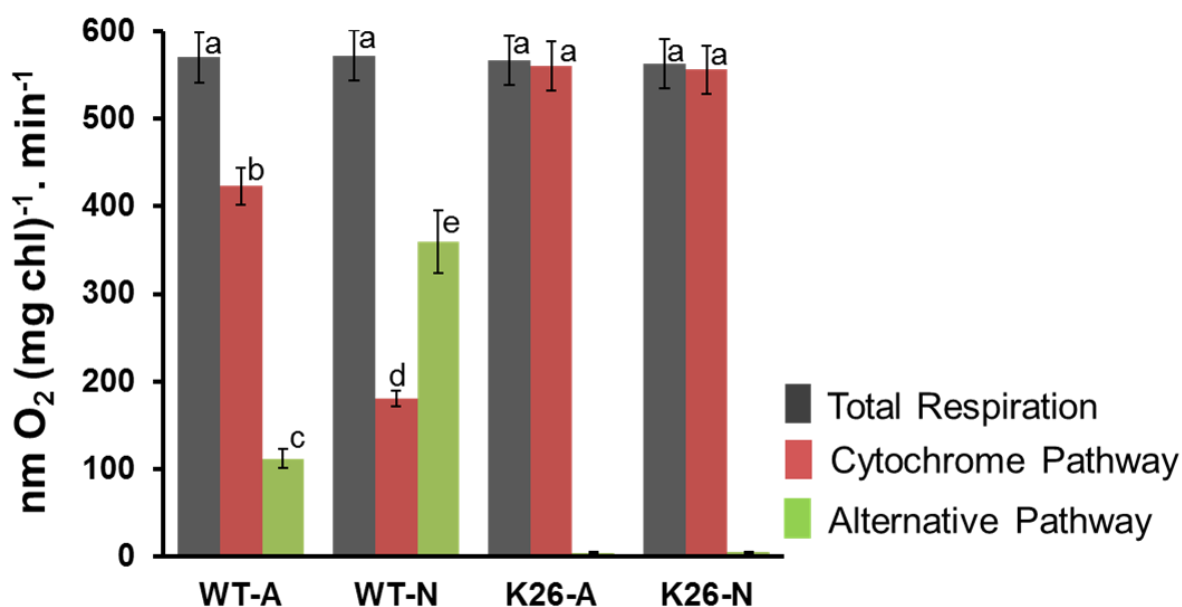


Figure 3.3 Respiration profile of WT and K26 strains. Total respiration, cytochrome pathway (CP) capacity and alternative pathway (AP) capacity in intact WT and K26 cells grown in HS medium containing ammonium (A) or nitrate (N). Data represent the mean \pm SE of four separate experiments. Values identified with different alphabets are significantly different as determined by two-way ANOVA, Post-hoc Tukey test ($P < 0.05$).

To determine whether AOX1 gene silencing has any differential effects on photosynthesis, light response curves for oxygen evolution were determined over a range of irradiances up to $1500 \mu\text{mol.m}^{-2} \text{s}^{-1}$ (Figure 3.4). Light response curves were generated for WT and K26 cells grown in HS-A and HS-N. From these curves, photosynthetic efficiency (apparent quantum yield of oxygen evolution) measured as the initial slope and the maximum rate of photosynthetic oxygen evolution (P_{max}) were calculated according to Falkowski and Raven (2004). The results from three independent experiments revealed that photosynthetic efficiency of K26 measured at lower light intensities is not very different from WT cells (WT-A - 0.55 ± 0.04 ; WT-N - 0.62 ± 0.06 ; K26-A -

0.53±0.07; K26-N – 0.56±0.04) while the maximum rate of photosynthesis (P_{max}) is reduced approximately by 15% and 23% in ammonium and nitrate grown cells respectively (WT-A - 195±4.5; WT-N – 205±5; K26-A – 162±3.5; K26-N – 145±5 $\mu\text{mol O}_2 (\text{mg Chl})^{-1} \text{ h}^{-1}$, Figure 3.4).

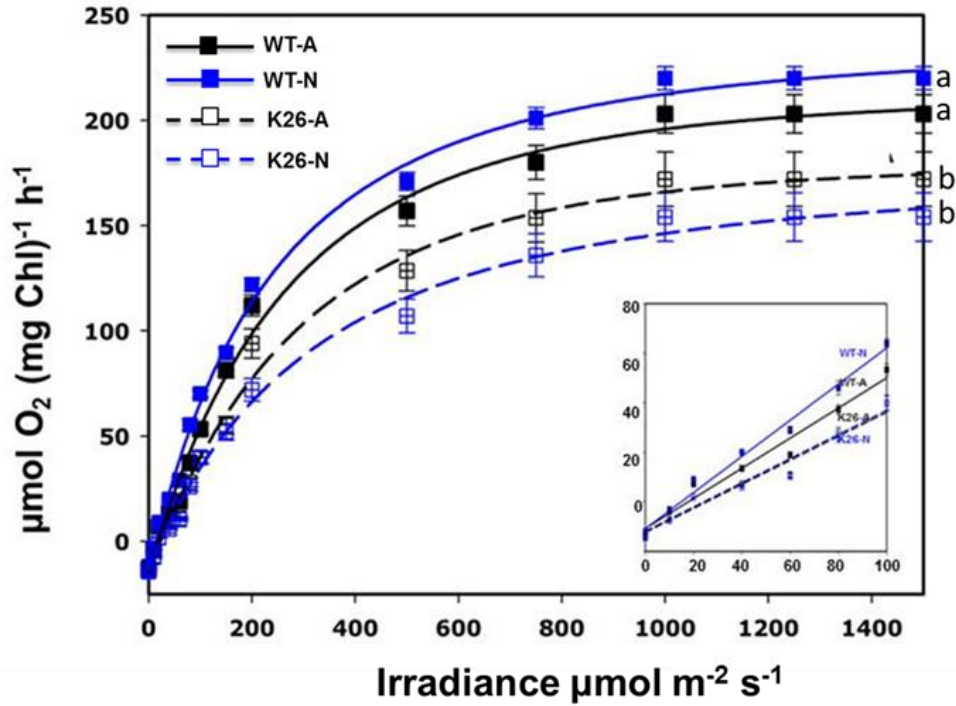


Figure 3.4 Measurement of photosynthetic oxygen evolution in WT and K26. Oxygen evolution measured as a function of irradiance for WT and K26 cells. Strains were cultured in high salt-ammonium (HS-A) and high salt-nitrate (HS-N) and mid-log phase cells were used at a chlorophyll concentration of 3-5 $\mu\text{g. mL}^{-1}$. The data presented is calculated from the means of three independent replicates. P_{max} (the maximum rate of photosynthetic oxygen evolution) values of WT and K26 curves are statistically significant between WT and K26 strains (two-way ANOVA, Post-hoc Tukey test $P < 0.05$). Inset graph shows the oxygen evolution of the cell samples at lower light intensities 10, 20, 40, 60, 80 and 100 $\mu\text{mol m}^{-2} \text{ s}^{-1}$.

3.3.3 Absence of AOX increased ROS abundance

An increase in intracellular ROS production has been shown to be one consequence of reducing the levels of AOX within mitochondria of tobacco cells (Maxwell et al., 1999). To see if this also occurs in *Chlamydomonas*, changes in intracellular ROS formation in WT and K26 strains was investigated with and without the treatment of antimycin A. Antimycin A has been shown in many systems to cause an increase in ROS formation (Maxwell et al., 2002, Vanlerberghe and McIntosh 1997). It is assumed that this occurs from over reduction of ubiquinone and its reaction with superoxide, which forms H_2O_2 .

Using the ROS-sensitive probe dichlorofluorescein acetate (DCF-DA), we found that irrespective of nitrogen form used in the growth medium, knocking down AOX1 in *Chlamydomonas* caused a substantial increase in intracellular ROS abundance (Figure 3.5). In addition, another interesting observation was made between the antimycin A treated WT cells and non-treated K26 cells. The level of increase in ROS generation in WT cells after adding antimycin A is almost equal to the ROS formation detected in the absence of antimycin A in K26 strain. This indicates that the endogenous ROS forming capacity of K26 cells is higher due to the absence of AP respiration in the mitochondria.

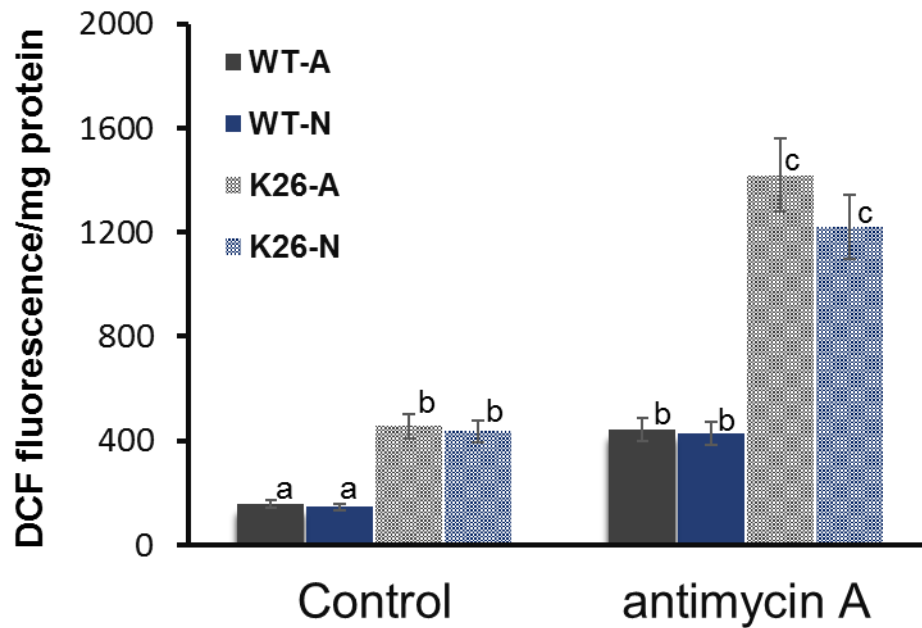


Figure 3.5 Changes in intracellular reactive oxygen species (ROS) abundance in WT and K26 cells. Cells were grown in high salt-ammonium (HS-A) and high salt-nitrate (HS-N) and loaded with 10 μ M dichlorofluorescein diacetate (H₂DCF-DA). After a 15-min incubation, cells were pelleted and resuspended in the respective medium treated with antimycin 10 μ M. Data represent the mean \pm SE of three or four separate experiments. Values significantly different between WT and K26 are denoted by different alphabets (two-way ANOVA, Post-hoc Tukey test, $P < 0.05$).

3.3.4 Nitrate and AOX1 silencing activates Photosynthetic Cyclic Electron Flow

Previous studies in *Arabidopsis* showed that in response to high light, the lack of AOX within the mitochondria affected photosynthetic function in the chloroplast (Yoshida et al., 2011). Although transcript levels of several genes related to antioxidant synthesis, malate-oxaloacetate shuttle, photo respiratory enzymes were increased to maintain redox homeostasis and minimize ROS production,

plants deficient in AOX1a could not sustain photosynthesis compared to WT plants (Yoshida et al., 2011; Dinakar et al., 2010; Vishwakarma et al., 2014).

To determine the effect of reduced AOX abundance on photosynthesis in *Chlamydomonas*, western blotting was performed to monitor the abundance of common proteins of the photosynthetic apparatus of WT and K26 cells (Figure 3.6). Western blot analysis was carried out using the polyclonal antibody specific for the major proteins of PSI (PsaA/B) and PSII (D1) as well as CYTB6F (cytochrome B6f complex, intersystem electron carrier), and PETF/FDX1 (ferredoxin), light harvesting proteins (Lhcb1, Lhcb2) with RBCL (large subunit of RUBISCO) as internal control.

For most of the proteins, their abundance did not change in K26 cells, as compared to WT, or in response to a change in nitrogen source. Two exceptions to this were found for PsaA, a component of the reaction center of PSI and CYTB6F, a component of the intersystem CYTB6F complex. The abundance of PsaA was lower in knockdown line irrespective of the nitrogen source (Figure 3.6), while the abundance of CYTB6F was lower only in K26 cells grown in ammonium.

The changes to PsaA and CYTB6F abundance seen in response to a change in nitrogen source and/or the knockdown of AOX1 expression suggested that a major site of altered function was associated with PSI. This line of inquiry was explored further by assessing the abundance of ferredoxin (FDX), a protein that acts as an intermediary between electron flow from PSI and a range of downstream electron acceptors including NADPH reductase. *Chlamydomonas* has six plant type (Fe_2S_2)

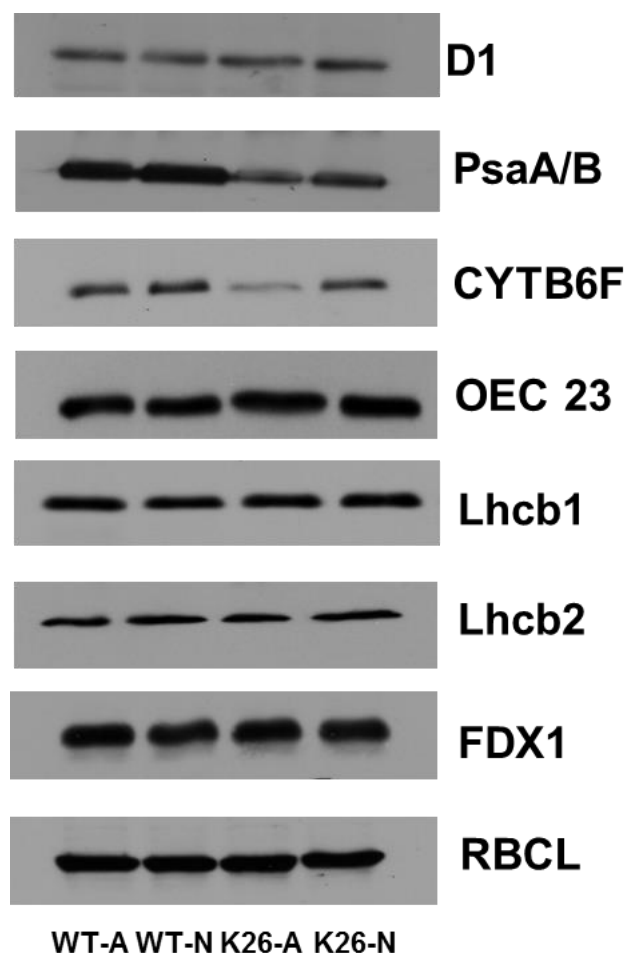


Figure 3.6 Representative Immunoblots showing the abundance of various photosynthesis-related proteins in WT and K26 strains grown in ammonium (A) or nitrate (N) containing media. D1, a protein component of PSII; PsaA/B, a protein component of PSI; CYTB6F, intersystem electron carrier; OEC23, oxygen evolving complex; Lhcb1&Lhcb2, light harvesting complex proteins; FDX1, ferredoxin; RBCL, large subunit of RUBISCO protein. Each lane of SDS-PAGE gel contains 25 µg of protein.

ferredoxins each being differentially regulated at the gene level by changes in nutrient supply (Terauchi et al., 2009). FDX1, the most common ferredoxin, does not change in cells lacking AOX, or in response to a change in nitrogen source (Figure 3.6). It has been shown that FDX2, a member of ferredoxin protein family was strongly induced by nitrate (Terauchi et al., 2009). This previous finding is in agreement with the data presented in Figure 3.7. The transcript level of FDX2 was largely increased in response to nitrate in both WT and K26 strains. Terauchi et al., (2009) suggested that FDX2 may play the specific role of transferring electrons from PSI to nitrite reductase, supporting the reduction of nitrite to ammonium.

The expression of two additional genes: NDA2 (NADPH dehydrogenase) and PGRL (Proton Gradient Related) were also examined as they play a role in electron transport pathways around PSI (Petroutsos et al., 2009, Jans et al., 2008). As shown in Figure 3.8, in WT cells, the expression of both genes was induced by nitrate. In addition, these two genes were also strongly upregulated in the K26 knockdown line, regardless of the nitrogen source. This result suggests that electron flow around PSI was altered not only by nitrate but also by the decreased capacity of AP respiration.

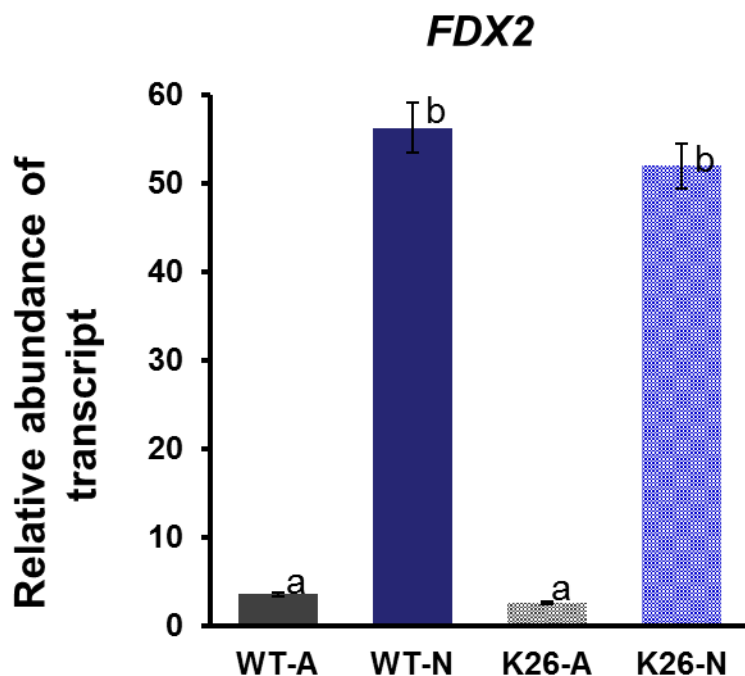


Figure 3.7 Quantitative PCR (qPCR) analysis of the abundance of *FDX2* transcripts in WT and K26 cells grown in ammonium (A) and nitrate (N) containing medium. Values are expression of *FDX2* normalized to the internal reference gene ubiquitin ligase (UBL) and represent the mean \pm SE of at least three biological replicates. Values significantly different are denoted by different alphabets as determined by two-way ANOVA, Post-hoc Tukey test, ($P < 0.05$).

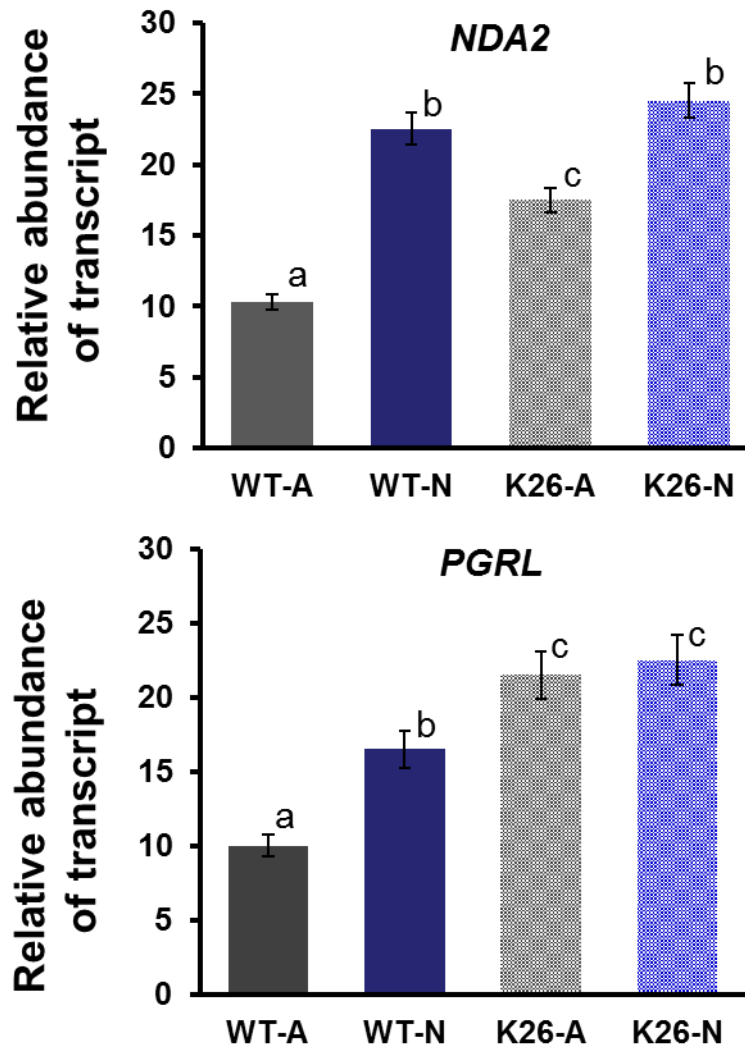


Figure 3.8 Quantitative PCR (qPCR) analysis of the transcript level of NDA2 and PGRL in WT and K26 strains grown in ammonium (A) and nitrate (N) containing medium. Values are expression relative to an internal reference ubiquitin ligase (UBL) and represent the mean \pm SE of at least three biological replicates. Expression levels which are significantly different (two-way ANOVA, Post-hoc Tukey test, $P < 0.05$) are denoted by different alphabets.

To directly investigate the functional changes of PSI in response to a change in nitrogen source or AOX abundance, 77K chlorophyll fluorescence spectroscopy was used to assess potential differences in the energy distribution between PSII and PSI (Weis 1985). At low temperatures (e.g. 77K), characteristic emission spectra of PSI, PSII, and their respective light harvesting complexes (LHCs) can be distinguished. Changes in these spectra have been shown to reflect acclimation to changing conditions such as low temperature (Ivanov et al., 2008) and nutrient availability (Morales et al., 1994; Ivanov et al., 2000 & 2006; Msilini et al., 2013). As shown in Figure 3.9, the 77K fluorescence emission spectrum is dominated by two peaks at 685 nm and 711 nm, which are attributed to emission from PSII and PSI respectively. In WT cells a shift from ammonium to nitrate resulted in a strong increase in PSI emission (711 nm) relative to PSII, resulting in a decrease in the PSII/PSI emission ratio (WT-A – 1.05, WT-N - 0.77; Figure 3.9, Appendix S1). Interestingly in the K26 strain, there was strong PSI emission, regardless of the nitrogen source (K26-A – 0.58, K26-N – 0.53; Figure 3.9, lower panels). The Gaussian parameters for the sub-band decomposition of low temperature (77K) chlorophyll fluorescence emission spectra of wild type WT and K26 strains are presented in Appendix S1.

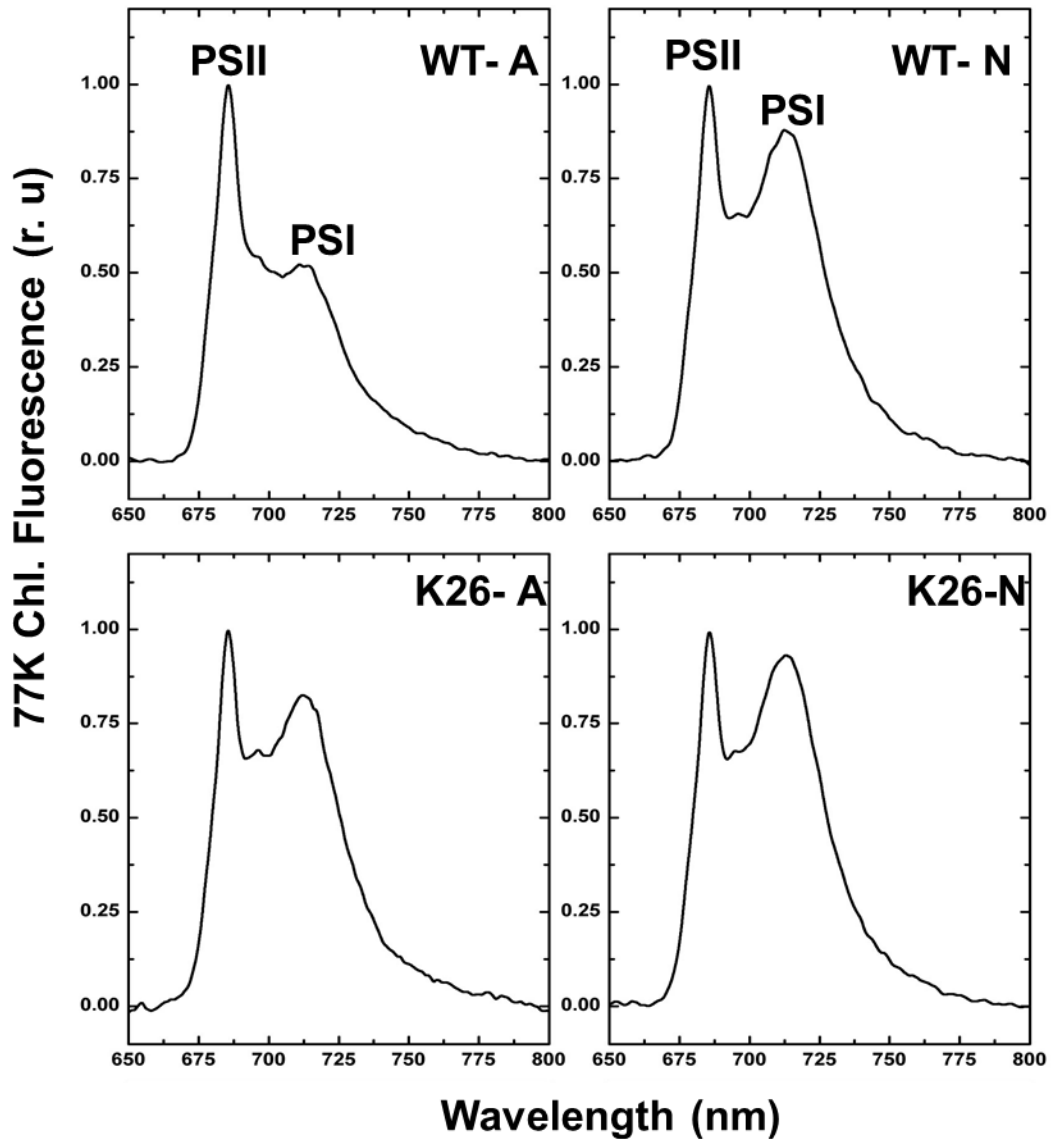


Figure 3.9 Energy distribution between PSII and PSI in WT and K26.77k emission spectra of WT and K26 strains grown in HS medium containing ammonium (A) or nitrate (N) at 28°C. The samples were excited at 436nm and the emission was recorded from 650 nm to 850 nm. Three to four independent readings collected were averaged and used to construct the curve by non-linear least squares algorithm. Chlorophyll concentrations of cell samples were maintained at 5µg/mL for all the measurements.

To measure cyclic electron flow, the rate of reduction of PSI reaction center (chlorophyll P700) was measured spectrophotometrically (see Materials and Methods for details). An example of this measurement is shown in Figure 3.10, which displays typical traces illustrating the oxidation and reduction of P700 in WT cells grown under ammonium (A) and nitrate (B). Illumination of the WT cells with far red light (FR), which preferentially excites PSI, after a short dark exposure results in a change A_{820} ($\Delta A_{820}/A_{820}$) reflecting the oxidation of P700 to P700⁺ (Schreiber et al., 1988). When the FR light is turned off, the kinetics of subsequent P700⁺ reduction in the dark can be used as measure of the rate of cyclic electron transport.

Table 3.1 shows the halftime ($t_{1/2}$) of the reduction of P700⁺ to P700 in the dark for WT and K26 cells grown in ammonium and nitrate. The values represent the rate of electron flow around PSI in milliseconds (ms). In WT cells, the decrease in the $t_{1/2}$ from 2.59 in ammonium to 1.29 in nitrate is consistent with the notion that growth in nitrate increased the rate of cyclic electron transport by one-fold. In K26 cells grown in ammonium, the rate of cyclic electron flow was determined to be approximately 40% greater than WT cells grown in ammonium. Compared to WT cells grown in nitrate the rate of cyclic electron flow in K26 cells in nitrate was found to be 18% greater.

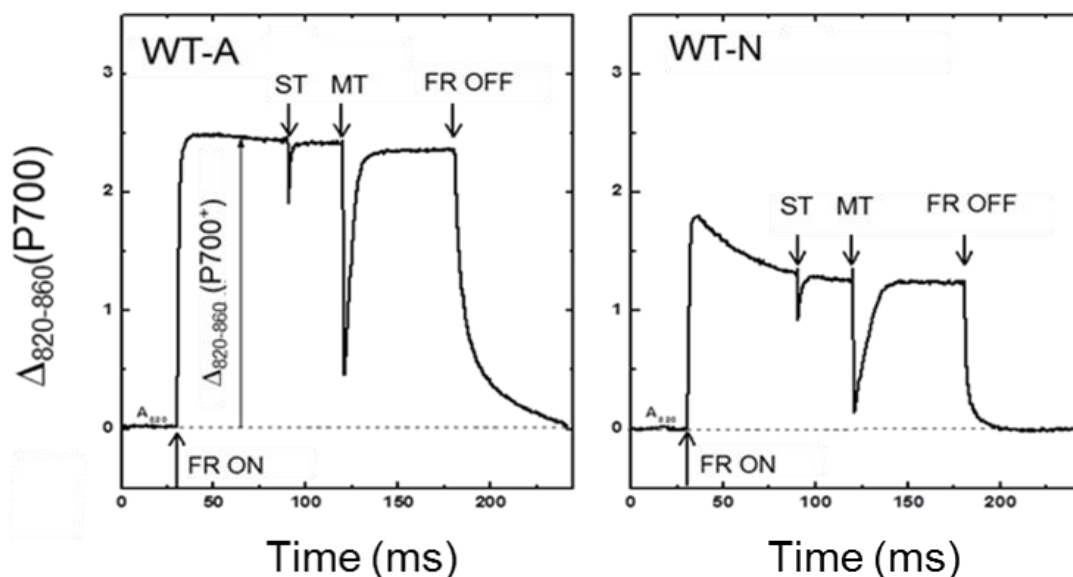


Figure 3.10 Representative traces of the spectrophotometric measurement of the redox state of P700 in WT cells grown in ammonium and nitrate. After reaching a steady state level of P700⁺ in the presence of far-red light (FR ON), single-turnover (ST) and multiple-turnover (MT) flashes were applied that caused the transient reduction of P700. Switching the far-red light off (FR OFF) causes the reduction of P700⁺. The traces were derived from three to four independent experiments.

Table 3.1 Rate of dark reduction ($t_{1/2}$) of P700⁺ in the dark for WT and K26 cells grown in ammonium and nitrate. Data represent the mean \pm SE of four separate experiments. Values identified with different alphabets are significantly different (two-way ANOVA, Post-hoc Tukey test, $P < 0.05$).

Strain	P700 ⁺ , $t_{1/2}$ (ms)
WT-A	2.59 \pm 0.61(a)
WT-N	1.29 \pm 0.09(b)
K26-A	1.47 \pm 0.60(a)
K26-N	1.09 \pm 0.09(d)

3.4 Discussion

Using the technique of RNA interference, the expression of AOX1 was successfully silenced in the *Chlamydomonas* strain CC4351. The genome of *Chlamydomonas* encodes two alternative oxidase genes, AOX1 and AOX2. The nucleotide sequences of these two genes share 50.17 % similarity and there is 57.6% identity at the protein level. Hence artificial microRNA targets designed and selected for AOX1 could potentially target AOX2 if the selected target sequence matched with the gene sequence of AOX2. However, the web based artificial microRNA designing platform took care of this issue by scanning the whole genome to identify the potential so-called "off targets", that would include AOX2 and provided only the target sequences specific for AOX1. So, the selected amiRNA targets, which are cloned and expressed in *Chlamydomonas* cells, were expected to be very specific and bind only the mRNA of AOX1.

The role of AOX2 in *Chlamydomonas* remains unknown as it has been shown to exhibit very low expression that seems to lack inducibility (Molen et al., 2006). In this study, where AOX1 is knocked out there is no evidence that this is compensated by expression of AOX2. In the K26 knocked down line immunoblot analysis using a polyclonal antibody against AOX showed barely detectable protein accumulation. As well, the K26 line showed a complete loss of AP pathway capacity. These data suggest that perhaps AOX2 is a pseudogene (Long and Langley 1993), and thus lacks any real function.

Respiration measurements in WT and K26 cells revealed certain features that seem unique to *Chlamydomonas* as they are not seen in other systems (Baurain et al., 2003, Pakkiriswami et al., 2009, Maxwell et al., 2002, Vanlerberghe and McIntosh 1997). The present study supports previous work (Pakkiriswami et al., 2009) showing that in response to nitrate, there is a large increase in AP capacity accompanied by a substantial decrease in CP capacity. Interestingly, the response of respiration to nitrate observed in *Chlamydomonas* is different from other biotic and abiotic stress factors known to stimulate AP capacity. Specifically, since AP respiration is not coupled to ATP synthesis, high AP

capacity is usually associated with a substantial increase in the overall respiration rate as determined by oxygen consumption (Reviewed in Vanlerberghe et al., 2013). However, in *Chlamydomonas*, the total respiration rate remained relatively constant under nitrate. These data support a previous suggestion that induction of AOX and AP respiration in response to a shift from ammonium to nitrate is a response that is distinct from the typical stress responses known to induce AOX (cold, H₂O₂, antimycin A) (Molen et al., 2006).

A major difference seen in respiration between WT and K26 cells is that in the AOX knockdown strain CP capacity is higher than in WT cells and is insensitive to a change in nitrogen source. This finding is not seen in WT cells, where CP capacity drops substantially when cells are shifted into nitrate containing media. The increase in the CP capacity of nitrate grown K26 cells indicates that cellular respiration in the K26 strain is maintained primarily by the CP respiration to sustain growth and development. Such an increase in the capacity of CP in K26 also suggests that knocking down AOX1 resulted in the modification of metabolome that perhaps removed the partial inhibition of CP capacity observed in WT cells. It has previously been shown in tobacco that the metabolite cysteine is a powerful inhibitor of the CP pathway and acts as a signal to induce increased AOX capacity (Vanlerberghe et al., 2002).

A key limitation of the measurements of AP and CP electron transport performed in this study is this approach measures only the capacity of each pathway and not the actual rate of electron transport that occurs in a specific condition. The capacity of each pathway is determined by blocking the other pathway and then measuring the rate of O₂ consumption. The technique of O₂ isotopic discrimination would need to be used to measure the actual rate of electron transport along either of these pathways under any specific conditions (Guy et al., 1989).

Under optimal growth conditions (150 $\mu\text{mol m}^{-2} \text{s}^{-1}$, 28°C), the lack of AP respiration resulted in a small but significant decrease in growth rate of K26

strain irrespective of the nitrogen source. Compared to *Chlamydomonas*, the knockdown of AOX in different plants had no effect on growth rate when they were grown under near optimal conditions (Vanlerberghe et al., 1997, Yoshida et al., 2011; Vanlerberghe et al., 2016). A decrease in growth rate in AOX knockdown lines was only observed when plants were subjected to stresses such as high light or drought (Yoshida et al., 2011, Vanlerberghe et al., 2016). That AOX deficiency results in a change in growth rate under optimal conditions in *Chlamydomonas* but not plants (Yoshida et al., 2011; Vanlerberghe et al., 2016) may indicate that in the green alga AOX is more closely tied to the metabolism of the entire organism, or rather, there are fewer compensatory changes that can be used in *Chlamydomonas* to counter the knockdown of AOX. Evidence for this comes from the fact that it is only in *Chlamydomonas* that AOX is strongly induced by a shift in nitrogen source from ammonium to nitrate, which as discussed in detail in Chapter 4 results in a total re-sculpting of metabolism. In addition, the decreased growth rate in *Chlamydomonas* in response to AOX1 silencing could be a consequence of the increased ROS formation shown in K26 cells as compared to WT. While increased ROS formation has also been shown in plants where AOX is knocked down (Umbach et al., 2005, Amirsadeghi et al., 2006), it may be the case that *Chlamydomonas* cells are more susceptible to the harmful effects of ROS (e.g. protein denaturation, lipid peroxidation) compared to plants.

The present data provide evidence to support that (i) a shift in nitrogen source from ammonium to nitrate in WT cells or (ii) silencing of AOX expression results in an increase in rate of electron donation to the PQ pool of photosynthetic electron transport through non-photochemical processes (Figure 3.10, Table 3.1). There are two distinct pieces of data that suggest this: First, a shift to nitrate in WT cells or AOX knockdown, results in increase NDA2 transcript abundance. The NDA2 protein is located on the stromal side of the thylakoid membrane and has been implicated in donating electrons from various molecules directly to the PQ pool (Jans et al., 2008). It is unfortunate that in the current study we did not have a NDA2 antibody to measure its abundance directly. Second, based on

previous research (Jans et al., 2008), increased NDA2 activity should result in increased electron flow to PSI, independently of PSII activity. Evidence for increased activity around PSI includes; increased PSI fluorescence emission peak (Figure 3.9), decrease in half-time of re-reduction of P700 (Table 3.1) and increased transcript abundance of PGRL (Figure 3.8), a component of cyclic electron transfer.

The increased PSI fluorescence emission or the shift in energy distribution between PSII and PSI seen under certain conditions as presented in Figure 3.9 is likely caused by a state I to state II transition (Allen 1992). Usually the light harvesting antenna surrounding PSII is larger than that surrounding PSI (State I), but under conditions where more light energy can be utilized by PSI, light harvesting pigment-protein complexes can migrate through the thylakoid and become more closely associated with PSI (State II). Such a shift would be reflected in an altered fluorescence emission as shown in Figure 3.9, where the PSI peak would be higher and thus the PSII to PSI emission ratio is reduced.

Changes to energy distribution between the photosystems triggered by a state transition often reflect a change to electron transport (Ivanov et al., 2000). Photosynthetic electron transport can exist in two distinct modes: in linear electron transport, PS II and PSI operate in series to generate both NAD(P)H and ATP. In cyclic electron transport, electrons are not donated to NADP⁺ but instead are cycled back to reduce the intersystem cytochrome b6f complex (CYTB6F). The effect of this electron flow around PSI is generation of additional ATP at the cost of NADPH.

Increased cyclic electron flow is associated with increased fluorescence emission from PSI. As shown in Figure 3.9, the strong PSI emission peak displayed for WT cells grown in nitrate and K26 cells grown in both ammonium and nitrate suggests conditions that promote increased cyclic electron transport. Besides the fluorescence data, additional data in support of increased cyclic electron flow in WT-N and K26 cells is increased expression of NDA2. This protein has been

shown to donate electrons to the PQ, resulting in its reduction by means other than electron donation from PSII (non-photochemical reduction). It is the over reduction of the PQ pool that has been shown to be a major sensing mechanism triggering a State I to State II transition.

A model is presented in Figure 3.11 to understand the significance of increased expression of NDA2. Besides donating electrons to the PQ pool, NDA2 has been implicated as supplying electrons for nitrite reduction through a unique ferredoxin isoform FDX2 (Terauchi et al., 2009). The proof for this possibility is shown as increased transcript accumulation of the specific ferredoxin FDX2, under nitrate in Figure 3.7. FDX2 has greater affinity for nitrite reductase enzyme and is implicated in supplying the reducing power for nitrite conversion to ammonium (Terauchi et al., 2009).

While we suggest that both WT cells shifted to nitrate and K26 knockdown cells may result in changes that trigger increased NDA2 mediated electron flow to PQ, it is our contention that this is for distinctly different reasons. In WT cells, the shift to nitrate puts increased demand on the chloroplast to generate reductant for nitrate reduction, which occurs within the chloroplast. Increased reductant generation could be achieved by oxidizing various substrates through NDA2, which would result in increased synthesis of NADPH and/or reduced ferredoxin. Testing this hypothesis is the focus of Chapter 4. In contrast, in K26 knock down cells, we speculate that increased NDA2 activity in the chloroplast is not the result of increased reductant generation by this organelle. Rather, it is the result of an increase in the reductant export from mitochondria as intermediates of the citric acid cycle, most notably oxaloacetate. It is important to realize that the pool of reductant in the stroma of the chloroplast is not independent of the pools of related molecules that exist in the cytosol and mitochondrial matrix. Through transporters including the oxaloacetate-malate shuttle, the reducing power can be distributed among chloroplast, mitochondria and the cytoplasm. It is because of this interconnectivity among the three compartments that a change in

respiratory metabolism (loss of AP pathway) could influence processes within the chloroplast.

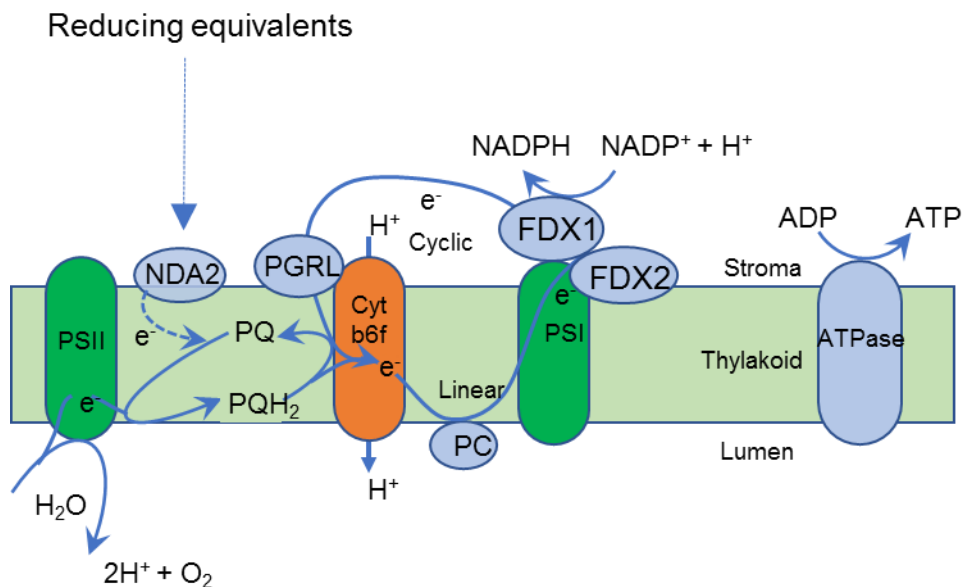


Figure 3.11 Model showing the non-photochemical reduction of PQ pool by the enzymic action of NDA2 complex.

Increased electron donation through NDA2 complex could either be used to increase the cyclic electron flow around PSI or reduce the ferredoxins. PSII- Photosystem II; PSI-Photosystem I; NDA2-NADPH dehydrogenase complex; PGRL-Proton Gradient Related protein; Fd-Ferredoxin; PQ-Plastoquinone (oxidized); PQH_2 -Plastoquinone (reduced); PC-Plastocyanin; ATPase- ATP synthase complex.

3.5 References

- Allen JF (1992) Protein phosphorylation in the regulation of photosynthesis. *Biochim. Biophys. Acta* 1098: 275-335.
- Amirsadeghi S, Robson CA, McDonald AE, Vanlerberghe GC (2006) Changes in Plant Mitochondrial Electron Transport Alter Cellular Levels of Reactive Oxygen Species and Susceptibility to Cell Death Signaling Molecules. *Plant Cell Physiol* 47: 1509–1519
- Asada K, Heber U, Schreiber U (1992) Pool Size of Electrons That Can Be Donated to P700+ As Determined in Intact Leaves: Donation to P700+ from Stromal Components Via the Intersystem Chain. *Plant Cell Physiol* 33: 927–932
- Baurain D, Dinant M, Coosemans N, Matagne RF (2003) Regulation of the Alternative Oxidase Aox1 Gene in *Chlamydomonas reinhardtii*. Role of the Nitrogen Source on the Expression of a Reporter Gene under the Control of the Aox1 Promoter. *Plant Physiol* 131: 1418–1430
- Cerutti H, Ma X, Msanne J, Repas T (2011) RNA-Mediated Silencing in Algae: Biological Roles and Tools for Analysis of Gene Function ▽. *Eukaryot Cell* 10: 1164–1172
- Dinakar C, Raghavendra AS, Padmasree K (2010) Importance of AOX pathway in optimizing photosynthesis under high light stress: role of pyruvate and malate in activating AOX. *Physiologia Plantarum* 139: 13–26
- Dinant M, Baurain D, Coosemans N, Joris B, Matagne RF (2001) Characterization of two genes encoding the mitochondrial alternative oxidase in *Chlamydomonas reinhardtii*. *Curr Genet* 39: 101–108
- Elthon TE, Nickels RL, McIntosh L (1989) Mitochondrial events during development of thermogenesis in *Sauromatum guttatum* (Schott). *Planta* 180: 82–89
- Falkowski PG, Raven JA (2004) Photosynthesis in continuous light. In *Aquatic photosynthesis*. 2nd ed. Princeton University Press, Princeton, N.J. pp. 273–274.
- Guy RD, Berry JA, Fogel ML, Hoering TC (1989) Differential fractionation of oxygen isotopes by cyanide-resistant and cyanide-sensitive respiration in plants. *Planta* 177: 483–491
- Ivanov AG, Krol M, Sveshnikov D, Selstam E, Sandström S, Koochek M, Park Y-I, **Vasil'ev S, Bruce D, Öquist G, et al** (2006) Iron Deficiency in Cyanobacteria Causes Monomerization of Photosystem I Trimers and Reduces the Capacity for State Transitions and the Effective Absorption Cross Section of

Photosystem I in Vivo. *Plant Physiol* 141: 1436–1445

Ivanov AG, Park Y-I, Miskiewicz E, Raven JA, Huner NPA, Öquist G (2000) Iron stress restricts photosynthetic intersystem electron transport in *Synechococcus* sp. PCC 7942. *FEBS Letters* 485: 173–177

Ivanov AG, Rosso D, Savitch LV, Stachula P, Rosembert M, Oquist G, Hurry V, Hüner NPA (2012) Implications of alternative electron sinks in increased resistance of PSII and PSI photochemistry to high light stress in cold-acclimated *Arabidopsis thaliana*. *Photosynth Res* 113: 191–206

Jans F, Mignolet E, Houyoux P-A, Cardol P, Ghysels B, Cuiné S, Cournac L, Peltier G, Remacle C, Franck F (2008) A type II NAD(P)H dehydrogenase mediates light-independent plastoquinone reduction in the chloroplast of *Chlamydomonas*. *PNAS* 105: 20546–20551

Jeffrey SW, Humphrey GF (1975) New spectrophotometric equations for determining chlorophylls a, b, c1 and c2 in higher plants, algae and natural phytoplankton. *Biochem Physiol Pflanz BPP*

Kindle KL (1990) High-frequency nuclear transformation of *Chlamydomonas reinhardtii*. *PNAS* 87: 1228–1232

Klughammer C, Schreiber U (1994) An improved method, using saturating light pulses, for the determination of photosystem I quantum yield via P700⁺-absorbance changes at 830 nm. *Planta* 192: 261–268

Long M, Langley CH (1993) Natural selection and the origin of jingwei, a chimeric processed functional gene in *Drosophila*. *Science* 260: 91–95

Maxwell DP, Nickels R, McIntosh L (2002) Evidence of mitochondrial involvement in the transduction of signals required for the induction of genes associated with pathogen attack and senescence. *The Plant Journal* 29: 269–279

Maxwell DP, Wang Y, McIntosh L (1999) The alternative oxidase lowers mitochondrial reactive oxygen production in plant cells. *PNAS* 96: 8271–8276

Mi H, Endo T, Schreiber U, Asada K (1992) Donation of electrons to the intersystem chain in the cyanobacterium *Synechococcus* sp PCC7002 as determined by the reduction of P700⁺ *Plant cell Physio* 33: 1099–1105

Molen TA, Rosso D, Piercy S, Maxwell DP (2006) Characterization of the alternative oxidase of *Chlamydomonas reinhardtii* in response to oxidative stress and a shift in nitrogen source. *Physiologia Plantarum* 127: 74–86

Molnar A, Bassett A, Thuenemann E, Schwach F, Karkare S, Ossowski S, Weigel D, Baulcombe D (2009) Highly specific gene silencing by artificial

microRNAs in the unicellular alga *Chlamydomonas reinhardtii*. *The Plant Journal* 58: 165–174

Montaigu A de, Sanz-Luque E, Galván A, Fernández E (2010) A Soluble Guanylate Cyclase Mediates Negative Signaling by Ammonium on Expression of Nitrate Reductase in *Chlamydomonas*. *The Plant Cell Online* 22: 1532–1548

Morales F, Abadía A, Belkhouja R, Abadía J (1994) Iron deficiency-induced changes in the photosynthetic pigment composition of field-grown pear (*Pyrus communis* L) leaves. *Plant, Cell & Environment* 17: 1153–1160

Morgan-Kiss RM, Ivanov AG, Modla S, Czymmek K, Hüner NPA, Prisco JC, Lisle JT, Hanson TE (2008) Identity and physiology of a new psychrophilic eukaryotic green alga, *Chlorella* sp., strain BI, isolated from a transitory pond near Bratina Island, Antarctica. *Extremophiles* 12: 701–711

Msilini N, Essemine J, Zaghdoudi M, Harnois J, Lachaâl M, Ouerghi Z, Carpentier R (2013) How does iron deficiency disrupt the electron flow in photosystem I of lettuce leaves? *Journal of Plant Physiology* 170: 1400–1406

Munekage Y, Shikanai T (2005) Cyclic electron transport through photosystem I. *Plant Biotechnology* 22: 361–369

Pakkiriswami S, Beall BFN, Maxwell DP (2009) On the role of photosynthesis in the nitrate-dependent induction of the alternative oxidase in *Chlamydomonas reinhardtii*. *Botany* 87: 363–374

Patel RP, McAndrew J, Sellak H, White CR, Jo H, Freeman BA, Darley-Usmar VM (1999) Biological aspects of reactive nitrogen species. *Biochimica et Biophysica Acta (BBA) - Bioenergetics* 1411: 385–400

Peltier G, Thibault P (1985) O₂ Uptake in the Light in *Chlamydomonas*. *Plant Physiology* 79: 225–230

Petroutsos D, Terauchi AM, Busch A, Hirschmann I, Merchant SS, Finazzi G, Hippler M (2009) PGRL1 Participates in Iron-induced Remodeling of the Photosynthetic Apparatus and in Energy Metabolism in *Chlamydomonas reinhardtii*. *J Biol Chem* 284: 32770–32781

Quesada A, Fernández E (1994) Expression of nitrate assimilation related genes in *Chlamydomonas reinhardtii*. *Plant Mol Biol* 24: 185–194

Quesada A, Galvan A, Fernandez E (1994) Identification of nitrate transporter genes in *Chlamydomonas reinhardtii*. *The Plant Journal* 5: 407–419

Quesada A, Gómez-García I, Fernández E (2000) Involvement of chloroplast and mitochondria redox valves in nitrate assimilation. *Trends in Plant Science* 5: 463–464

- Quesada A, Hidalgo J, Fernández E (1998) Three Nrt2 genes are differentially regulated in *Chlamydomonas reinhardtii*. *Mol Gen Genet* 258: 373–377
- Sager R, Granick S (1953) Nutritional Studies with *Chlamydomonas Reinhardtii*. *Annals of the New York Academy of Sciences* 56: 831–838
- Sakihama Y, Nakamura S, Yamasaki H (2002) Nitric Oxide Production Mediated by Nitrate Reductase in the Green Alga *Chlamydomonas reinhardtii*: an Alternative NO Production Pathway in Photosynthetic Organisms. *Plant Cell Physiol* 43: 290–297
- Schreiber U, Klughammer C, Neubauer C (1988) Measuring P700 Absorbance Changes around 830 nm with a New Type of Pulse Modulation System : *Zeitschrift für Naturforschung C*.
- Terauchi AM, Lu S-F, Zaffagnini M, Tappa S, Hirasawa M, Tripathy JN, Knaff DB, Farmer PJ, Lemaire SD, Hase T, et al (2009) Pattern of Expression and Substrate Specificity of Chloroplast Ferredoxins from *Chlamydomonas reinhardtii*. *J Biol Chem* 284: 25867–25878
- Umbach AL, Fiorani F, Siedow JN (2005) Characterization of Transformed *Arabidopsis* with Altered Alternative Oxidase Levels and Analysis of Effects on Reactive Oxygen Species in Tissue. *Plant Physiol* 139: 1806–1820
- Vanlerberghe GC, Day DA, Wiskich JT, Vanlerberghe AE, McIntosh L (1995) Alternative Oxidase Activity in Tobacco Leaf Mitochondria (Dependence on Tricarboxylic Acid Cycle-Mediated Redox Regulation and Pyruvate Activation). *Plant Physiol* 109: 353–361
- Vanlerberghe GC, Martyn GD, Dahal K (2016) Alternative oxidase: a respiratory electron transport chain pathway essential for maintaining photosynthetic performance during drought stress. *Physiol Plantarum* 157: 322–337
- Vanlerberghe GC, McIntosh L (1994) Mitochondrial Electron Transport Regulation of Nuclear Gene Expression (Studies with the Alternative Oxidase Gene of Tobacco). *Plant Physiol* 105: 867–874
- Vanlerberghe GC, McIntosh L (1997) ALTERNATIVE OXIDASE: From Gene to Function. *Annual Review of Plant Physiol and Plant Molecular Biology* 48: 703–734
- Vanlerberghe GC, Robson CA, Yip JYH (2002) Induction of Mitochondrial Alternative Oxidase in Response to a Cell Signal Pathway Down-Regulating the Cytochrome Pathway Prevents Programmed Cell Death. *Plant Physiol* 129: 1829–1842

Vanlerberghe GC, Vanlerberghe AE, McIntosh L (1997) Molecular Genetic Evidence of the Ability of Alternative Oxidase to Support Respiratory Carbon Metabolism. *Plant Physiol* 113: 657–661

Vishwakarma A, Tetali SD, Selinski J, Scheibe R, Padmasree K (2015) Importance of the alternative oxidase (AOX) pathway in regulating cellular redox and ROS homeostasis to optimize photosynthesis during restriction of the cytochrome oxidase pathway in *Arabidopsis thaliana*. *Ann Bot* 116: 555–569

Weis E (1985) Chlorophyll fluorescence at 77 K in intact leaves: Characterization of a technique to eliminate artifacts related to self-absorption. *Photosynth Res* 6: 73–86

Yoshida K, Watanabe C, Kato Y, Sakamoto W, Noguchi K (2008) Influence of Chloroplastic Photo-Oxidative Stress on Mitochondrial Alternative Oxidase Capacity and Respiratory Properties: A Case Study with *Arabidopsis* yellow variegated 2. *Plant Cell Physiol* 49: 592–603

Yoshida K, Watanabe CK, Terashima I, Noguchi K (2011) Physiological impact of mitochondrial alternative oxidase on photosynthesis and growth in *Arabidopsis thaliana*. *Plant, Cell & Environment* 34: 1890–1899

Zhao T, Wang W, Bai X, Qi Y (2009) Gene silencing by artificial microRNAs in *Chlamydomonas*. *The Plant Journal* 58: 157–164

Zhu H, Bannenberg GL, Moldéus P, Shertzer HG (1994) Oxidation pathways for the intracellular probe 2',7'-dichlorofluorescein. *Arch Toxicol* 68: 582–587

Chapter 4

4 Role of oxidative pentose phosphate pathway in the nitrate dependent induction of AOX

4.1 Introduction

One of the major findings presented in Chapter 3 was that a shift from ammonium to nitrate triggered an increase in cyclic electron flow around photosystem I. Together with the increased expression of NDA2, these data suggest that nitrate may trigger an increase in NADPH generation through pathways besides the light reactions of photosynthesis. It has previously been shown in *Chlamydomonas* and *Selenastrum* that nitrate stimulates the oxidative portion of the pentose phosphate pathway (oxPPP) (Huppe et al., 1992), which results in increased NADPH generation. It was found that this pathway is activated immediately at the onset of photosynthetic nitrate assimilation, whereas ammonium addition had a suppressive effect on its activity (Huppe et al., 1992).

Within the chloroplast the PPP is directly connected to the Calvin cycle, with the reductive phase serving to generate various carbon intermediates, which act as precursors for anabolic reactions. By contrast, the oxPPP converts glucose-6-phosphate to ribulose-5-phosphate with the production of two molecules of NADPH (Hopkins and Huner 2008). In the context of nitrate assimilation, this increased production of reducing power could be (i) transferred to the cytoplasm via metabolic shuttles to fulfill the high reductant demand for nitrate conversion to nitrite (Scheibe 2004) or (ii) used to reduce plastoquinone (Jans et al., 2008) of photosynthetic electron transport and thus contribute to increased ATP synthesis to meet the high energy cost of nitrate reduction within the chloroplast.

In plants, the oxPPP has been shown to supply necessary reducing power to support nitrate assimilation in non-photosynthetic tissues, including roots (Redinbaugh and Campbell 1998). In *Arabidopsis*, the requirement of plastidial oxPPP for nitrate assimilation was studied using the knockout mutant of the

oxPPP enzyme phosphogluconolactonase dehydrogenase (PGL3-1), which converts 6-phosphogluconolactone to ribulose-5-phosphate (Bussell et al., 2013). Based on that study it was concluded that oxPPP metabolites could act as signal molecules that can influence the expression of nitrate assimilation related (NAR) genes in the root cells. In addition, the specific inhibition of the oxPPP by glycerol or 6-aminonicotanamide was shown to modulate nitrate transporter gene expression in *Arabidopsis* roots (Lejay et al., 2008). From these findings, one can infer that in photosynthetic eukaryotes, oxPPP activity and NAR genes expression are tightly coupled to facilitate efficient nitrate assimilation.

The previous finding that the oxPPP is upregulated by nitrate in *Chlamydomonas* (Huppe et al., 1992) and that metabolites of the oxPPP can regulate NAR gene expression (Bussell et al., 2013; Lejay, et al., 2008), suggest that the oxPPP and NAR genes expression are tightly linked. This can be extended to include AOX1 (which is a NAR gene), which could be regulated by metabolite signals from the chloroplast or through changes in mitochondrial function in response to metabolic alterations in the chloroplast.

That the metabolism of the chloroplast and the mitochondrion are linked has been shown recently by the work of Dang et al. (2014). Plants deficient in PGRL1 a protein that mediates cyclic electron flow in the chloroplast were found to have a low growth phenotype only when respiratory electron transport was inhibited by antimycin A (Dang et al. 2014). Further support for tight metabolic linkage between these energy-transducing organelles comes from the analysis of mutants defective in CP respiration (Cardol et al., 2003). The reduction in mitochondrial ATP generation was found to be countered by a compensatory increase in the rate of photosynthetic electron transport. A common feature of these mutants is a stimulation of cyclic electron flow in the chloroplast, resulting in increased ATP generation (Cardol et al., 2003).

In the current study, the induction of AP respiration in response to a shift from ammonium to nitrate may be a result of increased activation of the oxPPP and

photosynthesis within the chloroplast. Specifically, nitrate may trigger an increase in ATP generation in the chloroplast by redirecting more reductants into photosynthetic electron transport obtained from the stimulation of oxPPP which would be compensated by the induction of AOX and concomitant decrease in ATP production within the mitochondria. This possibility was explored by taking a global metabolomics approach. By analyzing the changes to the major metabolites in both WT and K26 knockdown cells grown in ammonium and nitrate it should be possible to determine the overall metabolic rearrangement that has occurred in K26 cells including the metabolites specific to oxPPP.

4.2 Material and Methods

4.2.1 Analysis of cell metabolome by GC-MS method

Three biological replicates of WT and K26 cells grown in HS-ammonium and HS-nitrate growth medium were collected in the logarithmic growth stage and sent to West Coast Metabolomics Center (UC Davis Genome Center, Davis, CA 95616) for metabolite analysis based on GC-MS method (Lee and Fiehn, 2008). A total of 412 unique metabolic signatures were detected, 167 of which identified were used for data analysis. Multivariate statistics analysis of mass spectral data was performed using the Metaboanalyst 3.0, a software platform dedicated for metabolite analysis (Xia and Wishart (2016); www.metaboanalyst.ca).

Multivariate statistical method, principal component analysis (PCA) and partial least square discriminant analysis (PLS-DA) were used to project the variation in the abundance of various metabolites in WT and K26 cells resulted due to the change in nitrogen source and AOX absence (Eriksson et al., 2006). The scores and loading plot of PCA were obtained and used to present the overall pattern of accumulation of metabolites between the treatments. Variable importance in projection (VIP) scores determined through partial least square discriminant analysis method were used to identify the specific metabolites that contribute to the variation between the groups. Metabolites with the VIP score of more than 1.0 are considered for the analysis (Eriksson et al., 2006). Two-way ANOVA statistical technique was performed using Sigma Plot 14.0 to identify the data significance.

4.2.2 RNA extraction and Quantitative Polymerase Chain Reaction

For RNA isolation, 40 mL of cells harvested by centrifugation in 50 ml disposable centrifuge tubes was immediately frozen in liquid nitrogen and stored at -80°C. RNA was extracted using a modified hot phenol method described by Molen et al., 2006.

One mL of a hot (80°C) phenol/extraction buffer (P/EB) solution was added to the 40 mL of frozen pellet collected by centrifugation. The P/EB extraction

reagent consisted of one-part buffered phenol (pH 6.8) and one-part extraction buffer (1 M LiCl, 10 methylenediaminetetraacetic acid (EDTA), 1% SDS, 0.1 M Tris pH 8.0). Before vortexing the cells with the extraction reagent, (v/v) betamercaptoethanol and 4% (w/v) polyvinylpyrrolidone was added to the mixture. Then 0.5 mL of 24:1 (v/v) chloroform: isoamyl alcohol was added and vortexed for one minute. Immediately after, mixture was transferred to a microfuge and centrifuged at 16 000 *g* for 10 min at room temperature to collect the supernatant. The aqueous phase collected was used to selectively precipitate RNA by the addition of 1 vol. of 4 M LiCl. Then the whole mixture was stored at -20°C for at least 2 h, RNA was pelleted at 16 000 *g* for 10 min at room temperature. For final purification, the RNA pellet was dissolved in 400 µl of diethyl pyrocarbonate (DEPC)-treated water and precipitated using standard ethanol precipitation. The precipitated RNA was centrifuged to remove the supernatant and air dried to quantify using spectrometry.

Complementary DNA (cDNA), primed by oligo dT was prepared with the action of Superscript II Reverse Transcriptase (SS II RT) as described in Chapter 2, Material and Methods section 2.2.3 and used in the quantitative PCR. The amplification was performed in CFX96™ touch system (Bio-Rad laboratories) with qPCR reagents of iTaq Universal SYBR® Green Super mix qPCR kit (Bio-Rad Laboratories). All reactions contained the vendor's super mix, 200nm of each gene specific primer, and cDNA from WT or AOX1 knock down cells grown in HS-A or HS-N growth medium. The primers are designed as per the guidelines suggested by Bio-Rad Laboratories. The gene specific primers used for qPCR analysis of GLD1 and PGL are listed in the Appendix S2. The reaction was performed as per the manufacturer's protocol: 95°C for 5min, followed by 95°C for 15s, 65°C for 30s, 72°C for 30s up to a total of 40 cycles. The $2^{-\Delta\Delta CT}$ method was used to analyze the data (Livak and Schmittgen, 2001). The product was analyzed later by gel electrophoresis to verify that it represented the gene of interest based on its size. The final data are presented as fold change in mRNA abundance, normalized to an

endogenous reference gene, ubiquitin ligase (UBL) (Montaigu et al., 2010). The accumulation of endogenous gene mRNA did not vary between the WT and AOX1 knock down cells.

4.2.3 Glycerol treatment and protein blot analysis of AOX and COX

For glycerol treatment, WT and K26 cells were cultured to a logarithmic growth phase and shifted to fresh growth medium before adding glycerol (30 mM). Cell samples were collected after 8h of glycerol treatment and the abundance of AOX and COX protein was monitored using the western blot analysis as described in the Material and Methods section 3.2.3 and 3.2.4 of Chapter 3. Glycerol is used to inhibit the function of the enzyme, hexose phosphate isomerase which is involved in the formation of glucose-6-phosphate (Le Jay et al., 2008)

4.3 Results

4.3.1 AOX1 silencing alters the effect of nitrate on the cell metabolome

There is a large body of literature from both plants and algae detailing the metabolic alterations that occur in response to a change in nitrogen source from ammonium to nitrate (Geiger et al., 1999, Masakapalli et al., 2013). The goal of the current experiment was to assess the extent to which these changes in metabolites are solely dependent upon nitrate or influenced by the cell's ability to upregulate AOX and AP respiration.

Metabolite analysis was performed using whole cell extracts of WT and K26 cells grown in either ammonium or nitrate. To determine the effect of a change in nitrogen source and knocking down AOX on the accumulation of specific metabolites, pairwise comparisons of the following metabolomes was conducted: (i) WT-A was compared with WT-N to elucidate the metabolite changes in response to a change in nitrogen source; (ii) WT-N was compared to K26-N to identify the metabolite changes between the two genotypes. Evaluation of the metabolite differences between these two groups (WT-A/WT-N and WT-N/K26-N), allows one to determine those metabolites that are altered by nitrate as distinct from AOX knockdown. The metabolites that showed significant changes in abundance between the metabolomes were identified using variable importance projection (VIP) scores calculated by the multivariate statistics method partial least square-discriminant analysis (Eriksson et al., (2006) Xia and Wishart 2016).

The Venn diagram presented in Figure 4.1A compares the metabolites changed in response to a shift from ammonium to nitrate in WT cells (WT-A/WT-N) to the metabolites changed in response to knocking down AOX1 in nitrate (WT-N/K26-N). Of the 30 metabolites that are shared between the groups only two, aspartic acid and pentitol seemed to be regulated solely by nitrate (Figure 4.1B). This conclusion is based on the finding that, compared to WT-A cells, growth in nitrate

resulted in decreased levels of both metabolites, regardless of genotype (WT-N or K26-N). The data also indicates that 13 of these 30 metabolites are strongly induced in WT cells by a shift into nitrate medium, but these changes seem to be dependent upon the ability to upregulate AOX expression (Figure 4.1B). One can infer this because the abundance of these metabolites is not increased in K26-N cells. The other major finding was that 12 metabolites were found to have lower levels in WT cells grown in nitrate (WT-N) as compared to ammonium (WT-A) (Figure 4.1B). Again, this shift in abundance seems to be dependent upon the presence of AOX, as this downregulation was not seen in AOX knockdown cells (K26-N).

To visualize the clustering pattern of all four different metabolomes, Principle Component Analysis (PCA), another multivariate statistics method was employed. Figure 4.2 is the scores plot created by analyzing the metabolomics data obtained from three biological replicates of WT and K26 cells grown in ammonium and nitrate. As shown by the data presented in Figure 4.2, PC1 clearly delineated the two different genotypes (WT and K26). Alternatively, PC2 separated the metabolome of WT cells grown in ammonium from WT cells grown in nitrate (Figure 4.2). Interestingly, PC2 also showed that the two K26 treatments were not separated but rather formed a distinct cluster.

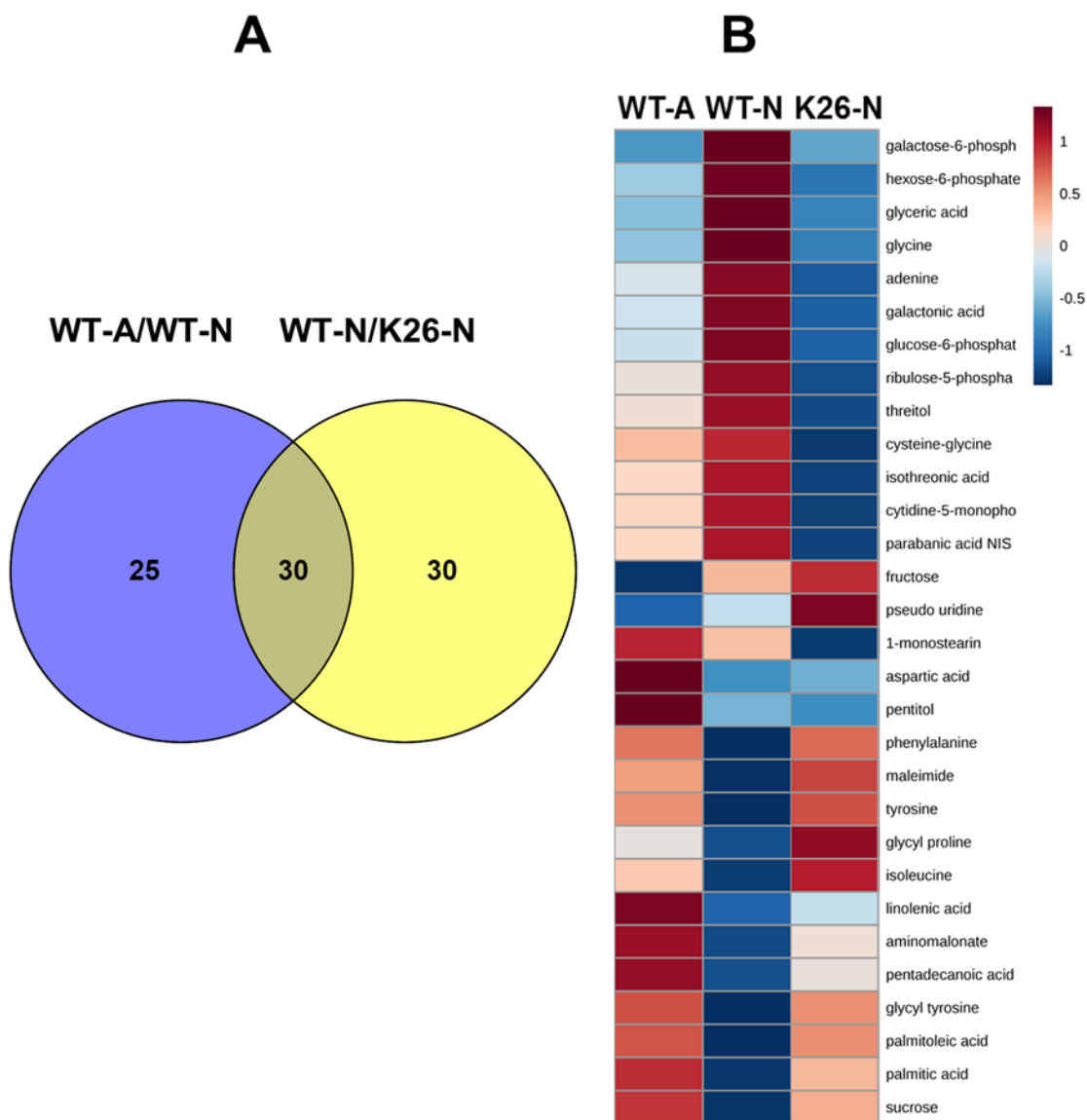


Figure 4.1 Venn diagram analysis and Heat map construction for metabolites altered in their status in WT and K26 in response to nitrate. (A) Two-way Venn diagram showing the number of common and unique metabolites that are changed in their abundance (either up or down regulated) in WT and K26 cells with respect to nitrate. (B) Heat map of 30 metabolites identified that are found to be modulated in their accumulation in the presence of nitrate in the absence of AOX. The average values from the three biological replicates are used to develop the heat map.

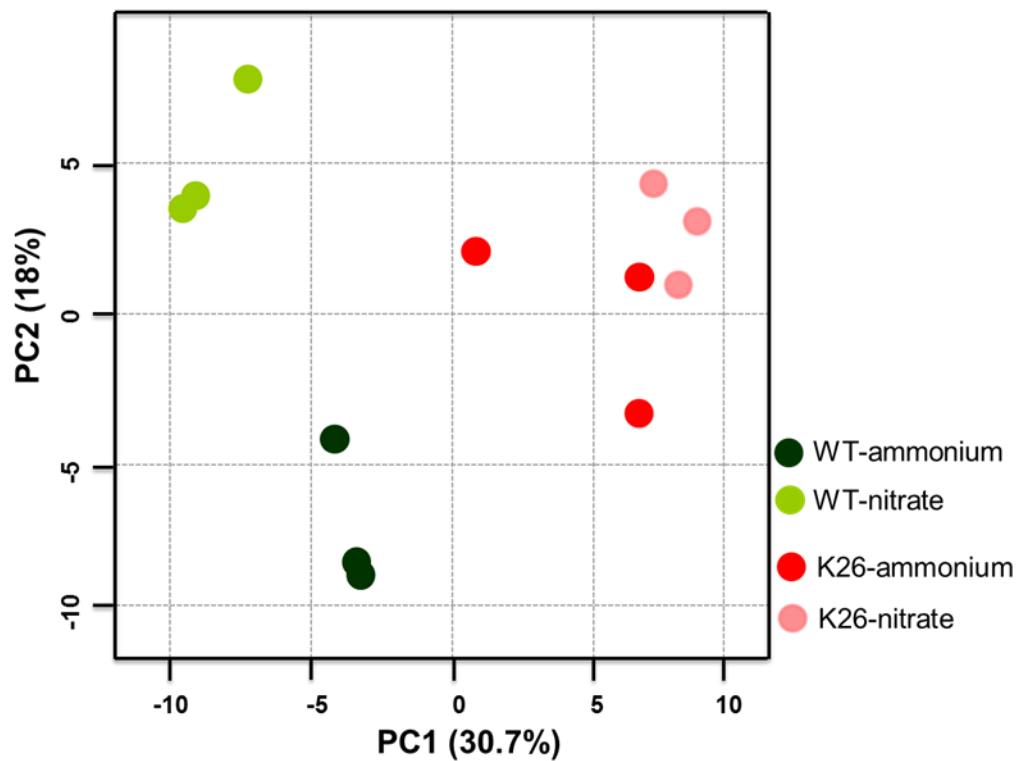


Figure 4.2 PCA scores plot showing the separation of the metabolome of WT and K26 cells grown in ammonium and nitrate. Each colored dot in the plot represents one replicate of each treatment class. Three biological replicates are used for each treatment class. PCA method was performed via Metaboanalyst 2.0, a specific statistics platform for metabolite data analysis.

To determine the specific metabolites that contributed to the distribution of all four classes as shown on the PCA scores plot, the PCA loading plot was examined. As shown in Figure 4.3, each dot in the loading plot represents one metabolite and the relative position of each metabolite in the plot indicates its level of influence on the separation of different groups (Xia and Wishart 2016). The metabolites located on the outmost area of the loading plot contribute strongly along the direction of separation as identified in the corresponding PCA score plot (Figure 4.2).

The metabolites that contributed most to the variation in PC1 (30%), and thus able to separate the two genotypes, were located and identified in the loading plot (red ovals). Knocking down AOX in *Chlamydomonas* increased the abundance of dehydroascorbic acid, threonic acid (a derivative of ascorbic acid), galactinol, uric acid, spermidine and citrulline. In addition, metabolism of various amino acids (cysteine, glycine, threonine, valine, and isoleucine), sugar derivatives (levoglucosan, myo-inositol) was altered by knocking down AOX.

The major metabolites that were found to accumulate specifically in K26 cells (dehydroascorbic acid, citrulline, spermidine, threonic acid, uric acid) have all been implicated in playing a role in the cell's antioxidant defense. The increased accumulation of dehydroascorbic acid most likely reflects stimulation in the activity of ascorbate peroxidase, a key hydrogen peroxide scavenging enzyme. The role of the other metabolites particularly citrulline, spermidine and uric acid in response to oxidative stress is not established yet in *Chlamydomonas*, although there is clear evidence for their potential roles in scavenging reactive oxygen species in *Arabidopsis* and other plants (Akashi et al., 2001, Brychkov et al., 2008).

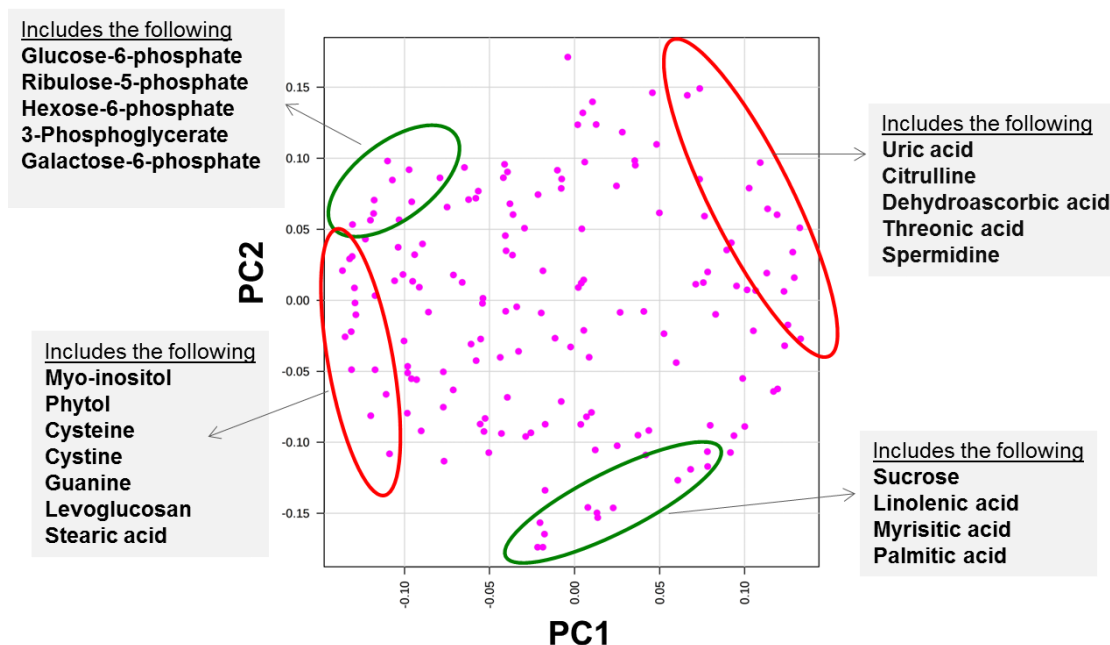


Figure 4.3 PCA Loading plot showing metabolites that contribute to the variation for PC1 and PC2. Each colored dot represents one metabolite. Metabolites positioned well away along the direction of separation of different groups as identified in the scores plot strongly contribute for the variation. The metabolites that contributed the most to the variation between WT and K26 are marked by red ovals and metabolites that contributed the most to the variation between nitrogen sources in WT cells are demarked by green ovals.

The metabolites that distinguished the metabolome of WT cells grown in ammonium as compared to nitrate are positioned in the top left and bottom right quadrant of the loading plot. These metabolites contribute towards the variation in PC2 (18%) and are circled by green ovals for identification. The levels of accumulation of these metabolites are either decreased or increased in response to the change in nitrogen source in WT cells. It was found that sugar derivatives (glucose-6-phosphate, ribulose-5-phosphate, hexose-6-phosphate and galactose-6-phosphate) are the metabolites that contribute positively to PC2, while fatty acids (myristic acid, palmitic acid and linolenic acid) contribute negatively for the separation displayed for PC2.

The abundances of a range of metabolites were found to change in response to a shift in nitrogen source in WT cells. However, significant changes were not seen in K26 cells in response to the change in nitrogen source. From the loading plot it can be seen that in response to nitrate there is an increase in the abundance of core sugar phosphates in WT cells. Figure 4.4, shows the abundance of hexose-6-phosphate, galactose-6-phosphate and glucose-1-phosphate. There are three clear trends one can observe in this data (i) except for glucose-1-phosphate, the shift to nitrate in WT cells increased the metabolite abundance (ii) K26 cells in ammonium had similar levels to WT cells in ammonium and (iii) unlike WT cells, in K26 cells, a shift to nitrate did not result in increased accumulation of the sugar phosphate.

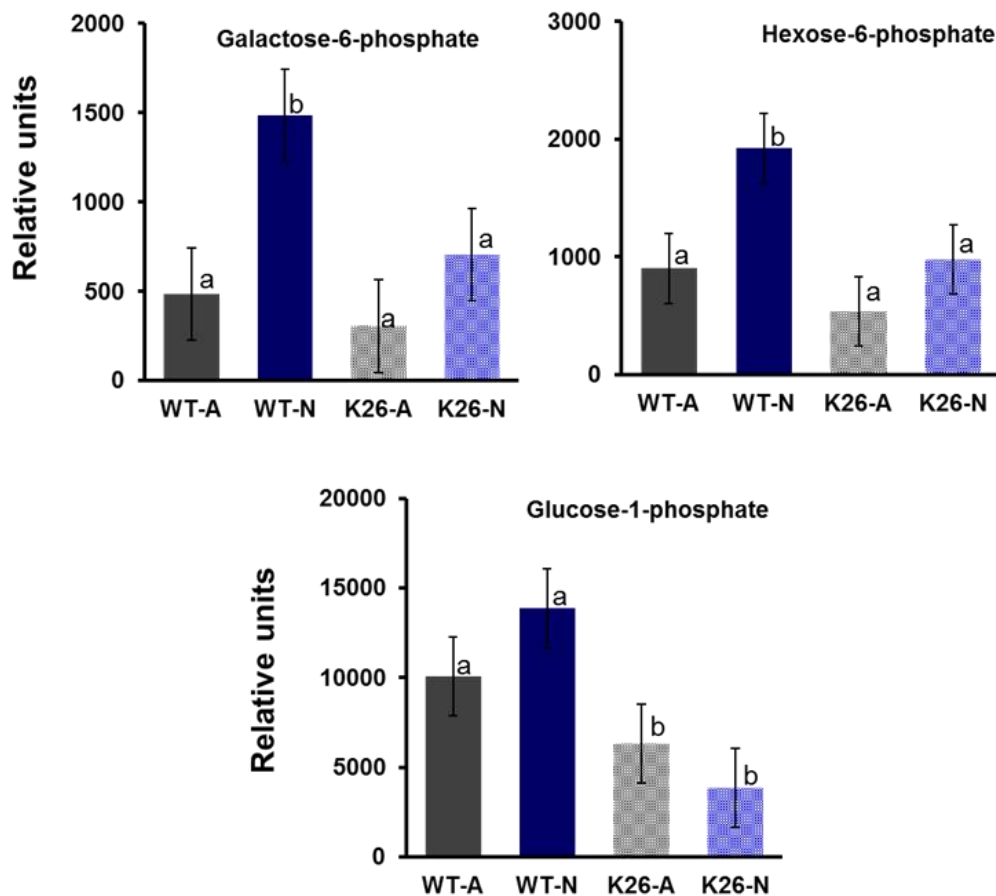


Figure 4.4 Abundance of specific sugar phosphates in WT and K26 grown in ammonium and nitrate. Values represent the mean \pm SE of three biological replicates. Values identified with different alphabets are statistically significant as determined by two-way ANOVA, Post-hoc Tukey test, ($P < 0.05$).

4.3.2 Oxidative Pentose Phosphate Pathway (oxPPP) activity is differentially modified by nitrate and alternative oxidase

One goal of this study was to determine how the lack of AOX and thus AP respiratory capacity in K26 cells could alter oxPPP activity in response to nitrate. This was assessed by measuring the levels of two metabolites of the oxPPP: glucose-6-phosphate and ribulose-5-phosphate. As shown in Figure 4.5A, compared to WT cells grown in ammonium, the abundance of both glucose-6-phosphate and ribulose-5-phosphate was doubled when cells were grown in nitrate. Interestingly, the levels of both of these metabolites were low in K26 strain, and insensitive to a change in nitrogen source. These data support the hypothesis that the oxPPP is stimulated by nitrate in WT cells, but the pathway is suppressed by the knocking down of AOX (Figure 4.5).

To lend support to the finding that oxPPP may be modulated by both nitrate and AOX abundance, transcript abundance of GLD1 and PGL/PGD that encode the oxPPP enzymes glucose-6-phosphate dehydrogenase and phosphogluconolactonase, respectively, was measured. As shown in Figure 4.6, there is a strong increase in the accumulation of GLD1 and PGD transcripts in response to nitrate in WT cells. But in the K26 strain, expression of both genes was lowered in nitrate grown condition. This agrees with the decreased accumulation of glucose-6-phosphate and ribulose-6-phosphate involved in the oxPPP. From these results, it can be inferred that in K26 strain, nitrate-dependent stimulation of oxPPP activity is subdued by the absence of AP capacity or restoration of mitochondrial respiration mainly through CP capacity.

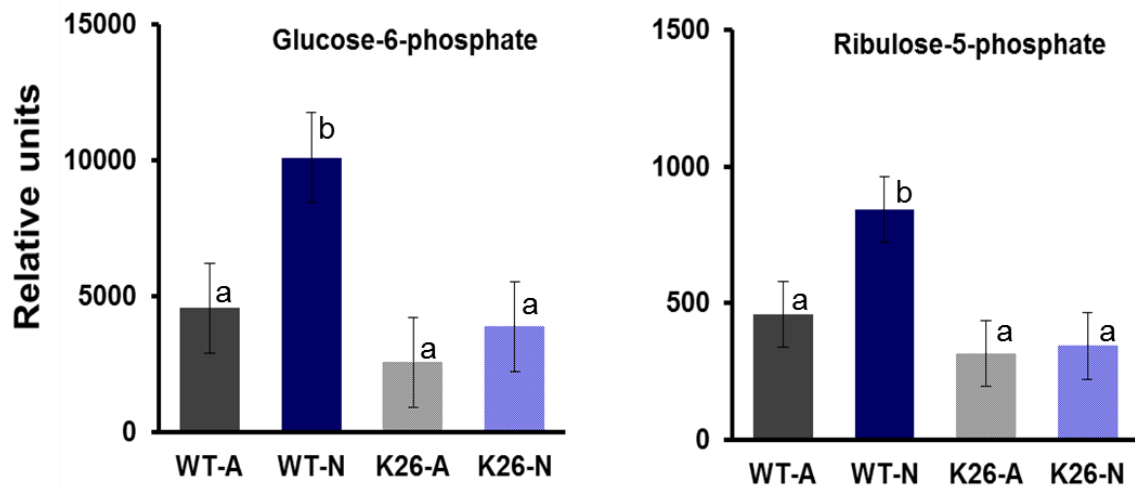


Figure 4.5 Changes in the abundance of metabolites glucose-6-phosphate and ribulose-6-phosphate in WT and K26 strains grown in ammonium (A) or nitrate (N). Values represent the mean \pm SE of three biological replicates. Values identified with different alphabets are statistically significant as determined by two-way ANOVA, Post-hoc Tukey test ($P < 0.05$).

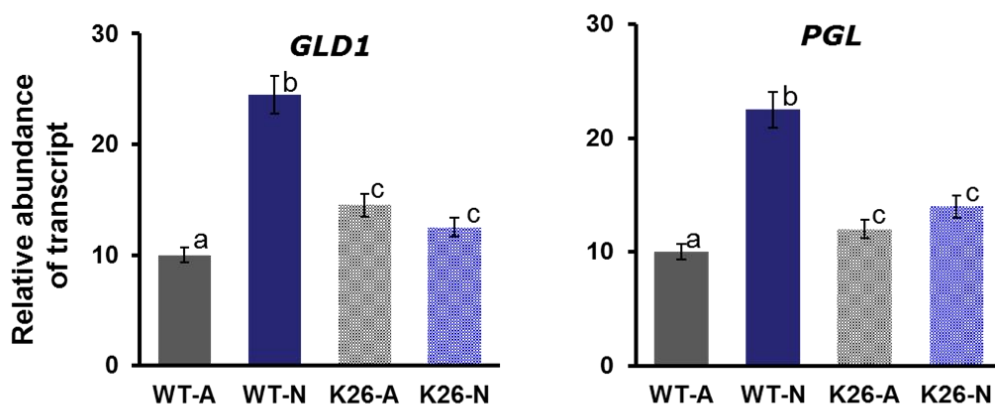


Figure 4.6 Quantitative PCR analysis of transcript abundance of *GLD1* (glucose-6-phosphate dehydrogenase) and *PGL*/PGD (phosphogluconolactonase) in WT and K26 strains. Values are expression relative to an internal reference gene ubiquitin ligase (UBL) and represent the mean \pm SE of three biological replicates. Values identified with different alphabets are statistically significant as determined by two-way ANOVA, Post-hoc Tukey test ($P < 0.05$).

4.3.3 Modification of oxPPP activity by glycerol downregulates AOX accumulation in the presence of nitrate

From the last section we showed that two metabolites of the oxPPP, glucose-6-phosphate and ribulose-6-phosphate have lower accumulation in response to AOX1 knockdown line in nitrate grown cells. This suggests that the oxPPP activity is being modified in the absence of AOX accumulation. To investigate if regulation also occurs in the opposite direction, we manipulated the oxPPP to see if it would alter AOX abundance. Previous studies in plants have shown that exogenous application of glycerol can inhibit the oxPPP by blocking gluocse-6-phosphate isomerase, thereby inhibiting the conversion of glucose into glucose-6-phosphate. Because of this, glycerol can act to downregulate the oxPPP (Lejay

et al., 2008). In the current study, it was expected that exposing *Chlamydomonas* WT cells to glycerol in the presence of nitrate would downregulate the oxPPP activity by reducing the glucose-6-phosphate availability. When the activity of the oxPPP is reduced in the chloroplast by glycerol addition, it was predicted that mitochondria would decrease the AOX accumulation. As shown in Figure 4.7, the addition of 30 mM of glycerol to WT cells grown in nitrate resulted in a strong decrease in AOX protein accumulation. The abundance of COX3, a protein of the CP pathway, was unchanged in glycerol treated cells indicating the presence of CP respiration and the absence of any detrimental effect due to glycerol in general. Based on this result it can be suggested that mitochondrial respiration is remodeled by downregulating AOX accumulation when the oxPPP is subdued in the chloroplast by glycerol.

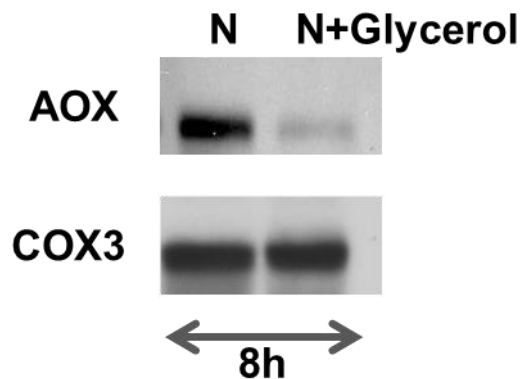


Figure 4.7 Representative Immunoblots showing the abundance of AOX and COX3 in WT cells grown in the presence of nitrate (N) with and without glycerol (30mM). Cells were collected after 8h from glycerol-treated and untreated cells and used for western blot analysis. Each lane contains 25 µg of protein.

4.4 Discussion

Using whole-cell metabolite analysis it was shown that shifting WT cells from ammonium to nitrate results in changes to a wide range of metabolites. Similarly, significant changes were seen in metabolite profiles in response to the knocking down of AOX abundance.

Comparing the metabolomes of WT and K26 cells, it was found that the accumulation of over half of the metabolites induced in WT cells by a shift into nitrate were dependent upon the ability to upregulate AOX expression. This dependence upon AOX is also shown by the fact that K26 cells shifted into nitrate displayed a muted response in its metabolite profile, which resembled an ammonium-grown metabolome. This muted response of K26 cells to nitrate indicates that the re-sculpting of the *Chlamydomonas* metabolome in response to nitrate requires the induction of AP respiration, which occurs within minutes of exposure to nitrate in WT cells (Molen et al., 2006, Pakkiriswami et al., 2009), but is prevented from occurring in K26 cells.

The metabolic alterations that occurred in response to nitrate and AOX deficiency were also evident in the clustering pattern of metabolomes obtained through PCA analysis. Based on this analysis, it was shown that there is clear separation between the metabolomes of WT cells grown in ammonium and cells grown in nitrate. That K26 cells did not show a clear separation between ammonium and nitrate metabolomes but the component PC2 indicates that the knocking down of AOX causes major alterations to metabolism that render any changes brought about by a change in nitrogen source largely insignificant. These data are further supported by the finding that metabolome of K26 cells grown in nitrate is similar to that of ammonium grown cells

The finding of increased glucose-6-phosphate and ribulose-5-phosphate accumulation in nitrate grown WT cell likely reflects the stimulation of the oxPPP. Further support for the upregulation of oxPPP comes from data that indicates the transcripts of two oxPPP-related enzymes, GLD1 and PGL, also increased in

response to nitrate. Induction of the oxPPP is thought to be required for the process of nitrate assimilation as it supplies additional reductants (NADH) (Huppe et al., 1992, Lejay et al., 2008, Bussell et al., 2013). This extra reductant could be channeled either through photosynthesis by NDA2, which donates electrons directly to the PQ pool of photosynthetic electron transport or alternatively it could be exported as reducing equivalents through metabolic shuttles to support nitrate assimilation in the cytosol (Scheibe 2004). The increased reductant transfer through NDA2 complex fulfills the demand of reducing power for nitrite reduction and in addition, could increase ATP generation by activating cyclic electron flow of photosynthesis (See Chapter 3).

The ATP required for the synthesis of sugar phosphates (e.g. glucose-6-phosphate and ribulose-5-phosphate) is generated primarily by the light reactions of photosynthesis. The increased sugar phosphate pool in WT cells grown in nitrate as compared to ammonium puts a heightened demand on adenine diphosphate (ADP) and inorganic phosphate (Pi) availability within the chloroplast. The increased accumulation of hexose phosphates (glucose-6-phosphate, glucose-1-phosphate, and fructose-6-phosphate) observed in response to nitrate may occur in response to increased transport of Pi into the chloroplast in exchange for sugar phosphates through the plastidic phosphate translocator (PPT). It would be expected that such events would deplete the cytosolic pool of ADP and Pi molecules. This would restrict their availability for oxidative phosphorylation within the mitochondria, which would through respiratory control, restricts the rate of CP electron flow. Support for this comes from the work in tobacco suspension cells, where phosphate deficiency restricts CP capacity and stimulates AP respiration (Rychter et al., 1992, Parsons et al., 1999, Vanlerberghe 2013).

This scenario is supported by the fact that cells lacking AOX (K26 line) are unable to upregulate the oxPPP and stimulate increased sugar phosphate production, as shown by their reduced levels of glucose-6-phosphate, ribulose-6-phosphate and other hexose phosphates, as compared to WT. In AOX deficient

cells there would be an absolute requirement for ADP and Pi levels within the mitochondrion to be sufficiently high to support high rates of CP respiration and oxidative phosphorylation. Further support for this link between oxPPP activity in the chloroplast and AP respiration in mitochondria is provided by the finding that exogenous glycerol, which has been shown previously to inhibit the oxPPP, was found to reduce AOX abundance. Inhibition of oxPPP would reduce the formation and conversion of hexose phosphates to glucose-6-phosphate and thereby reduce the demand of ADP and Pi in the chloroplast. This would, in turn increase the available pool of ADP and Pi in the cytosol, which could be transported to the mitochondria for ATP synthesis through CP respiration.

These data also suggest that either glucose-6-phosphate or other metabolites produced in the downstream of oxPPP might act as a signal and contribute to the regulation of AOX1 gene expression. It has been reported that metabolites of oxPPP control the expression of nitrate assimilation genes in Arabidopsis (Bussell et al., 2013). Since AOX1 is also a nitrate inducible gene, it is possible that sugar phosphates of the oxPPP might change the AOX1 expression level in Chlamydomonas like in Arabidopsis.

4.5 References

- Akashi K, Miyake C, Yokota A (2001) Citrulline, a novel compatible solute in drought-tolerant wild watermelon leaves, is an efficient hydroxyl radical scavenger. *FEBS Letters* 508: 438–442
- Brychkova G, Alikulov Z, Fluhr R, Sagi M (2008) A critical role for ureides in dark and senescence-induced purine remobilization is unmasked in the *Atxdh1* *Arabidopsis* mutant. *The Plant Journal* 54: 496–509
- Bussell JD, Keech O, Fenske R, Smith SM (2013) Requirement for the plastidial oxidative pentose phosphate pathway for nitrate assimilation in *Arabidopsis*. *The Plant Journal* 75: 578–591
- Cardol P, Gloire G, Havaux M, Remacle C, Matagne R, Franck F (2003) Photosynthesis and State Transitions in Mitochondrial Mutants of *Chlamydomonas reinhardtii* Affected in Respiration. *Plant Physiol* 133: 2010–2020
- Dang K-V, Plet J, Tolleter D, Jokel M, Cuiné S, Carrier P, Auroy P, Richaud P, Johnson X, Alric J, et al (2014) Combined Increases in Mitochondrial Cooperation and Oxygen Photoreduction Compensate for Deficiency in Cyclic Electron Flow in *Chlamydomonas reinhardtii*. *Plant Cell* 26: 3036–3050
- Eriksson L, Johansson E, Kettaneh-Wold N, Trygg J, Wilkstrom C Wold S (2006) Multi and Megavariable Data Analysis. 2nd Ed. Umetrics AB Sweden.
- Geiger M, Haake V, Ludewig F, Sonnewald U, Stitt M (1999) The nitrate and ammonium nitrate supply have a major influence on the response of photosynthesis, carbon metabolism, nitrogen metabolism and growth to elevated carbon dioxide in tobacco. *Plant, Cell & Environment* 22: 1177–1199
- Hopkins WG and Huner NP (2008). *Introduction to Plant Physiol*, Fourth Edition, New York: Wiley and Sons Inc. pp 207-208
- Huppe HC, Vanlerberghe GC, Turpin DH (1992) Evidence for Activation of the Oxidative Pentose Phosphate Pathway during Photosynthetic Assimilation of NO₃⁻ but Not NH₄⁺ by a Green Alga. *Plant Physiol* 100: 2096–2099
- Jans F, Mignolet E, Houyoux P-A, Cardol P, Ghysels B, Cuiné S, Cournac L, Peltier G, Remacle C, Franck F (2008) A type II NAD(P)H dehydrogenase mediates light-independent plastoquinone reduction in the chloroplast of *Chlamydomonas*. *PNAS* 105: 20546–20551
- Lee DY, Fiehn O (2008) High quality metabolomic data for *Chlamydomonas reinhardtii*. *Plant Methods* 4: 7
- Lejay L, Wirth J, Pervent M, Cross JM-F, Tillard P, Gojon A (2008) Oxidative

Pentose Phosphate Pathway-Dependent Sugar Sensing as a Mechanism for Regulation of Root Ion Transporters by Photosynthesis. *Plant Physiol* 146: 2036–2053

Masakapalli SK, Kruger NJ, Ratcliffe RG (2013) The metabolic flux phenotype of heterotrophic *Arabidopsis* cells reveals a complex response to changes in nitrogen supply. *Plant J* 74: 569–582

Molen TA, Rosso D, Piercy S, Maxwell DP (2006) Characterization of the alternative oxidase of *Chlamydomonas reinhardtii* in response to oxidative stress and a shift in nitrogen source. *Physiologia Plantarum* 127: 74–86

Nishizawa A, Yabuta Y, Shigeoka S (2008) Galactinol and Raffinose Constitute a Novel Function to Protect Plants from Oxidative Damage. *Plant Physiol* 147: 1251–1263

Pakkiriswami S, Beall BFN, Maxwell DP (2009) On the role of photosynthesis in the nitrate-dependent induction of the alternative oxidase in *Chlamydomonas reinhardtii*. *Botany* 87: 363–374

Parsons HL, Yip JYH, Vanlerberghe GC (1999) Increased Respiratory Restriction during Phosphate-Limited Growth in Transgenic Tobacco Cells Lacking Alternative Oxidase. *Plant Physiol* 121: 1309–1320

Redinbaugh MG, H. Campbell W (1998) Nitrate regulation of the oxidative pentose phosphate pathway in maize (*Zea mays* L.) root plastids: induction of 6-phosphogluconate dehydrogenase activity, protein and transcript levels. *Plant Science* 134: 129–140

Rychter AM, Chauveau M, Bomsel J-L, Lance C (1992) The effect of phosphate deficiency on mitochondrial activity and adenylate levels in bean roots. *Physiologia Plantarum* 84: 80–86

Scheibe R (2004) Malate valves to balance cellular energy supply. *Physiologia Plantarum* 120: 21–26

Vanlerberghe GC (2013) Alternative Oxidase: A Mitochondrial Respiratory Pathway to Maintain Metabolic and Signaling Homeostasis during Abiotic and Biotic Stress in Plants. *International Journal of Molecular Sciences* 14: 6805–6847

Xia J, Wishart DS (2002) Using MetaboAnalyst 3.0 for Comprehensive Metabolomics Data Analysis. *Current Protocols in Bioinformatics*. doi: 10.1002/cpbi.11

Chapter 5

5 General Discussion and Future Perspectives

5.1 Understanding the significance of AOX induction in response to nitrate in *Chlamydomonas*

Quesada et al (1998) identified AOX1 (originally naming it NAR5) in a study looking for additional NAR genes in *Chlamydomonas*. They showed that AOX1 was located near the nitrate transporter NRT2.3 and like other NAR gene, was shown to have expression that was strongly repressed by ammonium and induced by nitrate. Formal cloning and initial characterization of the nuclear gene encoding AOX1 in *Chlamydomonas* was carried out by Dinant et al., (2001). Subsequent work by Baurain et al., (2003) identified regulatory regions in the promoter of AOX1 that were required for nitrate-dependent induction of this enzyme.

The induction of AOX1 and in turn heightened AP respiratory capacity in response to nitrate is not seen in plants or fungi; it seems to be restricted to green algae, although nitrate-dependent induction of AOX has not been confirmed in species other than *Chlamydomonas*. In plants and fungi research suggests that a common feature of most stressors that induce AOX is an increase in intracellular reactive oxygen species (ROS) (see Vanlerberghe 2013). Research by Molen et al (2006) showed that many of these stressors (e.g. treatment with antimycin A, H₂O₂, cold stress) also induce AOX in *Chlamydomonas*. As well, they showed that induction of AOX by nitrate is distinctly different as it does not result in an increase in intracellular ROS (Molen et al. 2006).

The data provided by this earlier work (Quesada et al., (1998), Baurain et al., (2003) and Molen et al., (2006) failed to provide a physiological rationale for why growth in the presence of nitrate would induce AOX expression. It has been suggested previously that induction of AOX by nitrate was a mechanism of adjusting mitochondrial electron transport to the changing demands for reductant

and ATP generation within the chloroplast (Quesada et al., 2000). This thesis represents the first attempt to directly address this question by employing molecular strategies to effectively prevent AOX induction in the presence of nitrate.

Based on the findings presented in Chapters 3 and 4 of this thesis and incorporating the research of others (Bussell et al. 2013, Lejay et al., 2008, Huppe et al., 1992), a picture has emerged of how the metabolism of *Chlamydomonas* is remodeled when cells are shifted from a medium containing ammonium to one containing nitrate and the key role played by AOX in this remodeling. As described in this thesis, this remodeling involves major shifts in chloroplast metabolism, illustrating the interconnectivity of energy metabolism between the chloroplast and the mitochondrion. This research supports previous work that shows how membrane-bound transport shuttles and transporters move reductant, ADP and Pi between organelles and the cytosol supporting the integrated metabolism of the cell (Dang et al., 2014; Cardol et al., 2003),

Ammonium is the fully reduced form of nitrogen that is used for amino acid biosynthesis and is fully reduced. Because of this, growth in the presence of ammonium does not introduce additional energy demands on the cell. The reductant (NADPH) and ATP generated by linear photosynthetic electron transport is used primarily to support the reduction of CO₂ by the Calvin cycle (Figure 5.1). Within the mitochondrion, growth in the presence of ammonium is supported by high rates of electron flow along the cytochrome pathway generating ATP by chemiosmosis coupled to NADH and FADH₂ oxidation. The ATP generated in the mitochondria can be used for a range of biosynthetic reactions throughout the cell. As illustrated in Figure 5.1, engagement of the alternative pathway is very low and thus is not shown.

The energetics of nitrate assimilation are dramatically different than ammonium as both the enzymes nitrate reductase (cytosol) and nitrite reductase (chloroplast) require reducing power to convert nitrate into nitrite and nitrite to

ammonium, respectively. As shown in Figure 5.2, a key metabolic change that occurs in response to nitrate is the synthesis and activation of the two enzymes that constitute the oxidative pentose phosphate pathway (oxPPP). This activation was first reported by Huppe et al (1992), and is supported in this thesis by two pieces of data: (i) expression data showed induction of the genes encoding both glucose-6-phosphate dehydrogenase and 6-phosphoglucolactonase, the two enzymes of the oxPPP and (ii) metabolome analysis showed increased accumulation of glucose-6-phosphate and ribulose-5-phosphate, two metabolites of the pathway following a shift to nitrate (see Figure 5.2). As shown in Figure 5.2, the role of the oxPPP is to generate additional reducing power beyond what is possible through linear photosynthetic electron transport. The induction of the oxPPP by nitrate is explained by the additional demands put on the cell for reductant required to convert nitrate to ammonium.

Compared with the cells grown in ammonium, the activation of the oxPPP under nitrate was shown to increase the accumulation of hexose phosphates (fructose 6-phosphate, glucose 6-phosphate, glucose 1-phosphate) that are presumed to accumulate within the stroma of the chloroplast. This additional pool of hexose phosphate most likely comes from the diversion of sucrose synthesized from G3P of the Calvin cycle. This is supported by the metabolome data from Chapter 4 showing that levels of sucrose are lower when cells are grown in nitrate as compared to ammonium.

The other major metabolic shift seen in cells grown in nitrate as compared to ammonium is an increase in cyclic photosynthetic electron flow, which generates ATP but not NADPH (linear electron transport generates both). As described in Chapter 3, increased cyclic electron flow in the presence of nitrate comes from direct measurements of the re-reduction rate of $P700^+$ to P700 of PSI. Evidence also comes from transcript analysis showing induction of the gene coding for NDA2, a protein that donates electrons from NADPH to the plastoquinone pool (See Figure 5.2). Why would growth in nitrate trigger increased cyclic electron flow around photosystem I? With additional sources of NADPH (e.g. oxPPP), to

support not only the reduction of nitrate but also for biosynthetic reactions in the cytosol, photosynthetic electron transport can shift into a mode that generates more ATP. In the presence of nitrate, the additional ATP would be required to maintain high hexose phosphate pools and keep the oxPPP more active.

Growth under nitrate thus results in a remodeling of chloroplast metabolism that requires not only high levels of reductant but also high levels of ADP and inorganic phosphate. One consequence of this would be a reduction in the ADP and Pi pools found in other cellular compartments (cytosol and mitochondria). This in turn would cause a restriction in the rate of CP respiration, which is strongly coupled to the generation of ATP from ADP and Pi in the mitochondrion.

Respiratory control mechanisms activated by the limited pools of ADP and Pi within the mitochondria would restrict the rate of electron transport along the cytochrome pathway. This would in turn trigger the engagement of the alternative pathway, which in *Chlamydomonas* requires transcriptional activation of AOX1 as well as synthesis of AOX. Recall from Chapter 1, electron flow along the alternative pathway generates a smaller proton gradient than the cytochrome pathway, and thus generates less ATP. Under conditions of low adenylate levels within the matrix of the mitochondrion, activation of the alternative pathway is essential for the continued operation of the TCA cycle and upstream respiratory carbon flow (Parsons et al., 1999).

The elegant interplay between chloroplast metabolism and AOX expression within the mitochondrion seems to be governed by the relative needs of each organelle for ATP. In the presence of nitrate, the induction of AOX is coordinated with the activation of the oxPPP within the chloroplast and its heightened requirement for ATP. This interplay can be effectively manipulated through the addition of glycerol a potent inhibitor of the oxPPP. As described in detail in Chapter 4, when the oxPPP is prevented from operating, and thus the demand of the chloroplast for ATP falls, the induction of AOX within the mitochondrion is suppressed.

So, what is the consequence of genetically manipulating AOX1 in *Chlamydomonas* such that AP respiration is prevented from becoming engaged in the presence of nitrate? As shown by the model presented as Figure 5.3, in the K26 knockdown line, maintenance of respiratory electron flow would require engagement of the cytochrome pathway, which in turn is dependent upon mitochondrial concentrations of both ADP and Pi remaining high. A consequence of this would be a restriction in the levels of these metabolites within the chloroplast. Without sufficient ATP, the chloroplast would not be able to maintain the high hexose phosphate pools required to support activation of the oxPPP, which is what is reflected in the K26-N metabolite data. So, in this regard even though nitrate is present, carbon metabolism in the chloroplast in the knockdown line is more similar to ammonium-grown than nitrate-grown WT cells. It is interesting to note as shown in the K26-N model that cyclic electron flow occurs to a similar extent measured for WT-N cells.

In the absence of AP respiration (because of the knockdown of AOX1), high rates of cytochrome electron transport is essential to maintain the high rates of upstream carbon oxidation (glycolysis, pyruvate oxidation, TCA cycle). Oxidation of reduced carbon is essential not only for the generation of ATP but also because they are the carbon skeletons needed to support high rates of amino acid biosynthesis as well as being the precursors of a range of other molecules.

At the beginning of this work it was thought that cells deficient in AOX would not be able to grow in nitrate. The activation of AOX1 and AP respiration in response to nitrate was so strong and rapid that it was easy to conclude that the AOX induction is highly essential for nitrate assimilation to occur. However, at the conclusion of this work it does not come as a surprise that in fact cells deficient in AOX can still grow very well in the presence of nitrate. The difference between the growth characteristics in ammonium versus nitrate comes down to one of energy — specifically reducing power and ATP. The fact that WT cells grown in ammonium or nitrate have similar growth rates reflects the cells ability to upregulate energy production when necessary. Likewise, when it is unable to

upregulate AP respiration the cell elegantly adjusts its overall metabolism in other ways to maintain appreciable nitrate reduction.

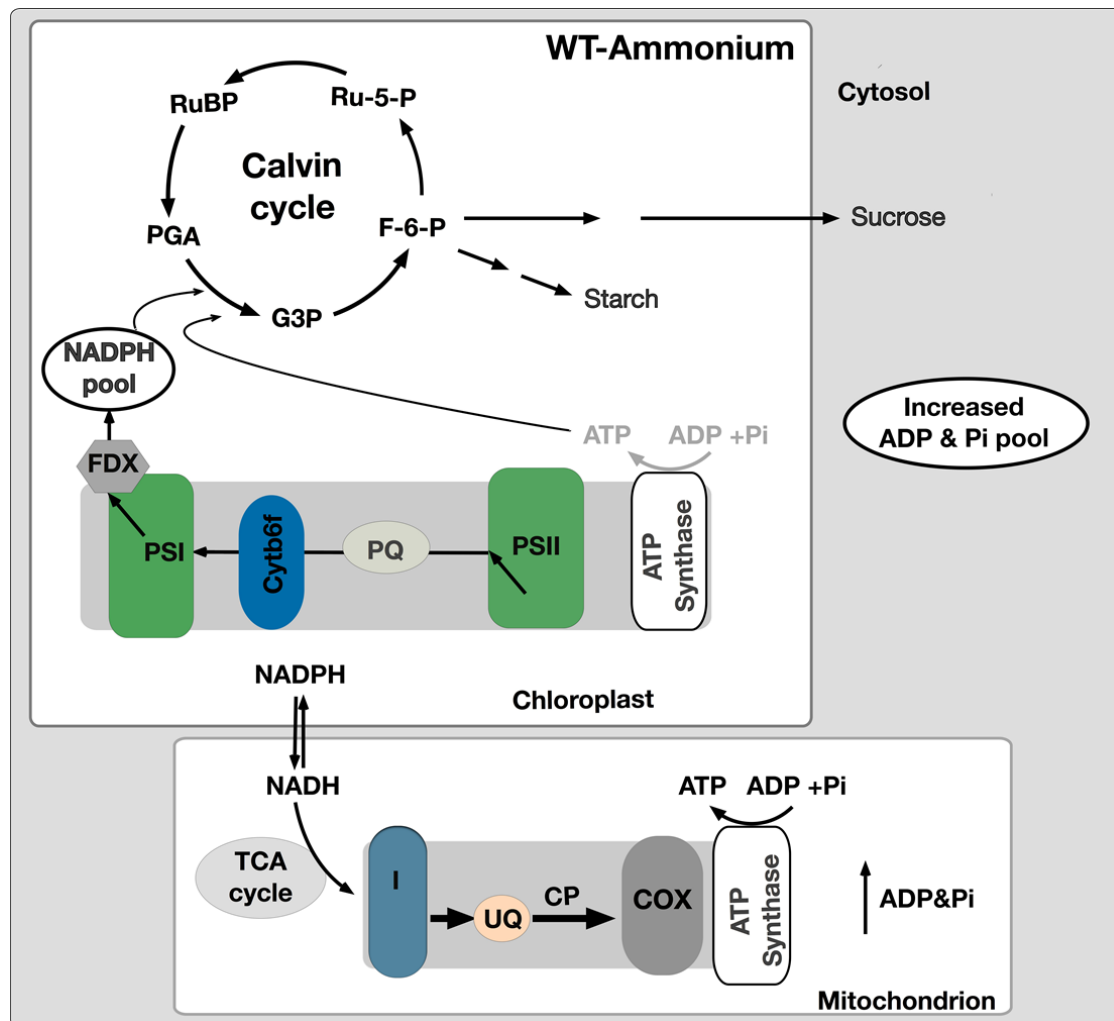


Figure 5.1 Model showing the metabolic interactions between the chloroplast and mitochondria in *Chlamydomonas* cells grown in ammonium. See text for explanation. The model is based on data presented in Chapters 3 and 4. Abbreviations; RuBP-Ribulose biphosphate, PGA- Phosphoglyceric acid, G3P-glyceraldehyde-3-phosphate, F-6-P-fructose-6-phosphate, Ru-5-P- ribulose-5-phosphate, FDX-ferredoxin, PSII-photosystem II, PSI-photosystem I, PQ-plastoquinone, COX-cytochrome oxidase, UQ- ubiquinone, I - Complex I of mitochondrial electron transport, ADP-adenine diphosphate, Pi- Inorganic phosphate

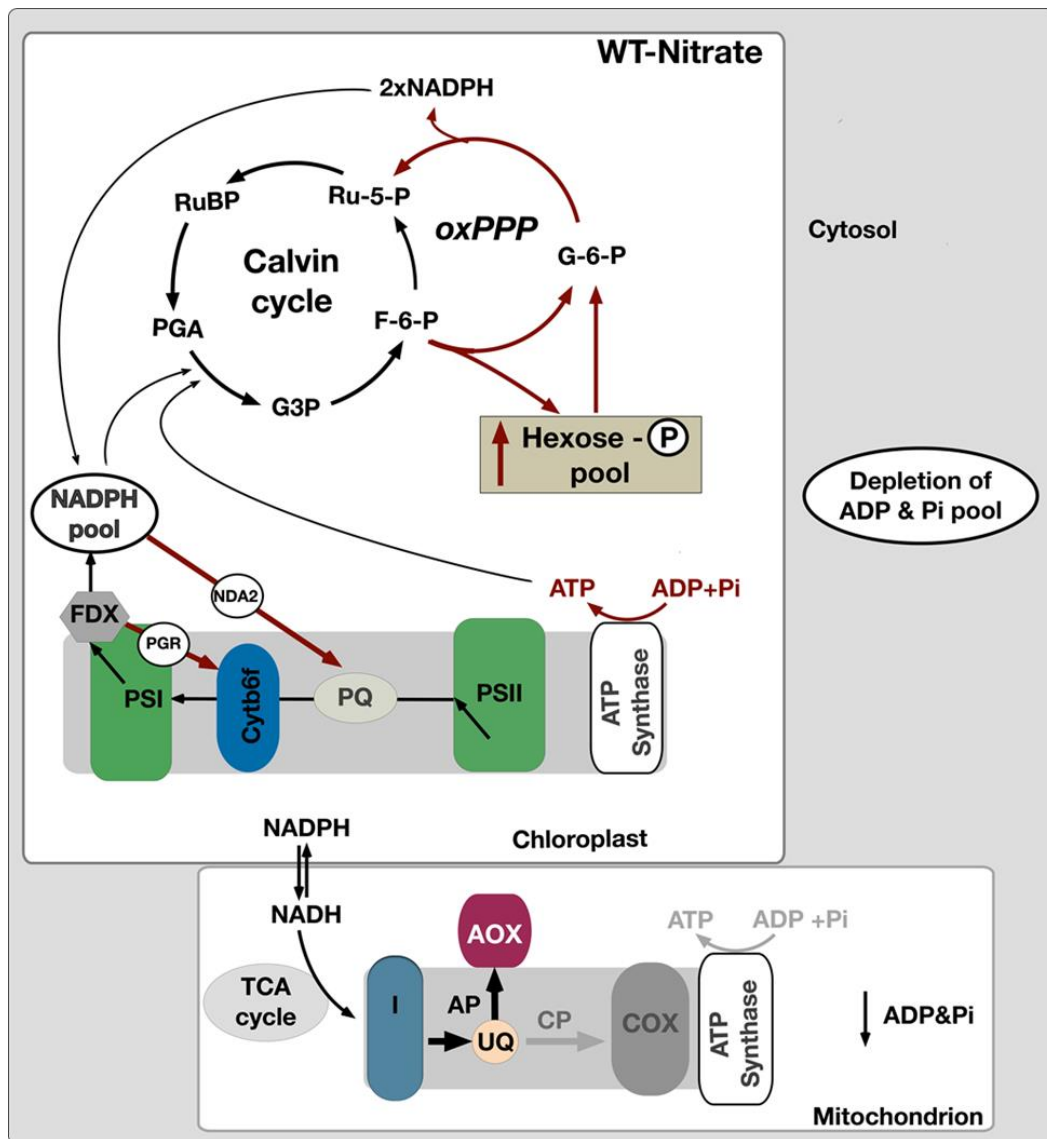


Figure 5.2 Model showing the relevant interactions between photosynthesis, Calvin cycle, oxPPP and mitochondrial electron transport in response to nitrate in WT cells. See text for explanation. Abbreviations: oxPPP-oxidative pentose phosphate pathway, RuBP-Ribulose biphosphate, PGA-Phosphoglyceric acid, G3P-glyceraldehyde-3-phosphate, F-6-P-fructose-6-phosphate, G-6-P-glucose-6-phosphate, Ru-5-P- ribulose-5-phosphate, FDX-ferredoxin, PSII-photosystem II, PSI-photosystem I, PQ-plastoquinone, COX-cytochrome oxidase, AOX- alternative oxidase, UQ- ubiquinone, I - Complex I of mitochondrial electron transport, ADP-adenine diphosphate, Pi- Inorganic phosphate

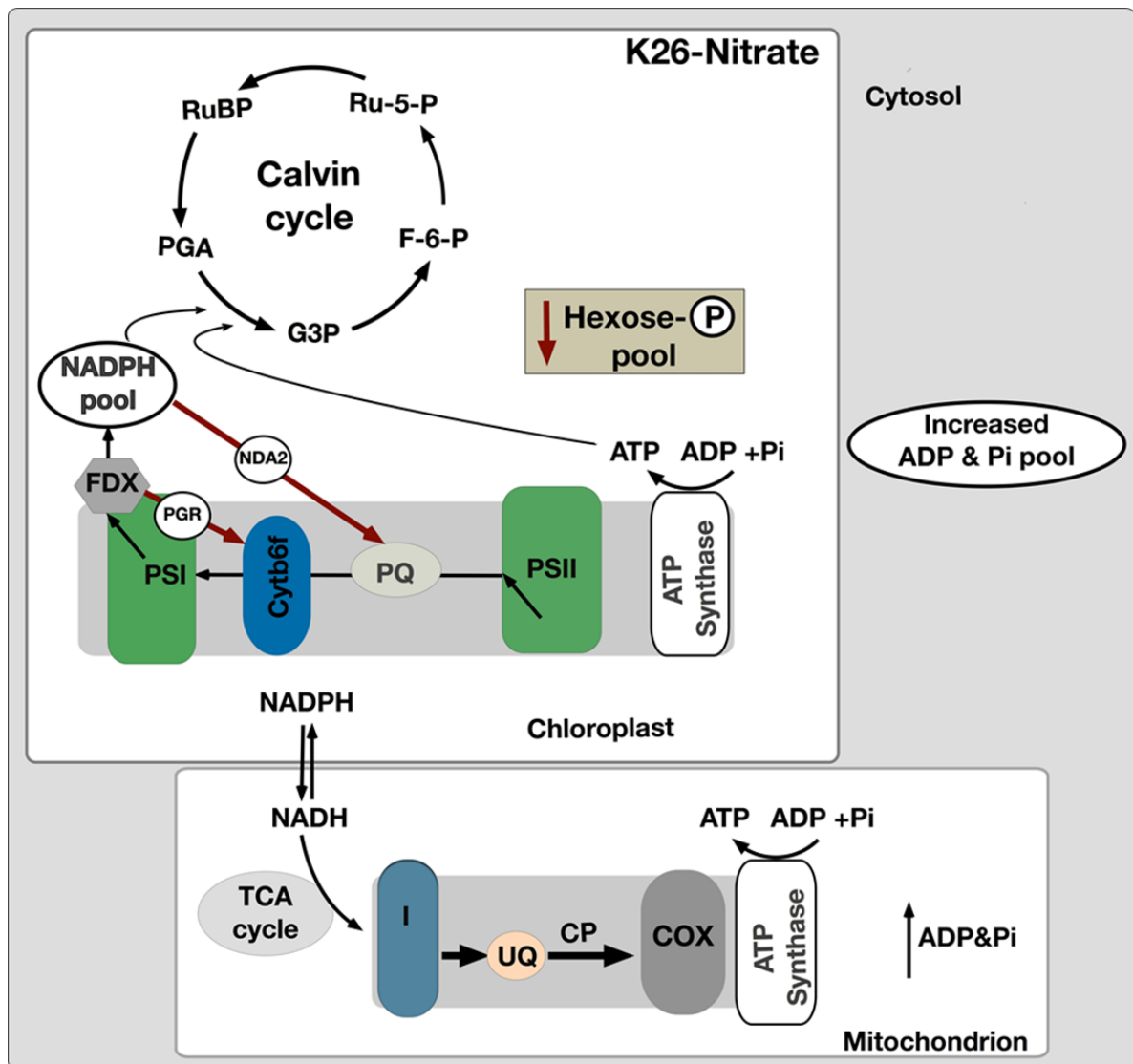


Figure 5.3 Model showing the relevant interactions between photosynthesis, Calvin cycle and mitochondrial electron transport in response to nitrate in K26 cells. See text for explanation. Abbreviations; oxPPP-oxidative pentose phosphate pathway, RuBP-Ribulose biphosphate, PGA-Phosphoglyceric acid, G3P-glyceraldehyde-3-phosphate, F-6-P-fructose-6-phosphate, G-6-P-glucose-6-phosphate, PGL-phosphogluconolactonate, Ru-5-P-ribulose-5-phosphate, FDX-ferredoxin, PSII-photosystem II, PSI-photosystem I, PQ-plastoquinone, COX-cytochrome oxidase, AOX- alternative oxidase, UQ-ubiquinone, I - Complex I of mitochondrial electron transport, ADP-adenine diphosphate, Pi- Inorganic phosphate

5.2 Summary of Major Contributions

The data from Chapter 2 provides *in silico* evidence for the distribution of NAR Cluster I and II in different green algal species by analyzing genomes available in the public databases. Based on the analysis, it was found that NAR cluster I is present in the Chlorophyceae, Trebouxiophyceae and Mamiellophyceae members of green algae available for analysis and NAR cluster II is restricted only to the members of Chlorophyceae. Further it was also observed that members of Trebouxiophyceae (*Coccomyxa* and *Chlorella*) analyzed in this study do not have a complete NAR cluster I and have lost one or more essential genes from the cluster. The loss of physical clustering in these algal species is coincidental with the improvement of other nitrogen acquisition strategies. It was noted that in the genomes of two green algal species, a greater number of amino acid transporter genes are present possibly reflecting the presence of organic nitrogen source in the environment from where they are normally found. From this data, this study showed that the form of nitrogen available in the environment strongly influence the organization of nitrogen assimilation genes in green algae. To my knowledge this is the first research linking NAR gene clustering with adaptation to specific nitrogen environments.

Chapters 3 and 4 were focused on determining the physiological significance of AOX induction in the presence of nitrate. By comparing the metabolomes of WT and knockdown cells grown in ammonium or nitrate it was discovered that induction of AP respiration in the mitochondria correlates activation of the oxPPP in the chloroplast. It was also shown for the first time that downregulation of AOX1 gene expression in K26 cells, reduced the accumulation of oxPPP metabolites in the chloroplast. These two pieces of data can be projected as evidence for the interplay between the chloroplast and mitochondrial energy metabolism under two different nitrogen environments.

The induction of AOX by nitrate seen in *Chlamydomonas* has been known for some time yet evidence indicating a clear metabolic rationale has been lacking. The data from the current study suggest that the stimulation of AP respiration in

the mitochondria is more likely to relieve the respiratory electron transport from adenylate control and sustain the operation of TCA cycle and NADH oxidation when mitochondrial adenylate levels are low. The stimulation of oxPPP in WT cells grown in nitrate resulted in the enhancement of cyclic electron transport around PSI. It reflects the heightened synthesis of ATP in the chloroplast through photosynthesis by increasing the transfer of ADP and Pi from the cytoplasm. This would deplete the ADP and Pi pool needed for the operation of the CP respiration in the mitochondria. Therefore, to overcome this situation, cell induces AP respiration in the mitochondria which generates small proton gradient and synthesize lesser ATP with the restricted supply of ADP and Pi from cytosol. Such induction of AP respiration would largely help to 1) sustain the operation of TCA cycle and NADH oxidation by respiratory electron transport and 2) reduce the formation of ROS by preventing the over reduction of ubiquinone pool.

5.3 Future Directions

One major conclusion that can be derived from the in-silico identification of NAR genes cluster organization in green algae is the physical grouping of NAR genes in the genome is advantageous for co-inheritance and co-regulation of the genes in the cluster. The loss of NAR gene clustering and the improvement of other nitrogen acquisition strategies observed in the genomes of *Chlamydomonas* and *Coccomyxa* suggest the role of selection pressure from the environment in the maintenance and formation of such gene clusters. This interesting coincidence is seen only in two of the green algal species and hence analysis of more algal genomes should be considered when their genome sequences become available in the future.

The clustering of AOX1 with NRT2.3 is unique and found to be present only in the three of the members of Chlorophyceae group. Initially when AOX1 was identified in *Chlamydomonas*, it was considered as one of the NAR genes (Quesada et al., 1998). It was predicted earlier that the localization of AOX1 proximal to NRT2.3 had no significance (Baurain et al., 2003). However, the data

presented in the chapter 4 support the notion that AOX1 in *Chlamydomonas* may be regulated like other NAR gene.

One question that arises from the data presented in Chapter 4 concerns the signals that regulate the expression of AOX1. Based on the content discussed in Chapter 4, it can be inferred that the metabolites of oxPPP may play a crucial role in the stimulation of AOX1 gene expression. Further support for this data comes from the study that demonstrated the analogous role played by oxPPP in *Arabidopsis*, wherein it was shown that the stimulated synthesis of oxPPP metabolites under nitrate regulates the expression of nitrate assimilation genes (Lejay et al., 2008 and Bussell et al., 2013). Hence future studies should be focused on assessing the status of expression of AOX1 gene in nitrate signaling mutants (Camargo et al., 2007 and de Montaigu et al., 2010) isolated in *Chlamydomonas*. This would be a first step to identify whether the regulatory network that regulates the expression of NAR genes could also control the AOX1 gene transcription.

In response to nitrate, absence of AOX did not lower the growth to any great extent. This is similar to what is reported in *Arabidopsis* and tobacco where altered levels of AOX did not affect the growth under optimal conditions. It affected the fitness of the organism only when it is exposed to stress conditions such as high light and low temperature (reviewed in Vanlerberghe et al., 2013). Hence to further understand the role of AOX induction in response to nitrate in *Chlamydomonas*; it is important to study the consequences of downregulating AOX1 gene expression by exposing the cells to various stress conditions like nutrient or temperature stress.

5.4 References

- Baurain D, Dinant M, Coosemans N, Matagne RF (2003) Regulation of the Alternative Oxidase Aox1 Gene in *Chlamydomonas reinhardtii*. Role of the Nitrogen Source on the Expression of a Reporter Gene under the Control of the Aox1 Promoter. *Plant Physiol* 131: 1418–1430
- Bussell JD, Keech O, Fenske R, Smith SM (2013) Requirement for the plastidial oxidative pentose phosphate pathway for nitrate assimilation in *Arabidopsis*. *Plant J* 75: 578–591
- Camargo A, Llamas Á, Schnell RA, Higuera JJ, González-Ballester D, Lefebvre PA, Fernández E, Galván A (2007) Nitrate Signaling by the Regulatory Gene NIT2 in *Chlamydomonas*. *The Plant Cell Online* 19: 3491–3503
- Cardol P, Gloire G, Havaux M, Remacle C, Matagne R, Franck F (2003) Photosynthesis and State Transitions in Mitochondrial Mutants of *Chlamydomonas reinhardtii* Affected in Respiration. *Plant Physiol* 133: 2010–2020
- Dang K-V, Plet J, Tolleter D, Jokel M, Cuiné S, Carrier P, Auroy P, Richaud P, Johnson X, Alric J, et al (2014) Combined Increases in Mitochondrial Cooperation and Oxygen Photoreduction Compensate for Deficiency in Cyclic Electron Flow in *Chlamydomonas reinhardtii*. *Plant Cell* 26: 3036–3050
- De Montaigu A, Sanz-Luque E, Galvan A, Fernandez E (2010) A soluble Guanylate Cyclase mediates negative signalling by ammonium on expression of Nitrate reductase in *Chlamydomonas*. *Plant Cell* 22:1532-1548
- Dinant M, Baurain D, Coosemans N, Joris B, Matagne RF (2001) Characterization of two genes encoding the mitochondrial alternative oxidase in *Chlamydomonas reinhardtii*. *Curr Genet* 39: 101–108
- Huppe HC, Vanlerberghe GC, Turpin DH (1992) Evidence for Activation of the Oxidative Pentose Phosphate Pathway during Photosynthetic Assimilation of NO₃⁻ but Not NH₄⁺ by a Green Alga. *Plant Physiol* 100: 2096–2099
- Lejay L, Wirth J, Pervent M, Cross JM-F, Tillard P, Gojon A (2008) Oxidative Pentose Phosphate Pathway-Dependent Sugar Sensing as a Mechanism for Regulation of Root Ion Transporters by Photosynthesis. *Plant Physiol* 146: 2036–2053
- Molen TA, Rosso D, Piercy S, Maxwell DP (2006) Characterization of the alternative oxidase of *Chlamydomonas reinhardtii* in response to oxidative stress and a shift in nitrogen source. *Physiologia Plantarum* 127: 74–86

Parsons HL, Yip JYH, Vanlerberghe GC (1999) Increased Respiratory Restriction during Phosphate-Limited Growth in Transgenic Tobacco Cells Lacking Alternative Oxidase. *Plant Physiol* 121: 1309–1320

Quesada A, Hidalgo J, Fernández E (1998) Three Nrt2 genes are differentially regulated in *Chlamydomonas reinhardtii*. *Mol Gen Genet* 258: 373–377

Vanlerberghe GC (2013) Alternative Oxidase: A Mitochondrial Respiratory Pathway to Maintain Metabolic and Signaling Homeostasis during Abiotic and Biotic Stress in Plants. *International Journal of Molecular Sciences* 14: 6805–6847

Appendices

Appendix S1: Gaussian parameters for the sub-band decomposition of low temperature (77K) chlorophyll fluorescence emission spectra of WT and K26 cells.

Parameters	WT-A	K26-A	WT-N	K26-N
1 λ max	681.1 \pm 0.1	680.9 \pm 0.4	680.3 \pm 0.3	681.1 \pm 0.2
FWHM	8.3 \pm 0.2	8.1 \pm 0.3	7.5 \pm 0.3	8.3 \pm 0.2
Area (%)	12.7 \pm 0.7	9.4 \pm 0.9	9.0 \pm 0.6	6.9 \pm 0.9
2 λ max	685.9 \pm 0.1	685.8 \pm 0.1	685.7 \pm 0.1	685.9 \pm 0.1
FWHM	5.0 \pm 0.1	5.3 \pm 0.2	5.6 \pm 0.1	5.1 \pm 0.1
Area (%)	8.2 \pm 0.5	7.9 \pm 0.9	10.3 \pm 0.9	9.0 \pm 0.2
3 λ max	691.9 \pm 0.2	692.5 \pm 0.2	692.5 \pm 0.2	691.9 \pm 0.2
FWHM	12.6 \pm 0.3	10.5 \pm 0.4	11.0 \pm 0.4	12.6 \pm 0.3
Area (%)	17.9 \pm 0.7	10.2 \pm 0.5	12.5 \pm 0.7	9.2 \pm 0.7
4 λ max	710.8 \pm 0.1	711.4 \pm 0.1	711.5 \pm 0.1	710.8 \pm 0.1
FWHM	23.8 \pm 0.2	24.5 \pm 0.2	23.7 \pm 0.2	23.8 \pm 0.2
Area (%)	36.5 \pm 0.7	46.9 \pm 0.7	40.9 \pm 0.7	47.3 \pm 0.8
5 λ max	727.3 \pm 0.6	726.6 \pm 0.6	724.3 \pm 0.5	727.3 \pm 0.6
FWHM	49.9 \pm 0.5	52.2 \pm 0.5	49.7 \pm 0.5	49.9 \pm 0.4
Area (%)	24.6 \pm 0.6	25.6 \pm 0.6	27.3 \pm 0.6	27.5 \pm 0.7
PSII/PSI	1.050	0.586	0.777	0.530

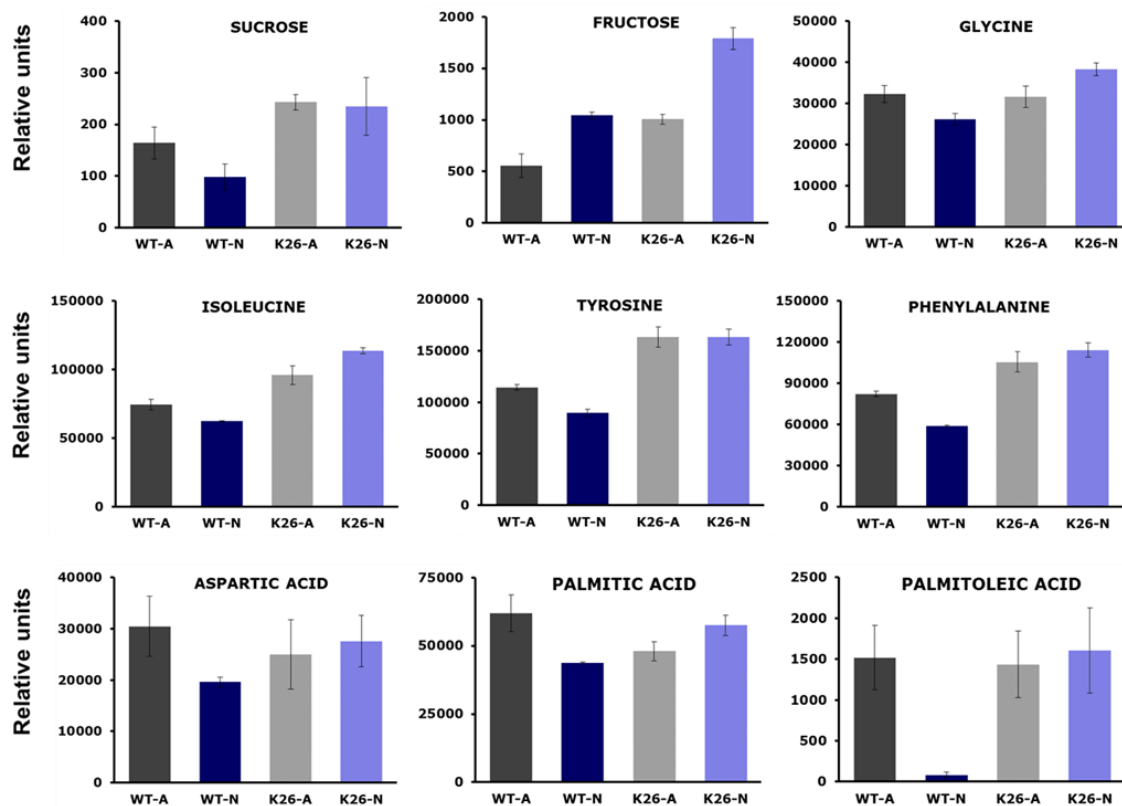
The percentage areas of the spectral forms have been calculated from the total area given by the sum of all bands. The FWHM of each band is the sum of the left and right HWHM values (FWHM - full width at half maximum). PSII/PSI represents the ratio between the areas of PSII related peaks (λ_1 , λ_2 and λ_3) and the area of PSI peak (λ_4). Data represent the mean \pm SE of four separate experiments.

Appendix S2: List of gene specific primers used in PCR

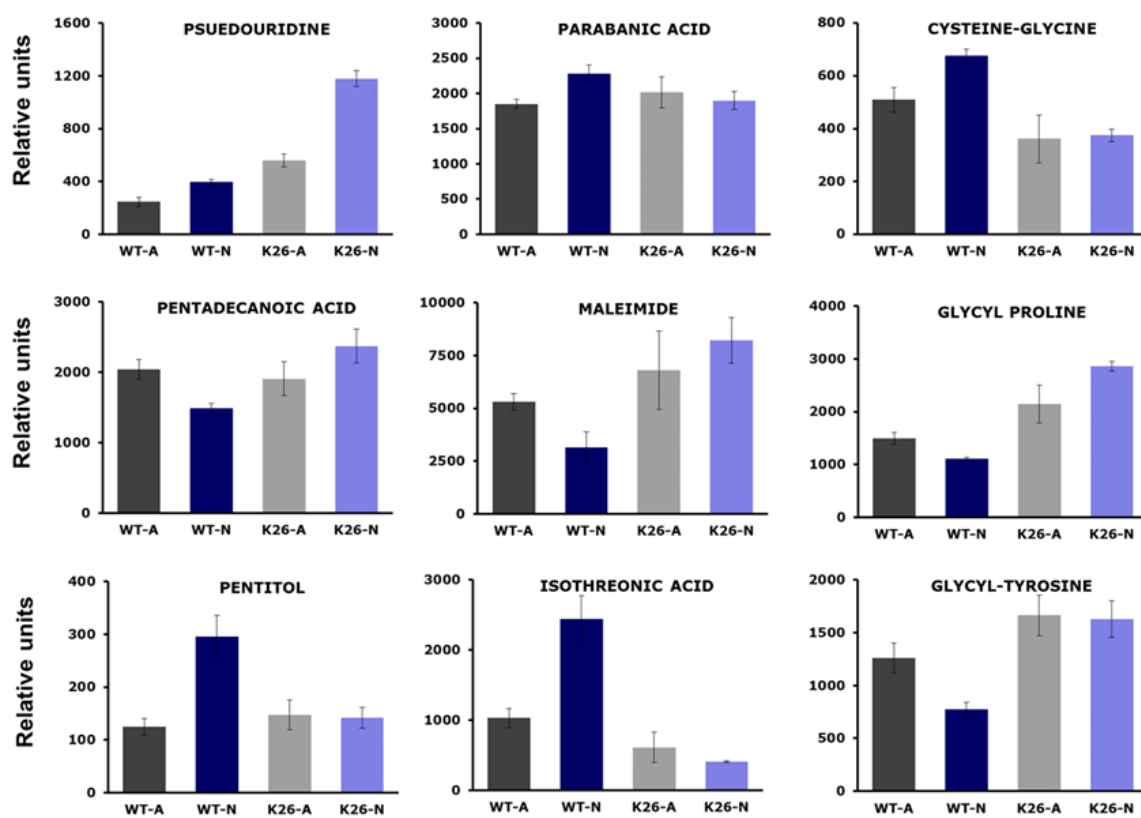
Gene Name	Sequence 5"to 3'
NIA1	FP-AGAACTTCTACCACTTCATGGACAAC RP-GTTGGCGGTTGCTCGTTTTGATGCCA
NII1	FP-GGAAAGGTACGTAGGAGCCG RP-ACAGACAAGCCACCCTAACG
NAR2	FP-CGCTCTATTTCCGCAACACG RP-TCTCGTCTCCCGATGTCCTT
NRT2.1	FP-ATGGCCACCGTTGAGAAGAA RP-AGATGCCATGAAGAGACGC
NRT2.2	FP-CACTTGTGGGCCTTTAGCTGC RP- GTGGAGAAGTCGGTGACCAG
NAR1.1	FP-TCGGTCTCTAAAACGGTGG RP-GAGTCAGGATGGGGTTGGTG
MDH5	FP-CGTAATGTCTGTGCCCCCAT RP-CCCTCACCAACACCCATACC
GLD1	FP-CGTGCGCCATGTACATCAAC RP-GAACTGCACTCGGATCTCGG
PGL	FP-ACTGTTGCACCCATCTCCAC RP-CTTCTCTCCCGTCACGTACA
UBL	FP- GTACAGGGCTAGAGGCAC RP-AGCGTCAGCGGCGGTTGCA
NDA2	FP-GTGTTGACCTGCCCAAGTT RP-ACTGGTTGCGGAAGGGAGAAC
PGRL	FP-AGATGTATGCCGATGCCGAG RP-GTCGAGTAGTCCACAGCGAA
FDX2	FP-ATGGACCTGCCCTACTCGT RP-GTCGCTGCCTTTAGAGCTTG

Appendix S3: Changes in the accumulation of 26 different types of metabolites in WT and K26 that are used for heat map analysis.

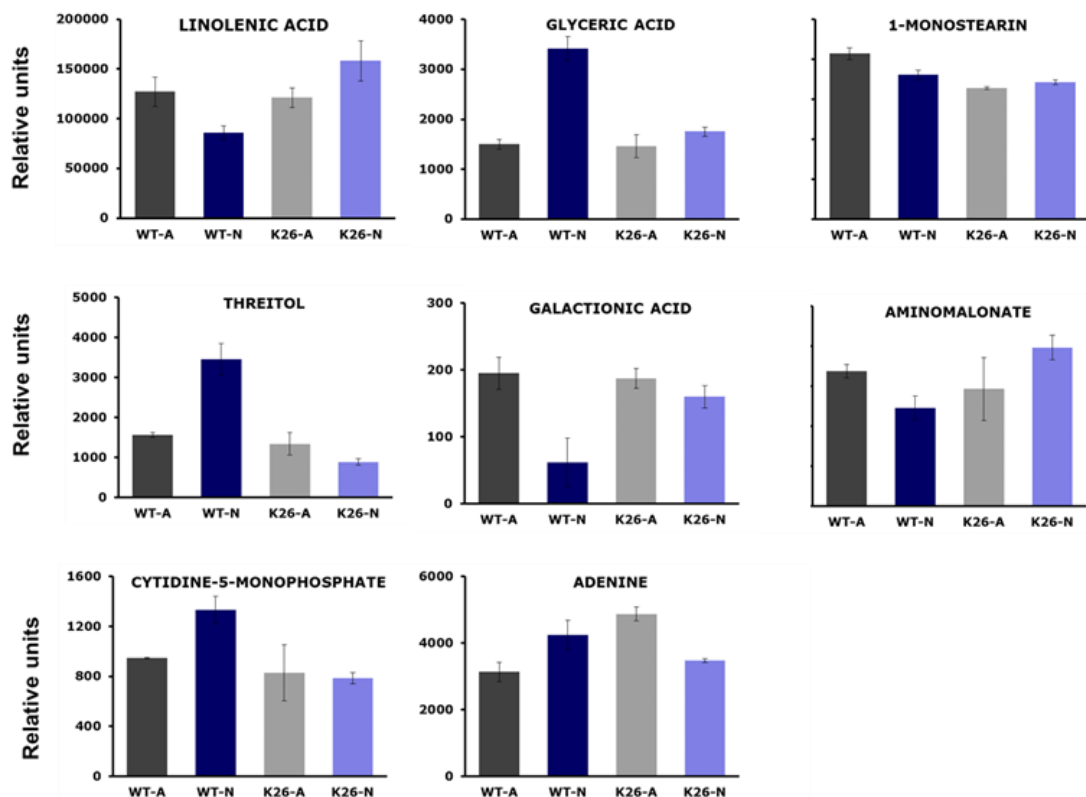
In total 30 metabolites are used for heat map construction, four of which are presented in 4.3.1 and 4.3.2 sections. Values represent the mean \pm SE of three biological replicates. Values marked by * are statistically significant as determined by ANOVA ($P < 0.05$). The following two pairs: WT-A and WT-N, WT-N and K26-N are compared to identify the differential accumulation of a particular metabolite.



Continued next page

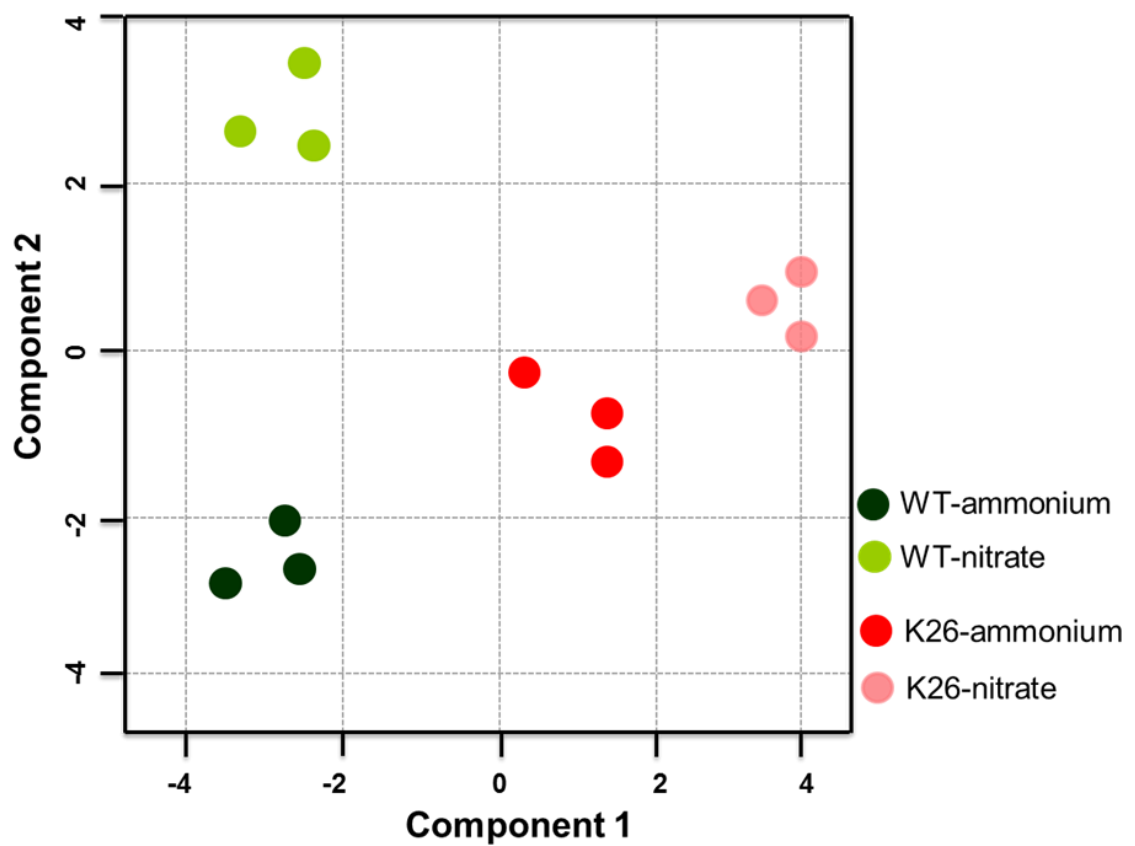


Continued next page



Appendix S4: PLS (DA) algorithm scores plot showing the separation of the metabolome of WT and K26 cells grown in ammonium and nitrate.

Each colored dot in the plot represents one replicate of each treatment class. Three biological replicates are used for each treatment class. PLS (DA) method was performed via Metaboanalyst 2.0, a specific statistics platform for metabolite data analysis.



Curriculum Vitae

Name: Shanmugasundaram Pakkiriswami

Post-secondary
Education and
Degrees: Western University
London, Ontario, Canada
2005-2008 MSc.

Western University
London, Ontario, Canada
2008-2017 PhD.

Honors and
Awards: Queen Elizabeth (II) Graduate Scholarship Sci. and Tech.
2011-2012

Related Work
Experience Teaching Assistant
Western University, London, Ontario, Canada

Publications:

Pakkiriswami S, Beall BFN, Maxwell DP (2009) On the role of photosynthesis in the nitrate dependent induction of alternative oxidase in *Chlamydomonas reinhardtii*. Botany 87(4):363-374